

Updated Recommendations Related to Spent Fuel Transport and Dry Storage Shielding Analyses

AVAILABILITY OF REFERENCE MATERIALS IN NRC PUBLICATIONS

NRC Reference Material

As of November 1999, you may electronically access NUREG-series publications and other NRC records at the NRC's Library at www.nrc.gov/reading-rm.html. Publicly released records include, to name a few, NUREG-series publications; *Federal Register* notices; applicant, licensee, and vendor documents and correspondence; NRC correspondence and internal memoranda; bulletins and information notices; inspection and investigative reports; licensee event reports; and Commission papers and their attachments.

NRC publications in the NUREG series, NRC regulations, and Title 10, "Energy," in the *Code of Federal Regulations* may also be purchased from one of these two sources:

1. The Superintendent of Documents

U.S. Government Publishing Office
Washington, DC 20402-0001
Internet: <https://bookstore.gpo.gov/>
Telephone: (202) 512-1800
Fax: (202) 512-2104

2. The National Technical Information Service

5301 Shawnee Road
Alexandria, VA 22312-0002
Internet: <https://www.ntis.gov/>
1-800-553-6847 or, locally, (703) 605-6000

A single copy of each NRC draft report for comment is available free, to the extent of supply, upon written request as follows:

Address: **U.S. Nuclear Regulatory Commission**
Office of Administration
Digital Communications and Administrative
Services Branch
Washington, DC 20555-0001
E-mail: Reproduction.Resource@nrc.gov
Facsimile: (301) 415-2289

Some publications in the NUREG series that are posted at the NRC's Web site address www.nrc.gov/reading-rm/doc-collections/nuregs are updated periodically and may differ from the last printed version. Although references to material found on a Web site bear the date the material was accessed, the material available on the date cited may subsequently be removed from the site.

Non-NRC Reference Material

Documents available from public and special technical libraries include all open literature items, such as books, journal articles, transactions, *Federal Register* notices, Federal and State legislation, and congressional reports. Such documents as theses, dissertations, foreign reports and translations, and non-NRC conference proceedings may be purchased from their sponsoring organization.

Copies of industry codes and standards used in a substantive manner in the NRC regulatory process are maintained at—

The NRC Technical Library

Two White Flint North
11545 Rockville Pike
Rockville, MD 20852-2738

These standards are available in the library for reference use by the public. Codes and standards are usually copyrighted and may be purchased from the originating organization or, if they are American National Standards, from—

American National Standards Institute

11 West 42nd Street
New York, NY 10036-8002
Internet: www.ansi.org
(212) 642-4900

Legally binding regulatory requirements are stated only in laws; NRC regulations; licenses, including technical specifications; or orders, not in NUREG-series publications. The views expressed in contractor prepared publications in this series are not necessarily those of the NRC.

The NUREG series comprises (1) technical and administrative reports and books prepared by the staff (NUREG-XXXX) or agency contractors (NUREG/CR-XXXX), (2) proceedings of conferences (NUREG/CP-XXXX), (3) reports resulting from international agreements (NUREG/IA-XXXX), (4) brochures (NUREG/BR-XXXX), and (5) compilations of legal decisions and orders of the Commission and the Atomic and Safety Licensing Boards and of Directors' decisions under Section 2.206 of the NRC's regulations (NUREG-0750), (6) Knowledge Management prepared by NRC staff or agency contractors (NUREG/KM-XXXX).

DISCLAIMER: This report was prepared as an account of work sponsored by an agency of the U.S. Government. Neither the U.S. Government nor any agency thereof, nor any employee, makes any warranty, expressed or implied, or assumes any legal liability or responsibility for any third party's use, or the results of such use, of any information, apparatus, product, or process disclosed in this publication, or represents that its use by such third party would not infringe privately owned rights.



NUREG/CR-7302, Revision 1
ORNL/TM-2023/2679

Updated Recommendations Related to Spent Fuel Transport and Dry Storage Shielding Analyses

Manuscript Completed: March 2023
Date Published: February 2024

Prepared by:
Georgeta Radulescu

Oak Ridge National Laboratory
Oak Ridge, TN 37831-6283

Lucas Kyriazidis, NRC Project Manager

Office of Nuclear Regulatory Research

ABSTRACT

This report provides updated recommendations for the important areas of the shielding review of applications for U.S. Nuclear Regulatory Commission (NRC) Certificates of Compliance for spent fuel dry storage cask and Type B radioactive material transportation package designs. The recommendations are based on a series of research studies sponsored by the NRC and performed by Oak Ridge National Laboratory. The main findings of this research are described and illustrated with graphs that allow for examination of representative source terms and dose rates, as well as expected effects of various input parameters on source terms and dose rates for transportation packages and storage casks. The principal recommendations cover: spent nuclear fuel limiting characteristics for loadings; relationships between decay heat and external dose rate; bounding depletion parameters for fuel assembly radiation source term calculations; the neutron source from subcritical multiplication; secondary gamma dose rates; reconstituted fuel assemblies with irradiated stainless-steel fuel rods; air density and soil composition specifications for storage cask far-field dose rate calculations; and models for activated metals in Type B waste packages. The recommendations are intended to provide staff with updated guidance on the performance of shielding analyses that account for modern methods, different application systems, and benchmark experiments.

FOREWORD

This report documents the findings from the U.S. Nuclear Regulatory Commission sponsored research project titled *Shielding Guidance Related to Transport and Storage*.¹ Project activities include seven tasks. The first six tasks consist of specific research studies designed to provide the bases for the last task, the purpose of which is development and documentation of recommendations for shielding evaluations reflective of current regulatory conditions for radioactive material transportation packages and spent nuclear fuel (SNF) storage casks. The supporting research studies are documented in a series of Oak Ridge National Laboratory (ORNL) sponsor reports, which are available from DOE Office of Scientific and Technical Information (OSTI.GOV):

- Task 1—ORNL/SPR-2020/1441 describes a study on the relationships between dose rate and decay heat for SNF casks.
- Task 2—ORNL/SPR-2020/1586 describes a series of shielding analyses for activated metals and spent resins from reactor operations.
- Task 3—ORNL/SPR-2021/2093 provides reference information for pressurized water reactor (PWR) and boiling water reactor (BWR) fuel assemblies and non-fuel hardware (NFH) for use in SNF radiation source term and dose rate calculations. The information consolidated in this report includes publicly available light water reactor fuel assembly design data dated 1992 or older.
- Task 4—ORNL/SPR-2021/2373 describes a study on the characteristics of SNF and NFH radiation source terms for shielding applications. A parametric study in that report extended the range of depletion parameters, previously analyzed in NUREG/CR-6802, for the treatment of PWR and BWR fuel with increased enrichment and higher burnup. The analyzed average fuel assembly burnup and maximum initial UO₂ fuel enrichment values were 80 GWd/MTU and 12%, respectively.
- Task 5—ORNL/SPR-2022/2518 provides a summary of available experimental data for validating computer codes used in shielding calculations for spent fuel storage and transportation systems.
- Task 6—ORNL/SPR-2022/2692 provides a review of SCALE validations applicable to SNF shielding calculations.

SCALE was used to perform the source term and shielding calculations that support the research described in this report. However, the recommendations provided in this report are code independent.

¹ NRC Agreement Number 331310019N0011.

TABLE OF CONTENTS

ABSTRACT	iii
FOREWORD	v
TABLE OF CONTENTS	vii
LIST OF FIGURES	ix
LIST OF TABLES	xi
EXECUTIVE SUMMARY	xiii
ACKNOWLEDGMENTS	xv
ABBREVIATIONS AND ACRONYMS	xvii
1 INTRODUCTION	1-1
1.1 Background.....	1-2
1.2 Purpose and Scope	1-3
1.3 Report Structure and Organization.....	1-4
1.4 Summary Recommendations	1-5
1.4.1 Fuel Assembly Burnup, Enrichment, and Cooling Time for Shielding Analyses.....	1-5
1.4.2 Conservative Radiation Source Term Calculations	1-5
1.4.3 Fuel Material Composition in the Fuel Assembly Model.....	1-5
1.4.4 Fuel Assembly Type	1-6
1.4.5 BWR Fuel Assembly Model.....	1-6
1.4.6 Cobalt Impurity Concentrations in Fuel Hardware and NFH Materials.....	1-6
1.4.7 Activation Sources in the Stainless-Steel Replacement Rods of Reconstituted Fuel.....	1-6
1.4.8 Neutron Source from Subcritical Multiplication	1-6
1.4.9 Secondary Gamma Dose Rate.....	1-6
1.4.10 Far-Field Dose Rates.....	1-7
1.4.11 Source Terms for Type B Waste Packages	1-7
1.4.12 Uncertainties Associated with Nuclear Data and Computational Methods.....	1-7
2 GENERAL SHIELDING CHARACTERISTICS OF DRY STORAGE SYSTEMS AND TRANSPORTATION PACKAGES	2-1
2.1 Canister-Based Systems	2-2
2.2 Non-Canistered Spent Fuel Systems.....	2-3
2.3 Dual-Purpose Storage and Off-Site Transport Systems.....	2-3
2.4 Type B Waste Transportation Packages.....	2-3
2.5 Regulatory Requirements for Transportation Packages Relevant to Shielding Analyses.....	2-3
2.6 Regulatory Requirements for SNF, HLW, and GTCC at ISFSIs Relevant to Shielding Analyses.....	2-4
3 SOURCE TERM CALCULATIONS	3-1
3.1 Spent Fuel.....	3-1

3.1.1	Neutron Sources	3-1
3.1.2	Photon Sources Originating in Irradiated Fuel	3-4
3.1.3	Bremsstrahlung Radiation	3-5
3.1.4	Activation Gamma Sources	3-5
3.1.5	Burnup, Enrichment, and Cooling Time for SNF Source Terms Calculations.....	3-7
3.1.6	Source Term Sensitivity to Depletion Parameters	3-9
3.1.7	Relationships between Decay Heat and External Dose Rates.....	3-11
3.1.8	Axial Burnup Profiles.....	3-12
3.1.9	Activation Sources in the Stainless-Steel Replacement Rods of Reconstituted Fuel.....	3-14
3.2	Non-Fuel Hardware for PWRs.....	3-14
3.3	Source Term Characterization for Type B Waste Packages	3-16
3.3.1	Activated Metals.....	3-17
3.3.2	Spent Resins from Power Plant Operations.....	3-19
3.3.3	Type B Waste Packages Containing a Variety of Waste Materials	3-20
3.4	Neutron Source from Subcritical Multiplication	3-21
3.5	Secondary Gamma Source	3-22
3.6	Source Term Computer Codes and Validation	3-22
3.6.1	ORIGEN	3-23
3.6.2	TRITON.....	3-23
3.6.3	POLARIS.....	3-23
3.6.4	ORIGAMI.....	3-24
3.6.5	Depletion Code Validations	3-24
4	SHIELDING CALCULATIONS.....	4-1
4.1	Methods	4-1
4.1.1	Deterministic Transport Codes	4-1
4.1.2	Monte Carlo Transport Codes	4-1
4.2	Modeling.....	4-3
4.2.1	Spent Fuel Transportation Package Model.....	4-4
4.2.2	Spent Fuel Storage Model.....	4-11
4.3	Computer Code Validation.....	4-19
5	CONCLUSIONS.....	5-1
6	REFERENCES.....	6-1

LIST OF FIGURES

Figure 2-1	3D View of the Geometry Model for a NUHOMS® Storage Module, where Concrete Wall Opacity was Reduced to 20% to Reveal SNF Canisters	2-2
Figure 3-1	Fractional Contributions of Neutrons from SF and (α ,n) Reactions to the Total Neutron Source Strength as a Function of Fuel Burnup and Cooling Time: WE 17x17 Assembly.....	3-2
Figure 3-2	Percentage Increase in the Total Neutron Source Strength Due To Bounding Light Element Impurities in UO ₂ Matrix as a Function of Fuel Burnup and Cooling Time: WE 17x17 Fuel Assembly	3-4
Figure 3-3	Trends of External Dose Rate Variation with Fuel Initial Enrichment for Various Fuel Cooling Times.....	3-8
Figure 3-4	Canister Heat Loading and 2 m Radial Dose Rate	3-12
Figure 3-5	Axial Burnup Profiles with Significant Axial Peaking for Various Ranges of PWR Fuel Assembly Burnup	3-13
Figure 3-6	Axial Burnup Profiles with Significant Axial Peaking for Various Ranges of BWR Fuel Assembly Burnup	3-14
Figure 3-7	Fractional External Dose Rates for ⁶⁰ Co and the Remainder of Radionuclides as a Function of Decay Time for (a) Type 304 Stainless Steel and (b) Reactor Vessel (Carbon Steel) Composition, Assuming a 10-cm Thick Steel Shield.....	3-18
Figure 3-8	Fractional External Dose Rates for Nuclides Reported in (a) NUREG/CR-2830 and (b) NUREG/CR-6567, Assuming a 10-cm Thick Steel Shield	3-20
Figure 4-1	Illustration of Generic Transportation Package Models for (a) NCT and (b) HAC.....	4-6
Figure 4-2	Spatial Dose Rate Distribution Produced in the Air Region External to a Generic Transportation Package under NCT by Each Radiation Source	4-7
Figure 4-3	Spatial Dose Rate Distribution Produced in the Air Region External to a Generic Transportation Package under HAC by Each Radiation Source	4-8
Figure 4-4	Axial Dose Rate Profiles Produced by Full-length Rod and Part-length Rod Fuel Assemblies at the Radial Surface of a Generic Transportation Package Model	4-11
Figure 4-5	Spatial Dose Rate Distribution Produced in the Air Region External to a Generic Dry Storage Cask Model by Each Radiation Source	4-12
Figure 4-6	Spatial Dose Rate Distribution Produced by BRPA and ORA in the Air Region External to a Generic Dry Storage Cask Model.....	4-13
Figure 4-7	Spatial Distributions of Irradiated Steel Replacement Rods in Reconstituted Fuel Assemblies and their Effects on External Gamma Dose Rate for a Generic Dry Storage Cask Model: (a) Reconstituted Assemblies in 9 Innermost Basket Locations; (b) All Assemblies Reconstituted	4-15

Figure 4-8	Dose Rate Variation as a Function of Distance and Fuel Assembly Cooling Time	4-17
Figure 4-9	Fractional Dose Rate Contribution by Each Radiation Source as a Function of Distance from a Generic Storage Cask and Cooling Time	4-18

LIST OF TABLES

Table 3-1	Primary Nuclides for Source of Neutrons in Spent Fuel	3-2
Table 3-2	Summary Information for Main Beta and Gamma Radiation Emitters in Spent Fuel.....	3-5
Table 4-1	Two Meter NCT Dose Rate Ratios for PWR and BWR Fuel Assembly Designs	4-10

EXECUTIVE SUMMARY

Current shielding analyses for radioactive material transportation packages and spent nuclear fuel (SNF) dry storage systems have a high degree of complexity and employ new analysis techniques to demonstrate compliance with regulatory requirements in Title 10 of the *Code of Federal Regulations*, Part 71 and Part 72. The complexity of these analyses derives from the purpose of newly developed spent fuel storage and transport systems. These systems allow flexible loading patterns for decay heat management and are intended to accommodate many fuel assembly designs as well as broad ranges of average fuel assembly burnups, enrichments, and cooling times. The contents of Type B waste packages typically include a broad range of nuclides, geometry configurations, and irradiated fuel or non-fuel materials. NUREG/CR-6716 and NUREG/CR-6802, published in 2001 and 2003, respectively, provide supporting analyses, evaluation findings, and recommendations on shielding analyses and dose rate measurement methods that significantly contributed to the review of both storage system and transportation package designs over approximately two decades. To support reviews of license applications for modern SNF storage and transportation systems that accommodate current industry needs, new recommendations for shielding analyses and reviews are needed. This report provides recommendations that are intended to reduce the complexity of relevant shielding analyses for current shielding designs. The recommendations are primarily based on a series of research studies sponsored by the U.S. Nuclear Regulatory Commission (NRC), which were performed and documented in a series of sponsor reports by Oak Ridge National Laboratory (ORNL).

To address the various aspects of radiation source term calculations for commercial SNF and Type B waste packages, this report describes the sources of radiation associated with SNF and other representative waste streams, analyzes the effects of various input parameter specifications on source terms and dose rate, describes methods for source term calculations, and presents available validations of nuclide inventories predicted by the SCALE code system developed at ORNL. Specifically, this report analyzes whether a relationship can be established between SNF decay heat, which is typically a limiting parameter for canister loadings, and other limiting SNF characteristics (i.e., combinations of fuel assembly minimum initial enrichment, average burnup, and cooling time) for shielding analyses. Other radiation sources—such as irradiated non-fuel hardware (NFH), stainless-steel replacement rods in reconstituted fuel assemblies, and activated metals in reactor internals and pressure vessels from decommissioned reactors—are analyzed to support better understanding of their contributions to the external dose rates of SNF dry storage and transportation packages.

This report also provides updated information and recommendations concerning computational methods for shielding calculations, modeling approaches, and the validation of shielding codes. Calculation results are included in this report to illustrate important aspects of radiation source term and shielding analyses as well as relevant current computer code capabilities. Generic shielding models for dry storage casks and transportation packages are used in all calculations. The graphs and tables included herein allow for examination of representative source terms and dose rates, and they illustrate expected effects of various input parameters on source terms and dose rates for SNF transportation packages and storage casks. Specific issues in the generation of source term and dose rate solutions that typically arise in preparation of a safety application are addressed. For SNF, these issues include source term/dose rate sensitivities to fuel assembly characteristics, fuel composition specifications in the shielding model, the level of fuel geometry details in the shielding model, design basis NFH type, reconstituted fuel assemblies containing irradiated stainless-steel replacement rods, and air and soil material specifications (far-field dry storage dose rates only). Fuel assembly design characteristics affect

both the total source strength and radiation self-shielding. For example, a fuel assembly with a higher initial heavy metal content produces a higher source strength but it also produces greater self-shielding effects. Some fuel assembly geometry details may be simplified without significantly increasing the external dose rate. For example, a BWR fuel assembly with partial-length rods may be represented as a BWR fuel assembly with full length rods. Reconstituted fuel assemblies containing irradiated stainless-steel replacement rods may be loaded in the innermost fuel basket locations to benefit from shielding by the fuel assemblies in the outer basket locations. Far-field dose rates are sensitive to air and soil material specifications.

This report provides a series of recommendations and the bases for these recommendations. The main recommendations in this report concern the following: SNF limiting characteristics for loadings; relationships between decay heat and external dose rate; bounding depletion parameters for fuel assembly radiation source term calculations; the neutron source from subcritical multiplication; secondary gamma dose rates; reconstituted fuel assemblies with irradiated stainless steel rods; air density and soil composition specifications for storage cask far-field dose rate calculations; and models for activated metals in Type B waste packages. SCALE was used to perform the source term and shielding calculations that support the research described in this report. However, the recommendations provided in this report are code independent.

ACKNOWLEDGMENTS

The work described in this report was accomplished with funding provided by the U.S. Nuclear Regulatory Commission. The author wishes to acknowledge the contributions of Oak Ridge National Laboratory (ORNL) staff members who contributed research studies to support the recommendations provided in this report, including Riley Cumberland, Brandon Grogan, Arzu Alpan, Peter Stefanovic,² and Kaushik Banerjee.² The guidance and technical comments provided by Lucas Kyriazidis and Don Algama³ of the Office of Nuclear Regulatory Research, Division of Systems Analysis, and Andrew Barto, Zhian Li, Daniel Forsyth, and Veronica Wilson³ of the Office of Nuclear Material Safety and Safeguards, Division of Fuel Management, were very important for the development of this report. The technical comments provided by ORNL staff members who reviewed the technical reports associated with this work, including William Wieselquist, Douglas Peplow, Joel Risner, Nicholas Kucinski, Germina Ilas, and Ugur Mertyurek, are much appreciated.

² Formerly with ORNL.

³ Formerly with U.S. Nuclear Regulatory Commission.

ABBREVIATIONS AND ACRONYMS

1D	one-dimensional
2D	two-dimensional
3D	three-dimensional
B&W	Babcock & Wilcox
BPR	burnable poison rod
BPRA	burnable poison rod assembly
BWR	boiling water reactor
CFR	Code of Federal Regulations
CISF	Consolidated Interim Storage Facility
CoC	Certificate of Compliance
DOE	Department of Energy
ENDF	Evaluated Nuclear Data File
ENSDF	Evaluated Nuclear Structure and Decay Data File
FQT	fuel qualification table
GE	General Electric
GTCC	Greater than Class C (waste)
HAC	hypothetical accident conditions
HLW	high-level radioactive waste
ICSBEP	International Criticality Safety Benchmark Evaluation Project
ISFSI	Independent Spent Fuel Storage Installation
ISG	interim staff guidance
LOPAR	low parasitic
LWR	light water reactor
MPC	multi-purpose canister
MTU	metric ton (tonne) of initial uranium
NEA	Nuclear Energy Agency
NCT	normal conditions of transport
NFH	non-fuel hardware

NRC	Nuclear Regulatory Commission
OECD	Organisation for Economic Co-operation and Development
OFA	optimized fuel assembly
ORA	orifice rod assembly
ORIGAMI	ORIGEN Assembly Isotopics
ORIGEN	Oak Ridge Isotope Generation and Depletion
ORNL	Oak Ridge National Laboratory
PWR	pressurized water reactor
RCA	radiochemical assay
SF	spontaneous fission
SINBAD	Shielding Integral Benchmark Archive and Database
SNF	spent nuclear fuel
TPD	thimble plug device
TRG	Technical Review Group
TRITON	Transport Rigor Implemented with Time-dependent Operation for Neutronic
VCC	vertical concrete cask
WE	Westinghouse

1 INTRODUCTION

Spent nuclear fuel (SNF) and reactor-related high-level radioactive waste (HLW), such as irradiated non-fuel hardware (NFH) and greater than class C (GTCC) waste from decommissioned commercial power reactors, are stored at Independent Spent Fuel Storage Installations (ISFSIs) at shutdown and operating sites throughout the United States. Currently, 164,840 SNF assemblies are loaded in 3,879 dry casks that are licensed as part of 93 different dry storage systems [1]. SNF storage at Consolidated Interim Storage Facilities (CISFs) emerged as a need for the management of continuously growing SNF inventory and HLW from commercial electricity generation. It involves storage of large quantities of SNF and reactor-related HLW at CISFs that are not co-located with a power reactor and would require large-scale transportation of the SNF and reactor-related HLW from their current storage locations [2]. The U.S. Nuclear Regulatory Commission (NRC) has recently licensed Interim Storage Partners LLC to build and operate a CISF [3] in Andrews County, TX, and is currently reviewing the application for Holtec's HI-STORE CISF [4] in Lea County, NM. The *Consolidated Appropriations Act of 2021* passed by Congress provides funding and directs the U.S. Department of Energy (DOE) to move forward with interim storage to support near-term action in managing the nation's SNF discharged from power reactors.

SNF dry storage and transportation systems accommodate a variety of assembly designs with broad ranges of average fuel assembly burnup, enrichment, cooling time, and irradiation conditions. Type B waste packages may contain a broad range of nuclides, geometry configurations, and irradiated non-fuel materials. Therefore, current shielding analyses have a high degree of complexity and employ new analysis techniques to demonstrate that dry storage casks and transportation packages comply with federal regulatory requirements. External radiation requirements for transportation packages are provided in Title 10 of the *Code of Federal Regulations* (CFR), Part 71 [5]. Specific dose rate limits for transport packages under normal conditions of transport (NCT) and hypothetical accident conditions (HAC) are provided in 10 CFR 71.47 and 71.51, respectively. The regulations in Title 10 of the Code of Federal Regulations (10 CFR) Part 72 [6] require that SNF, reactor-related GTCC waste, and HLW storage and handling systems be designed with adequate shielding to provide sufficient radiation protection under normal, off-normal, and accident conditions. Limits for the annual dose to any real individual located beyond the controlled area are provided in 10 CFR 72.104(a) for normal operations and anticipated occurrences. Specific limits are provided in 10 CFR 72.106(b) for dose from any design basis accident.

Specific guidance for review and approval of applications is documented in NUREG-2216 [7] and NUREG-2215 [8]. Although this guidance was specifically developed for NRC reviews, it clearly identifies all technical areas that an applicant ought to address in safety analyses that support license applications. Previous Oak Ridge National Laboratory (ORNL) research studies [9,10,11,12] provide supporting analyses, evaluation findings, and recommendations on shielding calculation and dose rate measurement methods that significantly contributed to the review of both storage system and transportation package designs. To support reviews of license applications for modern SNF storage and transportation systems that accommodate current industry needs, new recommendations for shielding analyses and reviews are needed. This report provides updated recommendations relevant to current shielding designs and analyses, which are primarily based on a series of ORNL research studies sponsored by the NRC. These research studies are documented in sponsor reports [13,14,15,16,17,18] that are publicly available from the DOE Office of Scientific and Technical Information (OSTI.GOV). More justification for updated shielding recommendations is provided in Section 1.1. The

purpose and scope of the report are discussed in Section 1.2. Specific technical areas addressed herein, and the report structure and organization are described in Section 1.3. A summary of technical recommendations is provided in Section 1.4. This report does not address accident tolerant fuels.

1.1 Background

The evaluation findings and recommendations on shielding analyses in two primary NUREG/CRs have been very useful to NRC staff in their performance of confirmatory calculations that support the review of license application submittals over approximately two decades. These two NUREG/CRs are NUREG/CR-6802 [9], “Recommendations for Shielding Evaluations for Transport and Storage Packages,” which was published in 2003, and NUREG/CR-6716 [10], “Recommendations on Fuel Parameters for Standard Technical Specifications for Spent Fuel Storage Casks,” which was published in 2001. Since the publication of these reports, shielding analyses supporting license applications have become more complex, fuel designs have evolved, applications involving high-burnup fuel have increased, and depletion and shielding codes employed in shielding evaluations have evolved.

Newer SNF systems include canisters with a loading capacity of up to 44 assemblies for pressurized water reactor (PWR) fuel and 89 assemblies for boiling water reactor (BWR) fuel. Loadings may include various fuel assembly types, low- and high-burnup fuel assemblies, intact and damaged fuel assemblies, and non-fuel hardware (NFH). Complex and flexible loading patterns are typically employed for these very large canister capacities to optimize fuel loading and to ensure adequate fuel cooling during storage and transportation. Heat load limits may include uniform, regionalized, and cell-by-cell decay heat limits. Because decay heat is typically the limiting parameter for canister contents, burnup, enrichment, and cooling time specifications for shielding analyses are based on limiting decay heat. Applicants’ analyses are becoming more sophisticated, and as a result, applicants can accommodate a wider range of contents and reduce margins to regulatory dose and dose rate limits.

For non-SNF radioactive material transportation, staff have started reviewing packages whose source varies (such as a waste package) using conservative analyses to encompass a broad range of contents. Applicants are pursuing more representative modeling approaches of sources that are not known at the time of shipment, causing shielding analyses to increase substantially in complexity. Each review of these kinds of packages is very complex, usually involving multiple rounds of requests for additional information. Operational procedures for determining loading limits are also very complex, which may increase human error in loading packages.

NUREG/CR-6802 provides useful recommendations for many areas of shielding analyses, including package descriptions expected in the submittals, fuel assembly and package modeling techniques, sensitivities of principal gamma and neutron emitters in spent fuel to various depletion parameters, and computer code capabilities relevant to source term and dose rate calculations at the time of writing. The depletion and shielding computer codes used to perform the calculations documented in NUREG/CR-6802 have been superseded by new computer codes with improved capabilities. For example, NUREG/CR-6802 extensively describes the capabilities and limitations of SAS2H, a one-dimensional (1D) depletion module available in SCALE Version 4, and provides the best techniques for modeling heterogeneous features of fuel assemblies—such as water holes and burnable poison rods (BPRs)—using 1D depletion calculations. However, SAS2H was superseded by depletion modules TRITON and Polaris with improved geometry modeling capabilities and cross-section data libraries in subsequent SCALE

releases [19,20]. In conclusion, additional research was needed to supplement existing staff guidance (e.g., the information in NUREG/CR-6802 and NUREG/CR-6716) to be reflective of current regulatory conditions.

The NRC sponsored research studies, which are documented in a series of ORNL sponsor reports as described in Section 1.2, to support revised shielding guidance. The main findings from these research studies served as the basis for the new recommendations on shielding analyses for spent fuel storage casks and transportation packages that are provided in this report.

1.2 Purpose and Scope

The purpose of this report is to provide recommendations for the important areas of shielding review of applications for NRC Certificate of Compliance for spent fuel storage cask [6] and Type B radioactive material package [5] designs. The objectives of this work are to provide staff with updated guidance on the performance of shielding analyses that account for modern methods, different application systems (higher burnups, fuel designs, etc.), and benchmark experiments as described in Section 1.1.

NRC-sponsored research studies documented in a series of ORNL sponsor reports are the bases for new recommendations for shielding analyses. ORNL/SPR-2020/1441 [13] describes a study on the relationship between dose rate and decay heat for spent nuclear fuel casks. ORNL/SPR-2020/1586 [14] describes a series of shielding analyses of activated metals and spent resins from reactor operations. ORNL/SPR-2021/2093 [15] provides reference information for PWR and BWR fuel assemblies and NFH for use in SNF radiation source term and dose rate calculations. The information consolidated in the report includes publicly available light water reactor (LWR) fuel assembly design data dated 1992 or older. ORNL/SPR-2021/2373 [16] describes a study on the characteristics of SNF and NFH radiation source terms for shielding applications. A parametric study in that report extended the range of depletion parameters previously analyzed in NUREG/CR-6802 for the treatment of PWR and BWR fuel with increased enrichment and higher burnup. The analyzed average fuel assembly burnup and maximum initial UO₂ fuel enrichment values were 80 GWd/MTU and 12%, respectively. ORNL/SPR-2022/2518 [17] provides a summary of available experimental data for validating computer codes used in source term and shielding calculations for spent fuel storage and transportation systems. ORNL/SPR-2022/2692 [18] provides a review of SCALE validations applicable to SNF shielding calculations.

SCALE was used to perform the source term and shielding calculations that support the research described in this report. However, the recommendations provided in this report are code independent. The purpose of the calculations presented in this NUREG/CR is to illustrate important aspects of radiation source term and shielding analyses as well as relevant current computer code capabilities. The graphs and tables included herein allow for examination of representative source terms and dose rates, and they illustrate expected effects of various input parameters on source terms and dose rates for SNF transportation packages and storage casks. Dose rate is a very complex physical quantity that varies with radiation source characteristics and shielding design. Therefore, the dose rate values provided in the report characterize generic transportation package and storage cask models developed for this research and should not be readily applied to other analysis models.

The structure of this report is similar to that of NUREG/CR-6802. Recommendations provided in NUREG/CR-6802 for many areas of shielding analyses—such as package descriptions

expected in the submittals, geometry modeling techniques, measurement techniques, and sensitivities of principal gamma and neutron emitters in spent fuel—are still applicable and are not repeated herein.

1.3 Report Structure and Organization

Section 2 provides brief descriptions of existing spent fuel dry storage casks and transportation packages and examples of representative storage and transportation systems, including canister-based systems, non-canistered spent fuel storage systems, dual-purpose storage and off-site transport systems, and Type B waste transportation systems. A summary of regulatory requirements related to the shielding performance of Type B packages for radioactive materials and spent nuclear dry storage is also provided in this section.

Section 3 is dedicated to radiation source term calculations. This section describes the various radiation sources in Type B spent fuel and waste packages, the effects of various input parameter specifications on source terms and dose rate, computer codes for source term calculations, and validations of nuclide inventory predictions. Specific spent fuel source term topics include (1) relationships between decay heat and external dose rates; (2) the combination of burnup, enrichment, and cooling time for shielding calculations; (3) source term sensitivities to depletion parameters; (4) axial burnup profiles; (5) material impurities that produce significant activation sources; and (6) sources associated with stainless-steel replacement rods in reconstituted assemblies. Section 3 is organized as follows:

- Spent fuel source terms (Section 3.1)
- Radiation source terms for PWR NFH (Section 3.2)
- Source term characterization for Type B waste packages (Section 3.3)
- Neutron sources from subcritical multiplication (Section 3.4)
- Secondary gamma sources (Section 3.5)
- Source term computer codes and validations (Section 3.6)

Section 4 is dedicated to shielding calculations. This section provides updated information and recommendations concerning computational methods for shielding calculations, modeling approaches with illustrations of dose rate spatial distributions for generic transportation package and dry storage cask models, and code validations. Specific issues in the generation of shielding and dose rate solutions that typically arise in preparation of a safety application are also addressed. These issues include source term/dose rate sensitivities to (1) fuel assembly design (e.g., BWR fuel assembly with full length rods vs. BWR fuel assembly with partial length rods); (2) fuel composition (i.e., fresh fuel vs. irradiated fuel compositions); (3) level of geometry details (i.e., pin-by-pin vs. homogeneous assembly model); (4) stainless-steel replacement rods in reconstituted fuel assemblies; and (5) air and soil material specifications (far-field dose rates only). Section 4 is organized as follows:

- Methods (Section 4.1)
- Modeling (Section 4.2)
- Computer code validations (Section 4.3)

1.4 Summary Recommendations

A summary of the specific recommendations contained in the text of this report is presented here. Further explanation of each of these recommendations is provided in the main body of the report.

1.4.1 Fuel Assembly Burnup, Enrichment, and Cooling Time for Shielding Analyses

The method presented in Section 3.1.5.1 is recommended as an adequate method for unequivocal determination of the sets of fuel burnup, enrichment, and cooling time values that satisfy the dose regulatory limits provided in 10 CFR 71 or 10 CFR 72.

1.4.2 Conservative Radiation Source Term Calculations

A set of input parameters that are conservative with respect to radiation source terms/external dose rate should be specified in depletion calculations. The effects of the selected input parameters should be evaluated for each source type (i.e., neutron, primary gamma—defined in Section 3.1.2, or ^{60}Co activation source in hardware). Most depletion conditions that were demonstrated to produce conservative neutron source terms also produce conservative source terms for primary gamma rays originating in active fuel and the ^{60}Co activation sources in fuel hardware regions. However, different trends of variation of the individual source types with certain input parameters were identified in previous studies. For example, the neutron source dose rate increases as initial fuel enrichment decreases at fixed burnup, but the primary gamma dose rate increases with decreasing initial fuel enrichment only up to approximately 10 years of cooling and then increases as initial fuel enrichment increases after 10 years of cooling at fixed burnup. Fuel assembly models that include inserts such as BPRs will produce conservative neutron and primary gamma radiation source terms, but non conservative ^{60}Co activation sources for fuel assembly hardware. The set of depletion parameter values for source term calculations may be based on their dose rate effects on the dominating source type (i.e., either neutron, primary gamma, or ^{60}Co activation source in hardware) with respect to external dose rate, for all burnups and cool times allowed. The shielding analysis should describe the set of depletion parameter values used to generate radiation source terms and evaluate the degree of conservatism relative to nominal parameters. See Sections 3.1.5 and 3.1.6.

1.4.3 Fuel Material Composition in the Fuel Assembly Model

Fresh fuel compositions are recommended in place of irradiated fuel compositions in the shielding model because fresh fuel produces higher neutron sources from subcritical multiplication than irradiated fuel, whereas fuel composition has a relatively negligible impact on external gamma dose rate. See Section 4.2.2.2.1.

Generally, bounding light-element impurity concentrations in UO_2 , such as those provided in ORNL/SPR-2021/2093 [15], Table 29, should be included in the fuel material for the purpose of determining neutron source terms. Pure UO_2 compositions may be used with proper justification. For example, the (α, n) source produced by bounding light-element concentrations in UO_2 would have a negligible contribution to the total dose rate if the total dose rate is dominated by the gamma dose rate, average fuel assembly burnup values are greater than 20 GWd/MTU, and fuel cooling times are less than 40 years. See Section 3.1.1.1.

1.4.4 Fuel Assembly Type

Use a fuel assembly type with the greatest initial uranium mass among the waste stream as the design basis fuel assembly type for general-purpose applications. Previous studies have shown that dose rate increases caused by reduced self-shielding effects are insufficient to offset dose rate reductions due to source strength effects associated with lighter fuel assembly types. See Section 4.2.1.3.1.

1.4.5 BWR Fuel Assembly Model

A BWR full-length fuel rod assembly model is recommended for use in shielding analyses. This model is more conservative with respect to dose rate than a partial-length rod fuel assembly model. See Section 4.2.1.3.2.

1.4.6 Cobalt Impurity Concentrations in Fuel Hardware and NFH Materials

Where available, cobalt impurity concentrations in fuel hardware and NFH materials based on plant records may be used in site-specific shielding analyses. The use of actual cobalt impurity concentrations in place of a bounding concentration value is especially important for short cooling times to avoid using excessive shielding material for overpack design. However, the importance of ^{60}Co production from neutron capture in iron isotopes might increase relative to the ^{60}Co production from the activation of the cobalt impurity and would have to be included in the total ^{60}Co activity. See Section 3.1.4.1.

1.4.7 Activation Sources in the Stainless-Steel Replacement Rods of Reconstituted Fuel

Specify a requirement for reconstituted fuel assemblies with irradiated fuel rods to be placed in inner fuel basket locations. Depending on the actual number of replacement stainless-steel rods within a reconstituted fuel assembly and the assembly cooling time, activation sources in irradiated steel can significantly increase external dose rates. See Sections 3.1.9 and 4.2.2.2.3.

1.4.8 Neutron Source from Subcritical Multiplication

Describe the method used to calculate the neutron source from subcritical multiplication and evaluate the safety margin that is associated with this neutron source over the range of fuel enrichments associated with the contents. See Sections 3.4 and 4.2.2.2.1.

1.4.9 Secondary Gamma Dose Rate

Perform coupled neutron photon transport calculations to calculate dose rate from secondary gamma rays because secondary gamma dose rate might be a significant contributor to total external dose rate. Although secondary gamma dose rate might be a negligible fraction of the total dose rate near a dry storage cask, the importance of secondary gamma dose rate increases with fuel burnup, cooling time, and distance from the cask. See Sections 4.2.1.2 and 4.2.2.3.1.

1.4.10 Far-Field Dose Rates

Include ample volumes of air and soil in an ISFSI model, extending beyond the location of interest for dose rate calculations, to properly simulate important radiation scattering events (i.e., skyshine and groundshine) that contribute to dose rates at remote locations. See Section 4.2.2.3.2.

For site-specific applications, use average air density values and soil compositions based on local conditions. Far-field dose rate increases with decreasing air density, and even small air density variations can have a very significant impact on dose rates at long distances from a cask because of the large volume of air considered in the geometry model. Soil composition affects the groundshine dose rate component. See Section 4.2.2.3.2.

1.4.11 Source Terms for Type B Waste Packages

To calculate activation sources for irradiated metal alloys in the pressure vessel and other internal components of decommissioned reactors, use bounding cobalt impurity concentration values based on plant records or measurements of representative samples. Previous studies have shown that the cobalt impurity concentration in the steel and Inconel alloys used in the reactor internals and pressure vessels of U.S. power reactors varies across a wide range. See Section 3.3.1.1.

For irradiated metal alloys in the pressure vessel, shroud, core barrel, etc. from decommissioned reactors, identify and document the magnitude of localized peak activation sources. External package dose rates may then be determined using a uniform source distribution with an activity density equal to the localized peak. Previous analyses have indicated that the activity densities of radionuclides in activated metals may vary by orders of magnitude, depending on their location in the reactor and the material composition. Therefore, activated metals from decommissioned reactors may present localized peak activation sources. See Section 3.3.1.3.

The crud (i.e., neutron-activated corrosion products) radiation source expected on reactor internals from decommissioned reactors should be modeled as a surface source. Homogenization of the neutron-activated corrosion products within the waste material is not recommended because this modeling approach would result in an underestimation of cask external dose rate. See Section 3.3.1.3.

To simplify the shielding model for Type B waste packages containing a variety of waste materials (e.g., Al, stainless steel, Zr), the waste may be represented as a single material with a mass density based on the total waste weight. However, the highest-Z material among the anticipated waste streams should be used for the purpose of generating the bremsstrahlung radiation produced by beta emitters. See Section 3.3.3.

1.4.12 Uncertainties Associated with Nuclear Data and Computational Methods

The consequences of biases and uncertainties associated with depletion and shielding computational methods may be mitigated by various analysis approaches, such as employing conservative modeling assumptions, increasing design margins in the analysis, and establishing bounding design-basis source terms with justified conservatism. See Sections 3.6.5 and 4.3.

2 GENERAL SHIELDING CHARACTERISTICS OF DRY STORAGE SYSTEMS AND TRANSPORTATION PACKAGES

SNF assemblies, various irradiated reactor inserts, and GTCC waste from commercial nuclear power reactors are currently stored at ISFSIs throughout the United States, including shutdown and operating sites [1,2]. GTCC waste is solid low-level radioactive waste from reactor operation and decommissioning, such as segments of irradiated pressure vessel internals and filter media, that is not generally acceptable for near-surface disposal [21] because of the presence of very-long-lived radionuclides in this waste stream.

Most SNF assemblies currently in dry storage are loaded in spent fuel canisters. Non-canistered dry storage systems (e.g., bolted casks) are also used for a small fraction of SNF assemblies (i.e., less than approximately 2%) [1]. A fuel basket assembly placed inside a canister or the non-canistered dry storage cask supports the fuel assemblies, provides neutron absorption to satisfy subcriticality requirements for the fuel assembly configuration, and facilitates decay heat transfer to the cask body wall. Most canister designs are licensed for both on-site SNF dry storage and transportation packages.

A transportation package consists of transportation packaging (canister, overpack, and impact limiters) and its contents. Type B packaging may be subdivided into several categories that indicate the type of contents, including Type B Waste Packages, Type B (Normal Form) Packages, Type B (Special Form) Packages, and Spent Fuel Packages. Only Spent (UO_2) Fuel Packages and Type B Waste Packages are addressed in this report. Transportation packages are designed based on regulatory requirements provided in 10 CFR Part 71. To satisfy the regulatory dose rate limits for transportation packages, radiation shielding for Type B transportation packages is typically provided by thick layers of steel, lead, and neutron absorber materials such as borated polymers and resins. Specific regulatory dose rate limits are discussed in Section 2.5 of this report. Design information and various analyses (e.g., structural, thermal, containment, shielding, and criticality) are documented by applicants for transportation package Certificates of Compliance (CoC) in a Safety Analysis Report to support NRC licensing review.

A dry storage system typically consists of several canisters, which are designed to accommodate a variety of SNF assemblies; a storage overpack, which contains a loaded canister during dry storage; and a transfer cask, which contains a canister during loading, unloading, and transfer operations. Concrete is the primary shielding material used in the construction of storage overpacks, but steel casks are also used for spent fuel storage, typically in bolted storage cask designs. The storage overpack and its fuel contents are referred to as a *spent fuel storage cask* herein. A storage cask typically requires maintaining an air flow around the fuel canister to control the cladding temperature of the stored fuel. The air flow is facilitated by a set of inlet and outlet vents or openings through the shielding layers. To minimize the impact of vents on dose rates produced by a dry storage cask, these vents are typically shaped as a labyrinth because such a configuration prevents a direct streaming path from the radiation source. The shielding materials for transfer casks may include carbon steel, lead, concrete, water, and borated materials. Dry storage systems are designed based on regulatory requirements of 10 CFR Part 72. Specific regulatory dose rate limits are discussed in Section 2.6 of this report. Design information and various analyses (e.g., structural, thermal, shielding, criticality, and confinement) are documented by applicants for general or site-specific licenses for dry storage systems or facilities in a Final Safety Analysis Report to support NRC licensing review.

There are a variety of dry storage and/or transportation systems designed by several vendors that have been licensed by the NRC. Representative dry storage and transportation systems are briefly described in Sections 2.1 through 2.4 of this report. Dry storage systems have been approved for either general use or site-specific use. Information about current dry storage system designs approved by the NRC for general use is available from the NCR website [22]. The RAMPAC website [23], which is maintained by the DOE Office of Environmental Management, Packaging Certification Program, provides information about most recent certificates issued by NRC for radioactive material packages as well as safety evaluation reports. A CoC for a spent fuel storage cask certifies that the dry storage design and contents described in the CoC meet the applicable safety standards in 10 CFR Part 72 for dry storage cask systems. A license for a site-specific ISFSI certifies that the dry storage facility meets the applicable safety standards in 10 CFR Part 72 for dry storage facilities. A CoC for radioactive material packages certifies that the packaging and contents described in the CoC meet the applicable safety standards of 10 CFR Part 71.

2.1 Canister-Based Systems

Canister-based SNF dry storage and transportation systems use spent fuel canisters. A canister is typically constructed of stainless-steel alloy and has a thin cylindrical wall (typically 0.5 in. thick), a base plate, and an inner and outer closure lid or closure ring. After SNF assemblies are loaded under water in the reactor spent fuel pool, canisters are drained, vacuum dried, filled with helium, and tested for leakage [24]. The canister constitutes the primary confinement/containment boundary for the radioactive material. More than 50 different welded metal canister designs have been licensed, and most of these canisters are licensed for both spent fuel storage and transportation [25]. Vendors use different names for their spent fuel canister designs. Examples of canister names include multi-purpose canisters (MPCs), dry shielded canisters, and transportable storage canisters. Canister-based dry storage systems include above-ground vertical concrete cask designs (e.g., MAGNASTOR® [26] and HI-STORM FW [27] systems), horizontal storage module designs (e.g., NUHOMS® Horizontal Modular Storage System [28]), and underground vertical ventilated module designs (e.g., the HI-STORM UMAX system [29]). Examples of canister-based transportation packages include the HI-STAR 190 [30], MAGNATRAN [31], and NUHOMS®-MP197 [32] packages. Figure 2-1 shows a 3D model for a canister-based dry storage system.

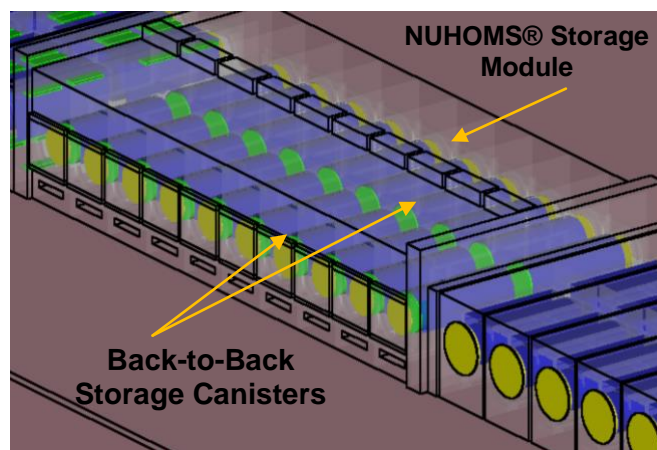


Figure 2-1 3D View of the Geometry Model for a NUHOMS® Storage Module, where Concrete Wall Opacity was Reduced to 20% to Reveal SNF Canisters

2.2 Non-Canistered Spent Fuel Systems

Non-canistered spent fuel storage systems (e.g., CASTOR designs V/21 and X33, MC-10, NAC I28 S/T, TN-32, TN-40, and TN-68) are currently used at five reactor sites [1]. NAC-STC [33] is an example of shipping cask that can be directly loaded with irradiated fuel assemblies. The design of these systems typically features a thick wall of carbon steel (for gamma shielding) surrounding a containment vessel. A basket assembly is placed inside the containment vessel. The containment boundary for these systems typically includes an inner shell and bottom plate, shell flange, and lid outer plate.

2.3 Dual-Purpose Storage and Off-Site Transport Systems

Examples of general use, canister-based, dual-purpose systems include the MAGNASTOR/MAGNATRAN, HI-STORM/HI-STAR, NUHOMS®/MP-197HB or MP-197 systems. For these systems, multiple canister designs can be used with both transportation and storage overpacks. HI-STAR 100 [34,35] is a canister-based dual-purpose storage and transport system. The system consists of the MPC and the HI-STAR 100 overpack. One MPC model for PWR fuel and two MPC models for BWR fuel with identical exterior dimensions are approved for this system. The non-canistered spent fuel storage systems TN-40 [36,37] and TN-68 [38,39] systems are also currently licensed for storage and transportation. The TN-40 cask is designed to store and transport 40 PWR spent fuel assemblies discharged from the Prairie Island Nuclear Generating Plant only.

2.4 Type B Waste Transportation Packages

Type B Waste transportation packages contain radioactive material in the form of solidified materials and waste that are typically packaged in secondary containers, such as filters, resins, scrap metals irradiated in a reactor, and transuranic-containing waste (e.g., 8-120B [40], 10-160B [41], RH-TRU 72-B [42], TRUPACT-II [43], HalfPACT [44], RT-100 [45] and OPTIMUS-L [46]). The contents of these packages may include a broad range of nuclides, geometry configurations, and irradiated non-fuel materials. The radiation source can be concentrated within a small volume or distributed within the packaging cavity volume. Type B waste packaging typically consists of a steel, lead shielded, shipping cask because the waste materials in these packages predominantly emit gamma radiation. Significant neutron sources produced by various means in the waste materials (e.g., spontaneous fission and alpha–neutron reactions) are typically not permitted.

2.5 Regulatory Requirements for Transportation Packages Relevant to Shielding Analyses

Specific dose rate limits for transportation packages under NCT and HAC are provided in 10 CFR 71.47 and 71.51, respectively. A presentation of applicable dose rate limits as a function of transport vehicle and conditions of transport is provided in NUREG-2216 [7], Table 5-2. Spent fuel packages and Type B waste packages often require transport under exclusive use because the dose rates at 1 m from the external surfaces of these packages typically exceed 0.1 mSv/h (10 mrem/h). The dose rate limits specified for the package surfaces are 2 mSv/h (200 mrem/h) for shipments made with an open (flatbed) vehicle and 10 mSv/h (1 rem/h) for closed vehicles and open vehicles with package enclosures such as personnel barriers. Maximum dose rates of 2 mSv/h (200 mrem/h) and 0.1 mSv/h (10 mrem/h) are also required for transport under

exclusive use at locations established as described in 10 CFR 71.47, which depend on the type of exclusive use vehicle. For example, the location of the 10 mrem/h dose rate limit for an exclusive-use closed vehicle is at 2 m from its outer lateral surfaces. Substantial reduction in the effectiveness of the packaging during NCT is not allowed (10 CFR 71.43). Requirements also apply for any normally occupied space unless exposed personnel are expected to wear radiation dosimetry devices in conformance with 10 CFR 20.1502. Under the HAC specified in 10 CFR 71.73, the dose rate limit is 10 mSv/h (1 rem/h) at 1 m from the external surface of the package.

2.6 Regulatory Requirements for SNF, HLW, and GTCC at ISFSIs Relevant to Shielding Analyses

Annual dose limits for any real individual located beyond the controlled area are provided in 10 CFR 72.104(a) for normal operations and anticipated occurrences at the site. These limits include an annual dose equivalent of 0.25 mSv (25 mrem) to the whole body and other annual limits for critical organs. Specific limits for the total effective dose equivalent are provided in 10 CFR 72.106(b) for dose from any design basis accident. The total effective dose equivalent cannot exceed 0.05 Sv (5 rem), and the minimum distance from the various radiation sources present at the site to the nearest boundary of the controlled area must be at least 100 m. Additional requirements in 10 CFR 72.104 concern implementation of operational limits to meet objectives as low as is reasonably achievable for direct radiation levels and radioactive materials in effluents. Thus, the safety analysis must provide information about near-field dose rates produced by dry storage casks.

A dry storage cask design must include confinement structures and systems, as well as components that provide redundant sealing of confinement systems (10 CFR 72.128 and 72.236). These casks are typically designed and tested to be leaktight as defined by the ANSI N14.5 [47] standard. The confinement boundary is to remain leaktight under all conditions [8]. Thus, the annual dose equivalent of 0.25 mSv (25 mrem) to the whole body can be used to establish the location of the owner-controlled area boundary for storage systems with leaktight confinement.

3 SOURCE TERM CALCULATIONS

This section addresses radiation source terms for shielding analyses of Type B transportation packages and SNF storage casks, including SNF radiation sources (Section 3.1), activation sources in PWR NFH (Section 3.2), radiation sources in Type B waste transportation packages (Section 3.3), neutron sources from subcritical multiplication (Section 3.4), and photon sources produced by radiative capture reactions of neutrons with nuclei in surrounding materials (Section 3.5). Source term computer codes and nuclide inventory prediction validations are presented in Section 3.6.

3.1 Spent Fuel

Most SNF dry storage and transportation systems accommodate a variety of assembly types with broad ranges of average fuel assembly burnup, enrichment, and cooling time. To ensure that the intended contents and the storage/package designs comply with regulatory shielding requirements, limiting fuel characteristics and depletion conditions must be identified for use in radiation source term calculations. This section describes the main characteristics of SNF fuel radiation sources used in shielding analyses of SNF transportation packages and dry storage casks and presents approaches for generating conservative radiation sources. Spent fuel must have a cooling time of at least one year to be stored in an ISFSI (10 CFR 72.2).

3.1.1 Neutron Sources

Neutrons are produced in spent fuel by (1) spontaneous fission (SF); (2) (α ,n) reactions with light elements in fuel oxide material; and (3) subcritical multiplication. Neutron sources from SF and (α ,n) reactions are calculated with an isotopic depletion and decay code. The neutron source from subcritical multiplication is discussed in Section 3.3. The overall importance of the neutron source relative to the primary gamma source (see Section 3.1.2) increases with increasing fuel burnup and cooling time [12].

The fractional contributions to the total neutron source strength of neutrons from SF and (α ,n) reactions are illustrated in Figure 3-1 for a Westinghouse (WE) 17 \times 17 fuel assembly. The graph in this figure shows that the (α ,n) contribution decreases as average fuel assembly burnup increases. This contribution increases with increasing fuel cooling time, but the rate of increase significantly decreases as average fuel assembly burnup increases. Table 3-1 shows primary transuranic nuclides that are important to the total SNF neutron source for various cooling time intervals. The transuranic nuclide ^{244}Cm ($T_{1/2}=18.1$ years) is the principal neutron emitter in spent fuel up to approximately 100 years of cooling [9]. For cooling times less than approximately 3 years, ^{242}Cm ($T_{1/2}=162.8$ days) is also an important contributor to the total neutron source [9]. The nuclides ^{238}Pu , ^{239}Pu , ^{240}Pu , and ^{241}Am are important contributors to the neutron source from (α ,n) reactions, which is a significant contribution to the total neutron source primarily for very low burnup and/or longer cooling times, as shown in Figure 3-1. At long cooling times (100 years or longer), ^{238}Pu , ^{239}Pu , ^{240}Pu , and ^{242}Pu , ^{241}Am , and ^{246}Cm are primary neutron source contributors through SF and/or (α ,n) reactions. In UO_2 fuel, $^{17}\text{O}(\alpha,n)^{20}\text{Ne}$ and $^{18}\text{O}(\alpha,n)^{21}\text{Ne}$ reactions are the principal source of neutrons from (α ,n) reactions because of the large amount of oxygen compared with other light elements that might be present in the fuel in trace quantities as impurities. However, nuclides with larger cross sections for neutron production might be present as impurities in the fuel oxide.

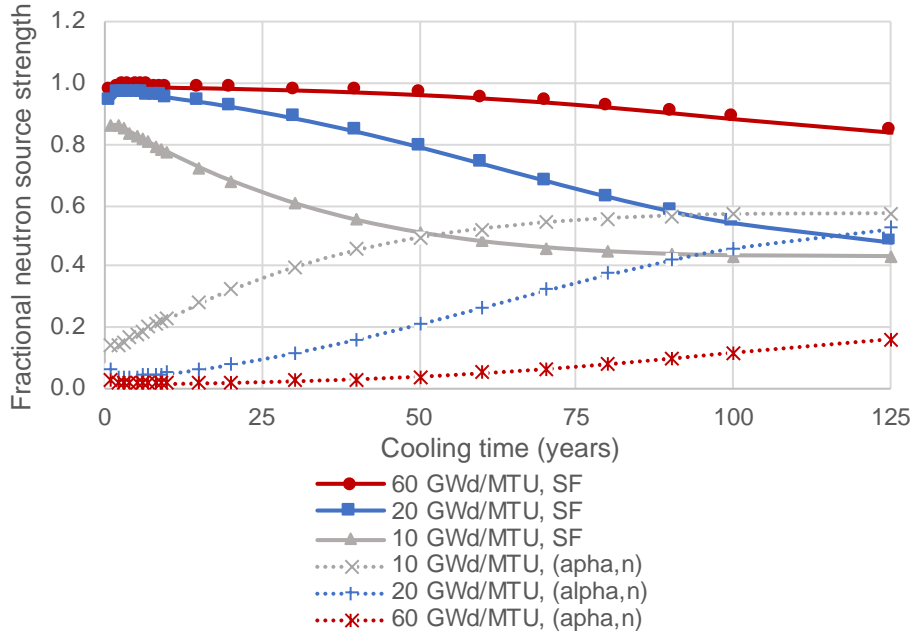


Figure 3-1 Fractional Contributions of Neutrons from SF and (α,n) Reactions to the Total Neutron Source Strength as a Function of Fuel Burnup and Cooling Time: WE 17x17 Assembly

Table 3-1 Primary Nuclides for Source of Neutrons in Spent Fuel

Storage Period	Isotope	Half-life (years)	Primary Nuclear Reaction ^a
1 < t ≤ 3 years	²³⁸ Pu	87.7	(α,n)
	²³⁹ Pu	2.41×10 ⁴	(α,n)
	²⁴⁰ Pu ^b	6.56×10 ³	SF, (α,n)
	²⁴¹ Am	433	(α,n)
	²⁴² Cm	0.446	SF, (α,n)
	²⁴⁴ Cm	18.1	SF, (α,n)
3 < t < 100 years	²³⁸ Pu	87.7	(α,n)
	²³⁹ Pu	2.41×10 ⁴	(α,n)
	²⁴¹ Am	433	(α,n)
	²⁴⁴ Cm	18.1	SF, (α,n)
t > 100 years	²³⁸ Pu	87.7	(α,n)
	²³⁹ Pu	2.41×10 ⁴	(α,n)
	²⁴⁰ Pu	6.56×10 ³	SF
	²⁴² Pu	3.75×10 ⁵	SF
	²⁴¹ Am	433	(α,n)
	²⁴⁴ Cm	18.1	SF
	²⁴⁶ Cm	4.73×10 ³	SF

^aThe neutron source from (α,n) reactions is a significant contribution to the total neutron source primarily for very low burnup (e.g., 10 GWd/MTU) and/or long cooling times

^bThis nuclide is only important for very low burnup (e.g., 10 GWd/MTU)

3.1.1.1 Light Element Impurities in UO₂ Matrix

Light nuclei—such as ^{6,7}Li, ⁹Be, ^{10,11}B, ^{12,13}C, ^{14,15}N, and ^{17,18}O—have large cross sections for neutron production [48,49]. NUREG/CR-6802 [9] indicates that for situations in which the (α,n) contribution to the total neutron source is significant, it is necessary to accurately quantify or establish bounding values for all impurities, especially light elements that are known to produce significant (α,n) quantities. In irradiated nuclear fuels that achieve a moderate-to-high burnup (e.g., > 30 GWd/MTU), the neutron source is typically dominated by ^{242,244}Cm spontaneous fission, but the (α,n) neutron processes can represent a larger component of the total neutron source in low-burnup fuels [50], as illustrated in Figure 3-1 for a WE 17x17 fuel assembly. Publicly available information on impurity concentration levels in LWR fuel was reviewed, and the effects of these impurities on the neutron source from (α,n) reactions relative to pure UO₂ were evaluated in ORNL/SPR-2021/2093 [15]. The reviewed data indicate that the maximum concentrations for H, Li, Be, and B are 1 μg or less per gram of U [51]. The contributions of the bounding values determined for light-element impurities in the UO₂ matrix to the neutron source from (α,n) reactions, as well as to the total neutron source, were calculated for the burnup range 10 to 60 GWd/MTU and cooling times from 1 to 125 years. The neutron source from (α,n) reactions was approximately 15 to 20% higher for the UO₂ composition including light-element impurities compared to the pure UO₂ composition for the entire range of burnups and cooling times evaluated. However, the effects of the bounding light-element impurities on the total neutron strength of the fuel assembly depend on the average fuel assembly burnup and cooling time.

The percentage increase in the total neutron source strength due to bounding light-element impurities is illustrated in Figure 3-2 as a function of burnup and cooling time for a WE 17x17 fuel assembly. The graph shows that these impurities make significant contributions to the total neutron source strength for a fuel assembly with a 10-GWd/MTU burnup value (e.g., up to 8% at a 125-year cooling time). However, this contribution is much smaller for higher average fuel assembly burnup and fuel cooling times less than 40 to 50 years. For example, this contribution is less than 2.5% for average fuel assembly burnup values greater than 20 GWd/MTU and cooling times less than 40 years. It is 1% or less for average fuel assembly burnup values greater than 40 GWd/MTU and cooling times less than 50 years. These calculations showed that the effects of bounding light element impurity concentrations in UO₂ on the total fuel assembly neutron source strength depend on average fuel assembly burnup and cooling time.

Generally, bounding light-element impurity concentrations in UO₂, such as those provided in ORNL/SPR-2021/2093 [15], Table 29, should be included in the fuel material for the purpose of determining neutron source terms. Pure UO₂ compositions may be used with proper justification. For example, the (α,n) source produced by bounding light-element concentrations in UO₂ would have a negligible contribution to the total dose rate, if the total dose rate is dominated by the gamma dose rate, average fuel assembly burnup values are greater than 20 GWd/MTU and fuel cooling times are less than 40 years.

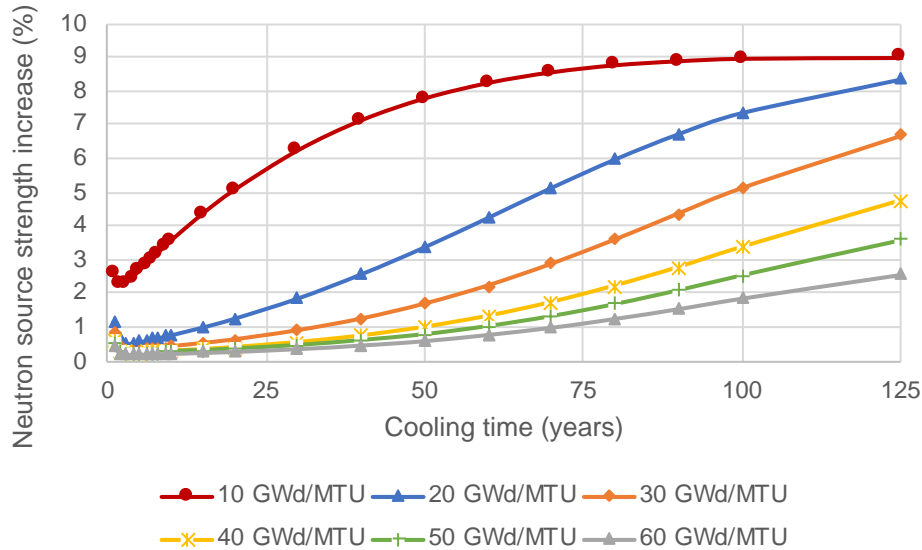


Figure 3-2 Percentage Increase in the Total Neutron Source Strength Due To Bounding Light Element Impurities in UO₂ Matrix as a Function of Fuel Burnup and Cooling Time: WE 17x17 Fuel Assembly

3.1.2 Photon Sources Originating in Irradiated Fuel

The main photon sources in irradiated fuel consist of gamma rays from radioactive decay. The principal gamma emitters in spent fuel include fission products and/or their daughter products ¹⁴⁴Ce ($T_{1/2}=284.89$ days)/¹⁴⁴Pr ($T_{1/2}=17.29$ min), ¹⁰⁶Ru ($T_{1/2}=1.02$ years)/¹⁰⁶Rh ($T_{1/2}=2.18$ hours), ¹³⁴Cs ($T_{1/2}=2.0652$ years), ¹⁵⁴Eu ($T_{1/2}=8.593$ years), and ¹³⁷Cs ($T_{1/2}=30.1$ years)/^{137m}Ba ($T_{1/2}=2.6$ min). Beta particles from fission product decay—such as ⁹⁰Sr ($T_{1/2}=28.78$ years)/⁹⁰Y ($T_{1/2}=64$ hours)—that are decelerated in the Coulomb field of nuclei produce bremsstrahlung radiation (see Section 3.1.3). Insignificant gamma sources are produced by other processes within the fuel, such as spontaneous fission and (α ,n) reactions [12]. Low-intensity gamma rays above approximately 4 MeV in spent fuel spectrum are entirely produced by spontaneous fission [12]. Photon sources originating in irradiated fuel are typically referred to as *primary gamma source* to differentiate it from the secondary gamma source that results from neutron capture reactions with nuclei within packaging materials and other surrounding materials such as air and soil. The importance to external dose rate of each gamma emitter fission product depends not only on its concentration in the SNF composition, but also on its gamma-ray energies and emission probabilities [52]. The overall importance of the primary gamma source relative to the neutron source decreases with increasing fuel burnup and cooling time [12]. The primary production paths and cumulative thermal fission yields [52] of the radionuclides important to gamma dose rates are summarized in Table 3-2.

Table 3-2 Summary Information for Main Beta and Gamma Radiation Emitters in Spent Fuel

Radionuclide	Half-life	Primary production path	Cumulative thermal fission yield from ²³⁵ U (%)	Cumulative thermal fission yield from ²³⁹ Pu (%)
¹⁴⁴ Ce	284.89 days	Fission	5.474	3.75
¹⁰⁶ Ru	1.02 years	Fission	0.41	4.188
¹³⁴ Cs	2.0652 years	¹³³ Cs thermal capture	6.60	6.99
¹⁵⁴ Eu	8.593 years	¹⁵³ Eu thermal capture	0.1477	0.38
⁹⁰ Sr	28.78 years	Fission	5.73	2.013
¹³⁷ Cs	30.1 years	Fission	6.221	6.588

3.1.3 Bremsstrahlung Radiation

Bremsstrahlung radiation is produced by electrons and positrons from radioactive decay decelerating in the Coulomb field of nuclei. However, only a fraction of their energy is converted to bremsstrahlung radiation. The fraction of the initial energy of a beta particle that is converted to bremsstrahlung, known as *radiation yield*, increases as the atomic number of the absorber material increases [53]. The radiation from bremsstrahlung has a continuous-energy spectrum, with a maximum (end point) energy given by the maximum energy of these electrons and positrons. Most pure beta emitters have end point energies of less than 300 keV and would probably be entirely absorbed in waste and shielding materials [54]. However, ⁹⁰Y, ³²P, ²⁰⁴Tl, and ⁴⁵Ca have much higher end point energies (i.e., 2.27, 1.71, 0.766, and 0.714 MeV, respectively), and their bremsstrahlung radiation may contribute to the external cask dose rate. For SNF, the percentage contribution of bremsstrahlung radiation to the total photon dose rate was estimated to be up to 10–20% [55], depending on gamma shielding thickness, fuel assembly burnup, cooling time, and dose point location.

3.1.4 Activation Gamma Sources

Activation gamma sources consist of photons from decay of activation products in fuel assembly hardware. Cobalt-60 is primarily produced by thermal and epithermal capture reactions in ⁵⁹Co, which is an impurity in fuel hardware and NFH materials, and reactor pressure vessel and other internal structural materials (typically steel and nickel-based alloys). The neutron irradiation of iron isotopes is also a well-known ⁶⁰Co production pathway. However, the production of ⁶⁰Co through activation of iron isotopes is much lower than the activation of ⁵⁹Co impurity because of differences in neutron capture cross sections between the iron isotopes and cobalt [56]. Therefore, only the ⁶⁰Co source from activation of ⁵⁹Co impurity is typically included in activation source terms. Previous studies [9] identified ⁶⁰Co (T_{1/2}=5.271 years) as a major contributor to external package dose rate because of its energetic decay gamma rays of 1.173 MeV and 1.333 MeV with close to 100% abundance. Other activation products in irradiated steel and Inconel alloys, such as ⁵⁹Fe (T_{1/2}=44.503 days), ⁵⁸Co (T_{1/2}=70.86 days), and ⁵⁴Mn (T_{1/2}=312.3 days), are primarily important to shielding at cooling times less than 2 years [14].

3.1.4.1 Cobalt Impurity Concentrations in Fuel Hardware and NFH Materials

As discussed in Section 3.1.4, cobalt activation sources in fuel hardware and NFH materials can significantly contribute to total external dose rates. However, significant uncertainty is

associated with this source term component, primarily because the actual cobalt impurity concentrations in hardware materials such as steel and Inconel alloys are generally unknown. Properties of alloys are specified by various material standards, such as American Society of Mechanical Engineers standards. However, concentration limits of trace elements are not specified in these standards, and the manufacturer is not required to report them.

A review of publicly available information about cobalt impurity concentrations in stainless steel and Inconel alloys is documented in ORNL/SPR-2021/2093 [15]. Almost all this information is dated 1992 or older. This old information indicates that the typical cobalt impurity concentration in stainless steel would be 0.1 wt % or less [9] (e.g., 800 ppm [57]). Limited new information exists about actual cobalt impurity concentrations for nuclear applications. Many nuclear utilities have implemented cobalt reduction plans—where high cobalt contributors in primary power plant systems have been identified and replaced [58]—because high concentrations of this impurity in contact with the coolant are undesirable. Therefore, it is expected that newer fuel assembly designs contain lower cobalt impurity than older designs. Lower cobalt impurity concentrations in stainless steel and nickel-based alloys can be requested, to the extent practicable, for nuclear applications. There are indications based on proven technology of 40 years of commercial U.S. and international LWR experience that the cobalt impurity can be specified as 0.05 wt % maximum and values as low as 0.02–0.03 wt % are achievable for stainless steel and nickel-based alloys [59]. Therefore, the cobalt impurity concentration in the hardware materials of newer fuel assemblies could be significantly lower than those of older assemblies. Where available, cobalt impurity concentrations in fuel hardware and NFH materials based on plant records may be used in site-specific shielding analyses. The use of actual cobalt impurity concentrations in place of a bounding concentration value is especially important for short cooling times to avoid using excessive shielding material for overpack design. However, the importance of ^{60}Co production from neutron capture in iron isotopes might increase relative to the ^{60}Co production from the activation of the cobalt impurity and would have to be included in the total ^{60}Co activity.

3.1.4.2 ORIGEN Scaling Factors for Hardware Regions that Are Outside the Fueled Region of the Reactor

SNF top and bottom hardware as well as many NFH components are not located within the fueled region during reactor operation. The neutron flux at these axial locations cannot be calculated with a 2D depletion code; therefore, a different method of calculation is required. A very popular method because of its simplicity consists of neutron flux adjustments based on flux scaling factors, as discussed in NUREG/CR-6802 [9]. For example, PNL-6906 Vol. 1 [60] provides flux scaling factors that were empirically derived from laboratory analyses of 38 samples of activated hardware from different SNF assembly types. Flux scaling factors were also evaluated in ORNL/SPR-2021/2093 [15] using a Monte Carlo N-Particle (MCNP) [61] detailed geometry model of a WE 17×17 core that was developed based on Virtual Environment for Reactor Applications benchmark specifications [62]. The calculation specified a neutron fission source with Watt energy spectrum and uniform spatial distributions. Therefore, the fission source spatial distribution is conservative with respect to the neutron flux in the fuel hardware regions because the axial neutron leakage is neglected in this model. The maximum flux scaling factors for the lower end fitting, gas plenum, and upper end fitting assembly regions were approximately 0.22, 0.22, and 0.05, respectively, which are approximately the same as the flux scaling factors provided in PNL-6906 Vol. 1. Although this calculation is limited to a WE 17×17 core, it confirms that the PNL-6906 flux scaling factors are adequate for conservative activation source estimations.

3.1.5 Burnup, Enrichment, and Cooling Time for SNF Source Terms Calculations

Main SNF assembly parameters used in source term calculations include fuel assembly type, the amount of heavy metal in a fuel assembly, fuel initial enrichment, assembly average burnup, and cooling time [63], as well as parameters related to fuel assembly irradiation conditions (see Section 3.1.6). The guidance in NUREG-2215 and NUREG-2216 indicates that bounding source terms should be used in shielding analyses and that the fuel assembly minimum initial enrichment, maximum burnup, and minimum cooling time are more appropriate for use as loading controls and limits. Previous parametric studies [9,10,16] have clearly shown that SNF neutron source strength—and consequently the neutron and secondary gamma dose rates—significantly increase with decreasing fuel enrichments at a fixed burnup. An increase of the fuel initial enrichment causes an increase of the ^{235}U absorption rate, a decrease of the absorption rates of other nuclides, a reduction of the thermal neutron flux, and hardening of the neutron spectrum. Fuel with higher enrichment will need lower neutron flux to achieve the same power density compared with fuel with lower enrichment. As the fuel initial enrichment decreases at a fixed burnup, the net effect is an increase of minor transuranic actinides [64], including main neutron emitters ^{244}Cm and ^{242}Cm . The increase of the neutron source is most pronounced when fuel is irradiated well beyond a typical discharge burnup as determined by the initial fuel enrichment. Therefore, technical specifications for canister contents have sometimes imposed a minimum fuel enrichment to limit the magnitude of the neutron source and reduce the overall conservatism [10].

However, fuel initial enrichment variations have a more complex effect on the primary gamma source terms, albeit less pronounced, than these variations' effect on the neutron source terms. The production rates of main gamma emitters depend on the relative concentrations of the fissile nuclides in the SNF composition and the decay characteristics of the gamma emitters. Fission products ^{144}Ce and ^{90}Sr have larger cumulative fission yields from ^{235}U compared with those from ^{239}Pu . The production of these fission products is expected to increase with increasing fuel initial enrichment due to a higher ^{235}U fission rate associated with higher initial fuel enrichment. Fission product ^{106}Ru has a larger cumulative fission yield from ^{239}Pu compared with that from ^{235}U , and the primary production paths for ^{154}Eu and ^{134}Cs are ^{153}Eu and ^{133}Cs thermal captures. The production of these fission products, as well as that of the ^{60}Co activation source, is expected to increase with decreasing fuel initial enrichment. The production of ^{137}Cs has a weak dependence on the fissile mixture in the fuel, based on its cumulative fission yields from fissile nuclides. The primary gamma source strength/external gamma dose rate was shown to increase with decreasing fuel initial enrichment for a 5-year cooling time [10,9]. However, the external gamma dose rate produced by primary gamma sources might actually increase with increasing initial fuel enrichment for longer cooling times, as shown in Figure 3-3 for a simplified concrete cask model which consists of PWR fuel surrounded by a 65-cm thick concrete shield [16]. Therefore, the initial fuel enrichment used in primary gamma source calculations should be justified, primarily for systems whose external dose rate is dominated by primary gamma dose rates or for combinations of burnup, enrichment, and cooling time that produce external dose rates close to regulatory dose rate values. The overall importance of the primary gamma source relative to the neutron source decreases with increasing fuel burnup and cooling time [12].

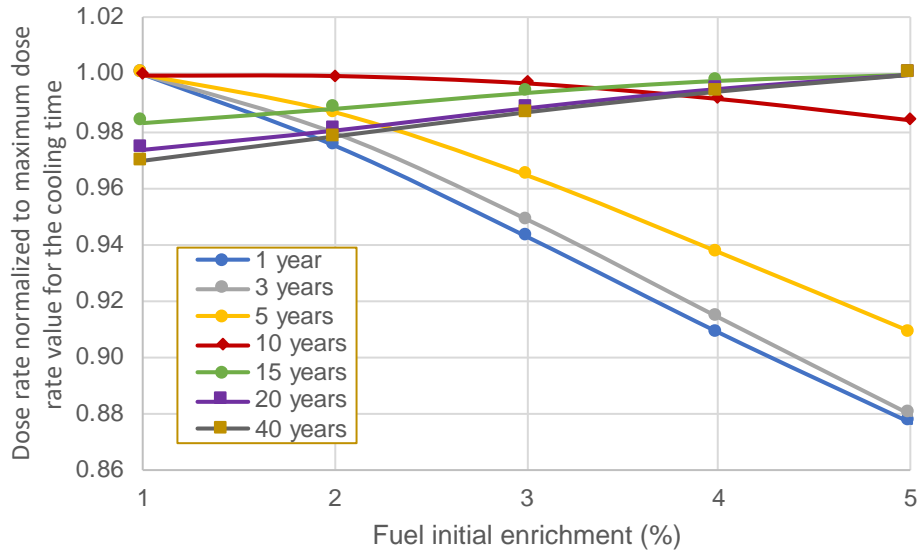


Figure 3-3 Trends of External Dose Rate Variation with Fuel Initial Enrichment for Various Fuel Cooling Times

3.1.5.1 Fuel Qualification Tables (FQTs)

A design-basis fuel assembly (i.e., single limiting condition) can be determined by performing an analysis of the SNF assemblies to be loaded and identifying SNF assembly characteristics that are bounding with respect to radiation source terms/external dose rates. This approach is suitable for site-specific shielding analyses. However, for systems dedicated to general use, another approach is typically used in license application submittals, which consists of defining a series of limiting conditions as multiple combinations of burnup, enrichment, and minimum cooling time. This approach offers much more flexibility than the single limiting condition with respect to fuel loading management because it readily identifies main characteristics of the fuel assemblies permitted to be loaded in canisters based on regulatory dose rate constraints. However, this approach significantly increases the complexity of shielding calculations and reviews. Further increasing the complexity of content specifications, a “zoning approach” has been used that specifies spent fuel of different characteristics for different zones of the cask radial cross section, which might also depend on fuel assembly type. The combinations of burnup, enrichment, and minimum cooling time permitted for loading are typically specified in an FQT. Previous analyses [9] have shown that neutron source strength increases with decreasing initial fuel enrichment at a fixed burnup; thus, the initial enrichment values for each burnup would be bounded by a minimum initial enrichment. Reasonably bounding minimum enrichment values for fuel assemblies on the burnup–cooling time curve are desirable to avoid unrealistic and excessively conservative initial enrichment values with respect to cask external dose rates.

To develop FQTs, an entirely different shielding analysis method is more practical than explicit calculations. The method requires many shielding calculations to determine cask external dose rate values for each source type (i.e., primary gamma, neutrons, secondary gamma, and the ⁶⁰Co activation source in irradiated fuel hardware), spatial region within the cask where source particle originates, and source particle energy group. Typical distinct spatial regions include the radial location of the fuel assembly in the basket, the axial zones of the active fuel in each fuel

assembly, where the number of the axial zones is dictated by the axial burnup profile specification, and assembly hardware regions. These dose rate values for each type of source, also known as *response functions*, are subsequently multiplied by the source strengths calculated for each energy group, and then the product values are summed over all energy groups and spatial regions to calculate the actual total dose rate at locations of interest external to the storage cask or transportation system that is analyzed. The method is also known as *on-the-fly*, referring to the speed of the calculation for the last step of the method [65], which can be implemented with spreadsheet applications or dedicated scripts. The response functions are typically generated for a specific fuel assembly model.

It is recommended that the method used to generate FQTs be described in full detail and that the most limiting combinations with respect to external cask dose rate of assembly enrichment, assembly average burnup, and minimum cooling time be identified in FQTs. Verification of the method should also be demonstrated in the shielding analysis by comparisons to explicit shielding calculations for selected combinations of fuel assembly minimum initial enrichment, average burnup, and cooling time.

3.1.6 Source Term Sensitivity to Depletion Parameters

Specific fuel assembly depletion conditions are generally not known, but a set of depletion parameters that are conservative with respect to radiation source terms may be specified in depletion calculations. Dose rate and/or nuclide concentration sensitivities to various depletion parameters have been analyzed in NUREG/CR-6802 [9] and NUREG/CR-6716 [10], and more recently in ORNL/SPR-2021/2373 [16] for PWR and BWR fuel with increased enrichment and higher burnup. For fuel with increased enrichment and higher burnup, the initial fuel enrichment would be increased up to 10% ^{235}U , which would enable an assembly burnup up to 75 GWd/MTU [66]. The parametric studies have shown that the neutron source terms are more sensitive to changes in depletion parameter values than primary gamma and ^{60}Co source terms. The neutron source terms, and consequently neutron and secondary gamma dose rates, increase with (1) increasing specific power; (2) increasing fuel temperature; (3) decreasing fuel density at a fixed heavy metal mass per fuel assembly; (4) decreasing moderator density; and (5) increasing soluble boron concentration (PWR fuel only) for a given burnup and cooling time. The primary gamma and ^{60}Co sources either exhibit similar trends as the neutron source terms or have negligible sensitivities to changes in these depletion parameter values. Therefore, a set of specific power, fuel temperature, fuel density, moderator density, and soluble boron concentration (PWR only) values that produce a conservative neutron source term would also produce conservative gamma radiation source terms.

Specific power affects the rate at which fission products are produced from fission events. The equilibrium level of unstable nuclides where the decay rate approaches the production rate is directly proportional to the specific power. The neutron flux increases with increasing specific power. Neutron energy spectrum hardening is also caused by an increase in the specific power [67]. The concentrations of the principal gamma and neutron emitters presented in Section 3.1 increase with increasing specific power for a fixed burnup. Therefore, a higher specific power value is more conservative than a lower specific power value with respect to SNF shielding analyses.

By increasing moderator density, the thermal flux is increased, the thermal absorption reactions are increased, and the resonance absorption reactions are decreased, causing lower ^{239}Pu and transplutonium nuclide production rates. Neutron, ^{60}Co , and primary gamma source strengths decrease with increasing moderator density (PWR) or decreasing void fraction (BWR).

Fuel temperature increase has a broadening effect on the resonance capture cross section of fertile nuclides (e.g., ^{238}U and ^{240}Pu), which increases the probability of neutrons with energies near resonances to be captured in the fuel pellet. Therefore, this effect is accompanied by slightly higher concentrations of transuranic nuclides compared to lower fuel temperature values as well as hardening of the neutron energy spectrum. Insignificant effects were observed on the primary gamma and ^{60}Co source strengths due to fuel temperature variations.

Neutron absorption probability is higher near the outer surface of the fuel pellet as compared to the inner region of the pellet (i.e., spatial self-shielding), especially for high burnup values, resulting in higher local burnup and density of transuranic nuclides at the radial outer edge of the fuel pellet. A higher fuel density will increase epithermal neutron resonance absorptions at the radial outer edge of the fuel pellet and decrease these absorptions within the inner pellet region at fixed burnup. A negligible overall effect was determined for primary gamma, neutron, and ^{60}Co source terms due to perturbations in fuel density at fixed burnup and heavy metal content [16].

Neutron absorption by boron diluted in PWR coolant results in hardening of the neutron energy spectrum, increased resonance captures in fertile nuclides (e.g., ^{238}U and ^{240}Pu), and increased production of transuranic nuclides. Therefore, the neutron source strength increases with increasing average soluble boron concentration in coolant. For PWR fuel with increased enrichment and higher burnup, there is an increase of the primary gamma and ^{60}Co source strengths with increasing average soluble boron concentration in coolant, but the effects of boron concentration changes on these parameters are smaller than those observed on the neutron source strength.

Previous parametric studies [10,16] also have shown that fuel radiation source terms are affected by fuel assembly exposures to integral and discrete burnable absorbers. The effects of integral burnable absorber on the neutron and gamma dose rates, which were analyzed in NUREG/CR-6716 [10], depended on fuel burnup for the neutron dose rate. As compared to pure UO_2 fuel, the neutron dose rate was higher at low burnup (e.g., 20 GWd/MTU) and approximately the same at high burnup (e.g., 60 GWd/MTU) for fuel with integral absorber. These effects were negligible for the gamma dose rate. A variety of discrete burnable absorbers are used during reactor operation (see Section 3.2). Both thermal neutron absorption in discrete absorbers and moderator displacement by these discrete absorbers result in hardening of the neutron energy spectrum, which increases resonance neutron captures in fertile nuclides (e.g., ^{238}U and ^{240}Pu) and production of transuranic nuclides. The analyses presented in ORNL/SPR-2021/2373 [16] analyzed the effects of BPRs on PWR source terms and the effects of control blades on BWR source terms. The neutron sources of fuel assemblies exposed to BPRs or control blades are significantly higher than the neutron sources of fuel assemblies with no such exposures, but the effect of exposure on the neutron source diminishes with increasing fuel assembly burnup. The BPR and control blade exposures have small or negligible effects on the primary gamma source terms. The ^{60}Co activation source will be slightly higher for PWR fuel assemblies with no exposure to BPRs and significantly higher for BWR fuel assemblies with no exposures compared to fuel assemblies exposed to control blades. Therefore, opposite trends of variation for the neutron and ^{60}Co activation sources were obtained by using fuel assembly models that simulate fuel assembly exposures to BPRs and control blades, compared to plain fuel assembly models.

3.1.7 Relationships between Decay Heat and External Dose Rates

The spent fuel canister loading limits for dry storage tend to be imposed by fuel cladding temperatures and related thermal loading limits, whereas for subsequent off-site transportation, the loading limits tend to be imposed by the 2 m external dose rate limits. Decay heat has been suggested as a single surrogate for the radiation source term [68] because assembly radiation source terms and decay heat are related in that these physical quantities result from decay of radionuclides in SNF. Moreover, the sets of nuclides identified as important to decay heat and radiation source terms are almost identical [9]. However, the physical processes responsible for decay heat and radiation source terms are relatively different. Decay heat is primarily produced by energy deposition in the fuel material by charged particles, including alpha particles from actinide nuclide decay, beta particles from fission product decay, and recoil nuclei. Radiation source terms primarily consist of photons and neutrons (i.e., indirectly ionizing radiation) from radioactive decay, spontaneous fission, and activation. In addition, the neutron source from subcritical multiplication (see Sections 3.4 and 4.2.2.2.1) depends on the fuel composition (typically fresh fuel) specified in the shielding model, which is unrelated to decay heat.

Nuclides that have important contributions to decay heat but either negligible or small contributions to radiation source terms, depending on fuel assembly burnup and cooling time, are ^{90}Sr ($T_{1/2}=28.78$ years), ^{90}Y ($T_{1/2}=64$ hours), and ^{238}Pu ($T_{1/2}=87.7$ years). The two successive beta decays of ^{90}Sr and its short-lived daughter ^{90}Y release a total energy of 2,736 keV and no accompanying gamma rays. However, the bremsstrahlung radiation (see Section 3.1.3) associated with $^{90}\text{Sr}/^{90}\text{Y}$ beta decay does contribute to the gamma source terms [14]. The contribution of ^{238}Pu to assembly decay heat significantly increases with fuel assembly burnup and cooling time, but this nuclide only has modest contributions to cask external dose rate at long cooling times [9]. In addition, ^{60}Co ($T_{1/2}=5.27$ years), primarily an activation product of the cobalt impurity in fuel hardware and NFH materials, can be a major contributor to dose rate depending on fuel cooling time, but it is only a minor contributor to decay heat [9].

As indicated in NUREG-2215, some applications may provide a bounding decay heat load (kilowatt per assembly) without specifying details about the SNF (e.g., design, enrichment, cooling time), but a significant variety of fuel assembly average burnup, enrichment, and cooling time combinations can result in a given amount of decay heat. Similarly, different combinations of fuel assembly average burnup, enrichment, and cooling time can produce the same maximum external cask dose rate values. ORNL performed a study on the relationship between dose rate and decay heat for spent nuclear fuel casks, which is documented in ORNL/SPR-2020/1441 [13]. In this study, dose rates were evaluated for 198 cases, which included various SNF systems (i.e., storage, transfer, and transport), SNF characteristics (e.g., fuel types, burnup, cooling time), and loading maps (e.g., uniform loading, zone loading) while a constant decay heat was maintained. The results of this study showed that a given decay heat does not correspond to a unique dose rate for a variety of fuel characteristics and package designs. The large variation in dose rates for a constant decay heat indicates that casks loaded based on decay heat—that is, allowing any burnup, cooling time, and enrichment combinations that yield the qualified decay heat limit(s)—cannot ensure that an ISFSI or a spent fuel transportation package will meet the regulatory limits set forth by the respective regulations (10 CFR 72 or 10 CFR 71).

Another analysis of actual canister heat loadings and the dose rate at 2 m from the lateral surface of the vehicle for five MPC-68s [35], which was performed with Used Nuclear Fuel-Storage, Transportation & Disposal Analysis Resource and Data System (UNF-ST&DARDS) [69], showed that the dose rate could be more limiting than the heat loading with respect to

regulatory requirements. The decay heat of the individual SNF assemblies within five canisters evaluated for year 2020 was lower than the assembly decay heat limit of 272 W for the MPC-68, as illustrated in Figure 3-4. However, four packages exceeded the regulatory dose rate limit of 10 mrem/h in 2020, and one package did not, as seen in the figure. This study shows that canister loadings complying with maximum decay heat can produce external dose rates higher than regulatory dose rate limits for transportation.

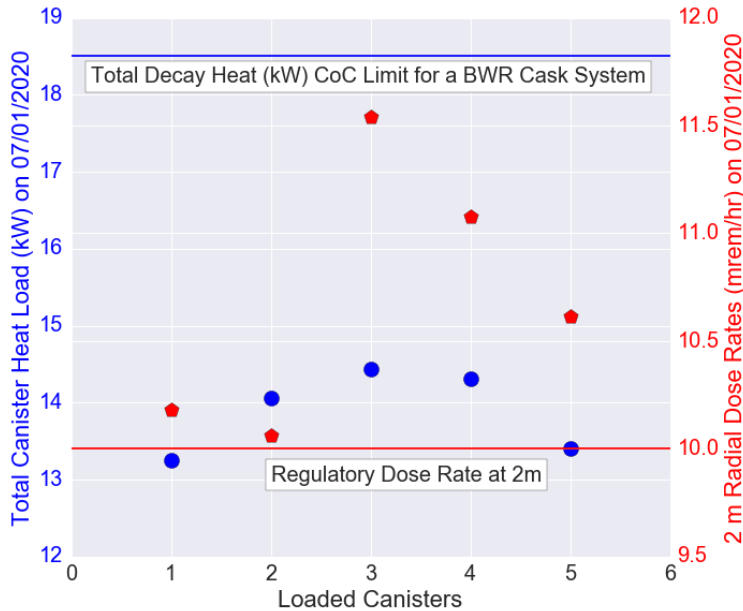


Figure 3-4 Canister Heat Loading and 2 m Radial Dose Rate

Although decay heat may be a limiting parameter for canister loadings, fuel assembly decay heat specifications should not replace FQT specifications (i.e., combinations of fuel assembly minimum initial enrichment, average burnup, and cooling time) as specifications for shielding analyses. This is especially important for transportation packages because the loading limits tend to be imposed by the 2 m external dose rate limits. As noted above, cask loadings based on decay heat cannot ensure that an ISFSI or a spent fuel transportation package will meet regulatory dose limits.

3.1.8 Axial Burnup Profiles

SNF assemblies exhibit axial burnup distributions that are important to shielding designs and analyses. The guidance in NUREG-2215 and NUREG-2216 indicates that an analysis of the effects of axial burnup profiles with significant axial peaking on gamma and neutron source terms should be available in the applicant's submittals, and these effects should be appropriately treated. Current reactor core operating limits include rod-averaged burnup values of approximately 62 GWd/MTU [70].

An axial burnup profile depends on reactor type (i.e., PWR versus BWR), fuel design (i.e., fuel with or without low enriched or unenriched axial blankets [7,15]), assembly average burnup (i.e., low burnup versus high burnup), and operation conditions (e.g., degree of exposure of fuel assemblies to control rods). Typically, the BWR fuel has a higher ratio of peak pellet average burnup to peak assembly average burnup than the PWR fuel with the same batch-average

burnup. For example, ratio values provided for BWR and PWR fuel assemblies with a batch-average burnup of 45 GWd/MTU [71] were approximately 1.3 and 1.16, respectively.

Typically, the most limiting dose rate for transportation packages is the radial dose rates at 2 m from the lateral surface of the transportation vehicle (see Section 3.1.7). Therefore, axial burnup profiles with high peaking factors (i.e., the ratio between the maximum and average values of the burnup profile) are bounding with respect to the radial dose rates of transportation packages because the SNF radiation source strength increases with increasing burnup. Examples of bounding PWR and BWR SNF axial burnup profiles with respect to radial dose rates are available in ORNL/SPR-2021/2093 [15]. These profiles were obtained from nonproprietary data [72,73] and may be used in shielding analyses.

A previous axial blanket demonstration program [74] showed that a PWR blanketed fuel assembly had an increase in assembly axial power peaking of 12.2% at beginning of life and 6.8% at 325 effective full power days relative to non-blanketed fuel (i.e., the increase in axial power peaking decreases with increasing burnup and irradiation time). The selected PWR axial burnup profiles in ORNL/SPR-2021/2093 [15] are from blanketed WE fuel assemblies. These profiles bound the axial burnup profiles of non-blanketed PWR fuel assemblies, that is, they are conservative with respect to external radial dose rates. The bottom half of a BWR fuel assembly typically achieves higher burnup than the upper half. However, a more uniform axial burnup profile is achieved with increasing assembly average burnup. The BWR axial burnup profiles in the analyzed database are representative of BWR blanketed and non-blanketed fuel assemblies, but no specific information about BWR fuel assemblies with partial length fuel rods is indicated in the data [73]. However, the axial burnup profiles of BWR fuel assemblies with partial-length fuel rods are expected to be flatter than the axial burnup profiles of BWR fuel assemblies with full-length fuel rods because partial-length fuel rods and inner channels are used in current BWR fuel assemblies to achieve a more homogeneous burnup distribution in the fuel [75]. Axial burnup profiles with significant axial peaking for PWR and BWR fuel assemblies are illustrated in the graphs presented in Figure 3-5 and Figure 3-6, respectively.

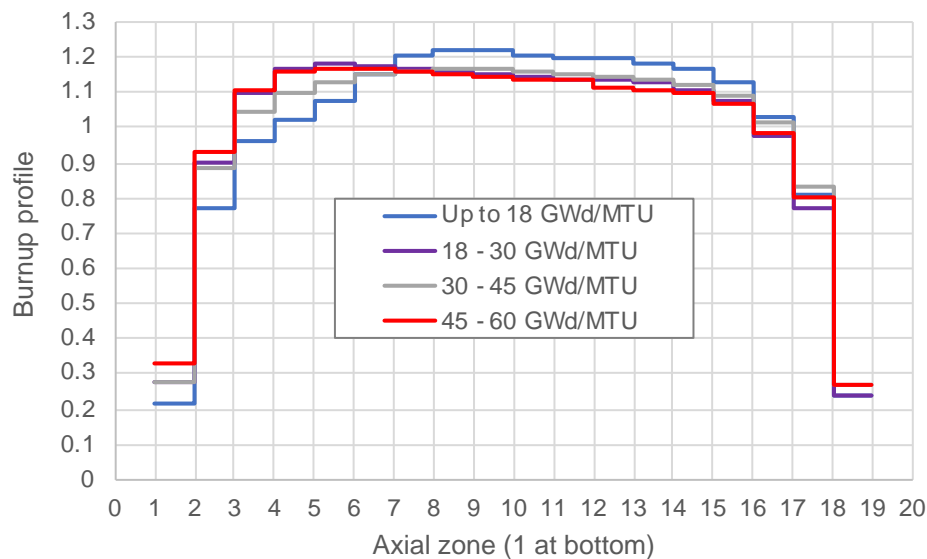


Figure 3-5 Axial Burnup Profiles with Significant Axial Peaking for Various Ranges of PWR Fuel Assembly Burnup

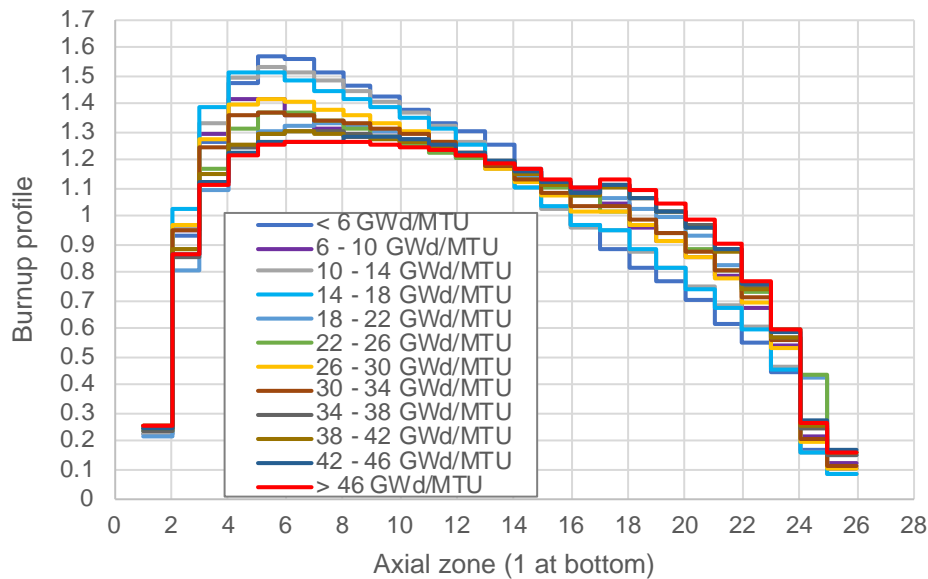


Figure 3-6 Axial Burnup Profiles with Significant Axial Peaking for Various Ranges of BWR Fuel Assembly Burnup

3.1.9 Activation Sources in the Stainless-Steel Replacement Rods of Reconstituted Fuel

Substitutions of zirconium alloy or solid stainless-steel filler rods are allowed for fuel rods that are found to be leaking during a refueling outage or could be sources of future leakage [76], if justified by cycle-specific reload analyses. The 2013 GC-859 survey [63] reported that approximately 850 fuel assemblies contained replacement rods as of 2013. Based on the survey data, these fuel assemblies contained fewer than 10 replacement rods. Depending on the actual number of replacement stainless-steel rods within a fuel assembly, assembly cooling time, and the location of the fuel assembly in the fuel basket (i.e., either peripheral or inner location), activation sources in irradiated steel could significantly increase external dose rates. The effects of stainless-steel replacement rods in reconstituted fuel assemblies on the external dose rate for a generic storage cask model are discussed in Section 4.2.2.2.3. Other fuel assemblies that might contain irradiated stainless-steel rods, such as the Shielding Fuel Assembly used in WE power reactors to reduce neutron fluence in the reactor vessel [77], are not analyzed herein.

3.2 Non-Fuel Hardware for PWRs

Nuclear power reactors use various components to control core reactivity and power distribution. These components, identified as NFH herein, are not an integral part of the fuel assembly. However, irradiated PWR NFH rods are usually inserted into the guide tubes of PWR SNF assemblies that are loaded in canisters for storage. Therefore, activation sources in irradiated NFH might have significant contributions to dry storage cask/transportation package external radiation dose rates. Generally, limits may be imposed on the number, basket locations, or cooling time of irradiated NFH to reduce their effects on external dose rates.

PWR NFH, including but not limited to control rod assemblies, axial power shaping rod assemblies (APSRAs) used in Babcock & Wilcox (B&W) reactors, burnable poison rod assemblies (BPRAs), neutron source assemblies, and thimble plug devices (TPDs), exhibit a wide range of physical and irradiation characteristics. Typical NFH activation sources include gamma radiation from ^{60}Co decay, primarily an activation product of the cobalt impurity in steel and Inconel alloys, and activation products in other materials such as the In-Cd-Ag alloy used in control rods. Summary information on NFH physical characteristics and operating conditions is provided in ORNL/SPR-2021/2093 [15]. This information was gathered from publicly available documents dated 1992 or older and may be used to generate NFH activation sources.

BPRs are inserted into the guide tubes of a PWR fuel assembly during full-power operations, but the BPR is typically removed after one irradiation cycle. The burnable absorber in BPRs typically consists of $\text{Al}_2\text{O}_3 - \text{B}_4\text{C}$ pellets or $\text{B}_2\text{O}_3 - \text{SiO}_2$ (Pyrex glass), and the cladding is either Zircaloy (e.g., BPR in B&W reactors and Wet Annular Burnable Absorber assemblies in WE reactors) or stainless steel (e.g., Pyrex Burnable Absorber Assembly in WE reactors). The BPR with steel cladding is often chosen as the design basis NFH in shielding analyses because BPRs are fully inserted during full-power operation, and the axial extent of BPRs is almost the same as that of the active fuel region. Therefore, the entire length of BPRs is exposed to the neutron flux within the active fuel region during operation. The BPR activation source for shielding analyses consists of ^{60}Co .

Other NFH have shorter rods than BPRs or may only be partially inserted during full-power operations. For example, TPDs (WE power reactors) and orifice rod assemblies (ORAs) (B&W power reactors) are inserted into empty burnable poison locations above the active fuel region, effectively blocking the flow of coolant through empty guide tubes. Therefore, ORAs/TPDs are exposed to the neutron flux within assembly gas plenum and upper end fitting axial regions. An estimated ORA/TPD exposure lifetime of 20 years during multiple cycles of operation is provided in DOE/RW-0184-R1 [78]. The ORA/TPD activation source for shielding analyses consists of ^{60}Co . Therefore, irradiated ORA/TPD stored inside SNF assemblies have the potential to significantly increase external dose rate near the upper regions of a dry storage cask—for example, where duct penetrations through the concrete shield typically exist.

Available data on PWR control rod assemblies indicate that they are either fully withdrawn at all times or mostly withdrawn during full-power operations. For example, a spent rod cluster control assembly was discharged after 12 cycles and 102,767 hours of service from the WE PWR Point Beach 1 power reactor, and measurements/analyses were performed for samples taken from activated metal, as documented in PNL-10103 [79] and NUREG/CR-6390 [80]. The tip, which was nearest the core, was highly activated, but the activation dropped off to negligible levels beyond a short distance less than 2 ft from the core. NUREG/CR-6390 indicates that the predominant radionuclides in irradiated In-Cd-Ag rods are $^{108\text{m}}\text{Ag}$, $^{110\text{m}}\text{Ag}$, and ^{60}Co , and the concentration of $^{108\text{m}}\text{Ag}$ in the In-Cd-Ag alloy is comparable to the ^{60}Co in the stainless-steel cladding on a per gram basis at 10 years after removal from service. The radionuclide $^{108\text{m}}\text{Ag}$ ($T_{1/2}=438$ years) decays mainly by electron capture accompanied by the emission of three gamma rays, the energies of which are approximately 434, 614, and 723 keV, with an approximately 91% emission probability. The radionuclide $^{110\text{m}}\text{Ag}$ ($T_{1/2}=249.8$ days) primarily decays by beta emission, followed by a cascade of gamma rays within the 133–2,005 keV energy range, the most abundant of which has an energy of 657 keV [81]. Although the gamma rays from $^{108\text{m}}\text{Ag}$ decay are less penetrating than those from the ^{60}Co decay, this gamma source might increase the external dose rate at the lower region of the package/dry storage cask with

reduced gamma shielding. Therefore, it is recommended that the effects of activation source in irradiated In-Cd-Ag rods be analyzed if spent control rod assemblies are allowed in outer basket locations.

In the current spent fuel inventory, APSRAs have only been used in B&W power reactors. There are two types of APSRAs: a black APSRA that uses Ag-In-Cd as neutron absorber and a gray APSRA that uses Inconel as neutron absorber. Their lower end plug and cladding material is stainless steel, and representative lengths of the absorber in the black and gray APSRAs are approximately 90 cm and 160 cm, respectively [82]. Irradiated APSRAs could have high activation sources because the absorber is exposed to the neutron flux in the fueled region during operation. Therefore, APSRAs should be allowed to cool down sufficiently and/or be placed only in the innermost basket locations. For example, the ^{60}Co source intensity decreases approximately by one order of magnitude over approximately 17.5 years of cooling. APSRAs located in the innermost basket locations are effectively shielded by the fuel assemblies outside this region, thereby reducing their contributions to the external gamma dose rate.

A limited study, including calculations of ^{60}Co activation sources associated with cobalt impurity in BPRs, TPDs (WE power reactors), and orifice rod assemblies (ORAs) (B&W power reactors), as well as an evaluation of their effects on the external dose rate of a generic dry storage cask, is provided in ORNL/SPR-2021/2373 [16]. The results of that study are summarized in this section to illustrate the magnitude of representative NFH activation sources.

A ^{60}Co activation source of 447 Ci was calculated using the following BPR input parameters: (1) Pyrex BPR assembly; (2) 24 rodlets per BPR assembly; (3) a total amount of cobalt in the active fuel region of approximately 9 grams (assuming 800 ppm of cobalt in stainless-steel); (4) cycle burnup of 28.8 GWd/MTU [83]; (5) and a cooling time of 5 years. The spatial distributions of the gamma dose rate produced by this activation source in the external region of generic transportation package and dry storage cask models are illustrated in Sections 4.2.1.2 and 4.2.2.1.

Among the ORA used with B&W 15×15 fuel assemblies and TPDs used with WE 14×14, 15×15, and 17×17 fuel assemblies, the ORA had the largest amount of cobalt impurity (2.72 g at the gas plenum location and 2.86 g at the upper end fitting location of the fuel assembly), followed by the TPD used with the WE 17×17 assembly, based on cobalt impurity concentrations of 800 ppm in stainless steel and 500 ppm in Inconel-718. The ^{60}Co activation sources at the gas plenum and the upper end fitting locations were 93.9 Ci and 51.8 Ci, respectively, assuming an NFH cooling time of five years. The spatial distribution of the gamma dose rate produced by this activation source in the external region of a generic dry storage cask model is illustrated in Section 4.2.2.1, Figure 4-6. The NFH material was neglected in the assembly model.

3.3 Source Term Characterization for Type B Waste Packages

The contents of Type B waste packages may include a broad range of nuclides, geometries, and non-fuel materials that may not be very well defined before loading. The materials, geometry shapes, and spatial source distributions of individual waste pieces may exhibit variations that cannot be easily characterized and/or considered in safety analysis models. Therefore, idealized bounding shielding models are typically developed for shielding analyses.

A series of studies documented in ORNL/TM-2020/1586 [14] evaluated bounding analysis approaches that may be used to reduce the complexity of shielding analyses for Type B waste packages. A study analyzed the contributions of activation products in irradiated steel and

Inconel alloys to steel cask external dose rates as a function of decay time. Self-shielding effects associated with various idealized source geometry configurations and material representations were analyzed assuming an arbitrary ^{60}Co gamma source and typical packaging materials (i.e., steel and lead). Radiation sources associated with spent resins from power plant operations were also analyzed. The findings of the studies and recommendations based on the studies are provided in this section.

3.3.1 Activated Metals

3.3.1.1 Characteristics of Radiation Source Terms

Material compositions including major constituents and impurities, which were measured in unirradiated samples of Type 304 stainless steel, carbon steel, and Inconel collected from various U.S. power reactors are provided in NUREG/CR-3474 [84]. The concentration of cobalt impurity varied from 93 ppm in carbon steel samples to 2,570 ppm in Type 304 stainless steel samples. The average cobalt impurity concentration varied from 122 ppm in carbon steel samples to 1,414 ppm in Type 304 stainless steel samples. The activation calculations documented in ORNL/TM-2020/1586 [14] showed that irradiated steel contains significant amounts of relatively short-lived radionuclides such as ^{56}Mn ($T_{1/2}=2.579$ hours) and ^{51}Cr ($T_{1/2}=27.704$ days) at reactor shutdown. Therefore, these radionuclides have negligible or small contributions to cask external dose rate after approximately 30 days to 1 year from reactor shutdown. Other activation products are pure beta emitters of low-energy electrons such as ^{63}Ni ($T_{1/2}=100.1$ years), or they emit weak gamma rays, such as ^{55}Fe ($T_{1/2}=2.73$ years). Irradiated steel also contains small amounts of the ^{54}Mn radionuclide ($T_{1/2}=312.3$ days), which is produced by the threshold reaction $^{54}\text{Fe}(n,p)^{54}\text{Mn}$ and whose decay produces gamma rays of 835 keV. The activation calculations showed that ^{60}Co is not a significant contributor to the total radioactivity. However, ^{60}Co was a principal contributor to total decay heat and the major contributor to the gamma dose rate external to a simplified package model, as seen in Figure 3-7. The external package dose rate was dominated by short-lived radionuclides at shutdown, but the ^{60}Co contribution to external dose rate increased with increasing decay time. At 30 days after shutdown, the ^{60}Co contribution to the total external package dose rate varied from approximately 60% to 95%, depending on material, initial cobalt impurity concentration, and shield thickness. Its maximum contribution of approximately 100% was reached within the time interval of 2 to 5 years after shutdown and was maintained for up to 45 to 60 years after shutdown, depending on material, initial cobalt impurity concentration, and shield thickness. Thereafter, the ^{60}Co contribution relative to other radionuclides in irradiated steel and Inconel alloys decreased, reaching negligible contributions at 100 years after reactor shutdown. The analyses in this report support the approach of defining the contents of packages dedicated to shipment of activated metals from reactor internals and pressure vessel in terms of ^{60}Co activity/source strength. Representing other radionuclides that contribute to the external package dose rates as ^{60}Co is conservative because ^{60}Co gamma ray emissions are bounding in terms of radiation source energy and intensity. It is recommended that bounding cobalt impurity concentration values based on plant records or measurements of representative samples be used in ^{60}Co source calculations for activated metals in pressure vessel, shroud, core barrel, etc. from decommissioned reactors.

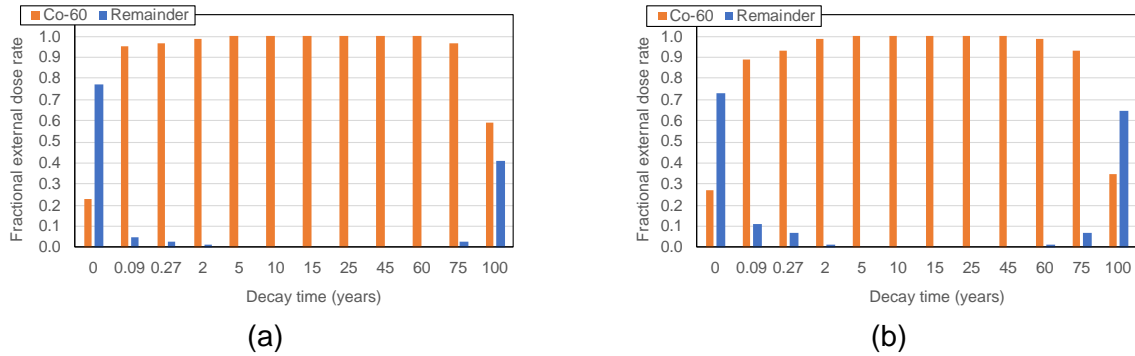


Figure 3-7 Fractional External Dose Rates for ^{60}Co and the Remainder of Radionuclides as a Function of Decay Time for (a) Type 304 Stainless Steel and (b) Reactor Vessel (Carbon Steel) Composition, Assuming a 10-cm Thick Steel Shield

3.3.1.2 Waste Geometry

The shapes of individual activated metal pieces loaded into a transportation cask might vary significantly. Therefore, safety analyses typically use idealized bounding geometry and spatial source distribution models. Self-shielding effects associated with various idealized geometry and material representations were analyzed in ORNL/TM-2020/1586 [14]. Dose rates produced by an arbitrary ^{60}Co source were calculated at multiple locations on the external surface of a generic waste package and at 2 m from its surface using SCALE/MAVRIC (see Section 4.1.2.2).

Source self-shielding effects on external package dose rate were analyzed for four idealized waste geometry models, where each model used the same material composition, total material weight, and total source strength. The waste material (Type 304 stainless steel) and radiation source were uniformly distributed within the geometry boundaries of the waste geometry model. One configuration consisted of a single cylindrical source with waste material extending throughout the available cask cavity volume. The other three configurations consisted of more compact waste shapes with higher mass densities, including multiple cuboids or cylinders. The mass densities of these four different waste geometry configurations varied from 4.35 g/cm^3 to 8.0 g/cm^3 . As expected, the configuration with homogeneous material and uniform volumetric sources extending throughout the available cask cavity volume was most conservative with respect to external package dose rate among the four configurations analyzed. This model is often used in safety analyses because it is considered to produce bounding dose rates due to (1) reduced self-shielding and (2) closer source proximity to dose rate locations than other geometry models. The greatest impact of the four different models on external dose rate was observed at 2 m from the package top and bottom surfaces (up to 23% dose rate differences), and the smallest impact was observed at 2 m from the package radial surface (up to 5% dose rate differences). Therefore, a waste geometry model describing homogeneous waste material throughout the available cask cavity volume is recommended for conservative external package dose rates.

3.3.1.3 Source Spatial Distributions

Nuclide activity densities (i.e., Ci per gram of material) are expected to vary widely among activated metals from decommissioned reactors because of flux and spectrum variations outside the reactor core region. Furthermore, the density of activation products is expected to

vary as a function of depth within reactor vessel and structural materials. High-fidelity, detailed reactor analyses [85] showed that the ^{60}Co and ^{55}Fe activity densities were much higher in the pressure vessel liner than deeper within the pressure vessel wall. These activity densities further decreased with increasing depth within the pressure vessel up to a certain depth and then slightly increased near the outer surface because of the neutron streaming in the annulus region between the pressure vessel and the biological shielding. Similarly, the analyses in NUREG/CR-0130 [86] and NUREG/CR-0672 [87] have shown that the dose rates due to activation products at the inner surface of the activated shroud, core barrel, and pressure vessel are higher than the dose rates at the outer surfaces of these reactor components. Based on these previous analyses, activity densities of radionuclides in activated metals may vary by orders of magnitude, depending on material compositions and their location in the reactor. Therefore, using a uniform volumetric source distribution in the shielding model may result in an underprediction of external package dose rate values, if the activated metals exhibit localized source peaks. The effects on the external package dose rate of spatial variations in ^{60}Co activity density were analyzed in ORNL/TM-2020/1586 [14] using idealized axial and radial source density distributions. The total source strength was constant for all analyzed spatial source distributions. The intent of the study was to determine the effects of localized source peaks on external package dose rate relative to uniform volumetric source models. The study showed that the uniform volumetric source distribution would not be conservative if individual waste units exhibit localized peaks of activity density/source strength, which emphasizes the need for accurate characterization of the peak source activities for the waste stream expected to be loaded in the cask. A simple modeling approach would be to assume that the entire waste has an activity density equal to the localized specific activity peak. External package dose rates may then be determined using a uniform source distribution with an activity density equal to the localized peak.

The composition and the quantity of neutron-activated corrosion products deposited on reactor internals depend on structural material compositions; reactor size, design, and operating history; and reactor fuel conditions. This radioactive material is known as Chalk River unidentified deposits (crud). The effects on external dose rate of two different spatial source representations (i.e., surface and volumetric) for crud were analyzed. A surface source was found to produce much higher external dose rates, by a few orders of magnitude, than a volumetric source. Therefore, the activation source in the crud deposited on reactor internals should be modeled as a surface source.

3.3.2 Spent Resins from Power Plant Operations

Spent organic ion exchange resins from nuclear power plants contain a mixture of neutron-activated corrosion products and fission products. These resins may also contain low or undetectable levels of actinides. Dose rates external to a steel cask model were estimated for radiation sources associated with neutron-activated corrosion products and fission products (see Section 3.3.2.1) and actinides (see Section 3.3.2.2) using available data on the levels of radionuclide loadings on spent resins. However, no specific recommendation can be provided on spent resin shielding analyses based on those studies because data were only available for a small sample of spent resins from power plant operations.

3.3.2.1 Neutron-activated Corrosion Products and Fission Products

ORNL/TM-2020/1586 [14] analyzed the data available in NUREG/CR-2830 [88] and NUREG/CR-6567 [89], which describe the levels of radionuclide loadings (in $\mu\text{Ci/g}$) on samples of spent resin from reactor coolant cleanup that were shipped for disposal. The data in

NUREG/CR-2830 consist of maximum radionuclide loadings on spent resins shipped for disposal from 5 power plants: Hatch 1, Maine Yankee, Peach Bottom, Trojan, and Vermont Yankee. These data are representative of the time of resin removal from service at U.S. power plants during 1980 and 1981. NUREG/CR-6567 provides measured activities for long-lived radionuclides on a bead resin from Crystal River at 3.08 years after removal from service. The individual radionuclides and the magnitude of radionuclide loadings on spent resins varied significantly among these power plants.

Gamma dose rates external to a simplified cask model with a 10-cm thick steel shield were calculated. The graphs in Figure 3-8 show the radionuclides important to external gamma dose rate and their dose rate fractional contributions for the analyzed resins. The dominant fraction consisted of fission products (e.g., ^{134}Cs and ^{137}Cs) at some plants and activation products (e.g., ^{60}Co , ^{58}Co) at other plants.

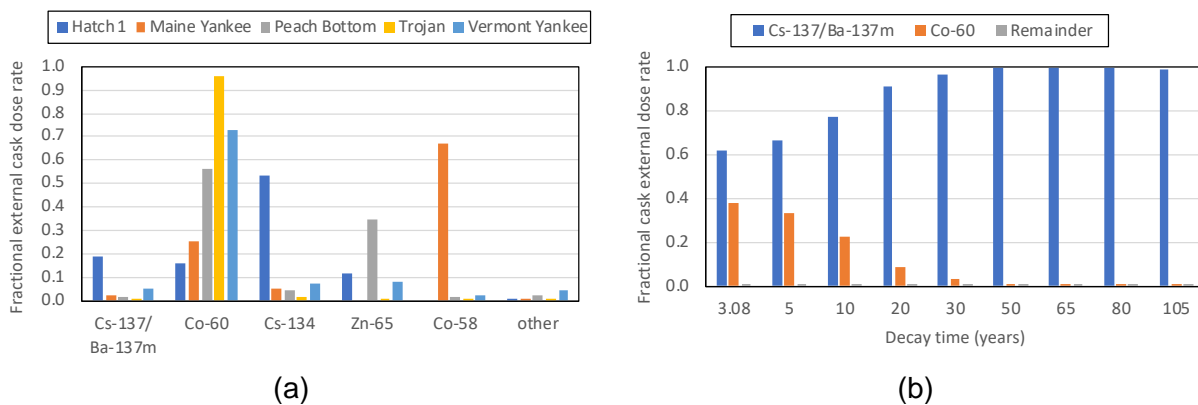


Figure 3-8 Fractional External Dose Rates for Nuclides Reported in (a) NUREG/CR-2830 and (b) NUREG/CR-6567, Assuming a 10-cm Thick Steel Shield

3.3.2.2 Actinides

Low levels of actinides might be present in spent resins. Neutrons are produced by spontaneous fission of actinides and (α, n) reactions of the alpha particles from actinide decay with light nuclei in the waste matrix material. Thus, the neutron source depends on the actinides present in the waste and the resin elemental composition. A significant neutron source can be produced from ^{17}O (α, n) and ^{18}O (α, n) reactions, as well as (α, n) reactions with light-element impurities in the waste matrix material. Actinide neutron and gamma source terms were calculated in ORNL/TM-2020/1586 [14] based on spent resin actinide loading data provided in NUREG/CR-2830 [88] and DOE/EIS-0375 [90]. In these calculations, it was assumed that the resin matrix material is polystyrene cross-linked with divinylbenzene and that this matrix contains 1% oxygen by weight. This calculation showed that the neutron and gamma dose rates produced by actinides on spent resins are negligible compared to the total dose rate, which is dominated by activation and fission products.

3.3.3 Type B Waste Packages Containing a Variety of Waste Materials

For Type B waste packages containing a variety of waste materials, using a single material in the shielding model would significantly simplify shielding analyses. Waste material specifications might affect external dose rates as well as the bremsstrahlung radiation source term. A study

documented in ORNL/SPR-2020/1586 [14] analyzed the effects of different waste material specifications, including Al, stainless steel, and Zr, on the external gamma dose rates of a generic steel/lead cask model while assuming constant waste weight. The waste geometry configuration consisted of a cylinder with homogeneous material and uniform volumetric ^{60}Co sources extending throughout the available cask cavity volume. Material weight, material density, and source intensity were the same for each of these materials, that is, electron density was approximately constant. The dose rates for all cases were within their 3-sigma statistical uncertainties. The results demonstrate that different waste materials may produce similar external gamma dose rates, provided that waste mass and source volumetric distribution are the same.

Many radionuclides decay by emitting beta particles (i.e., energetic electrons in β^- decay and positrons in β^+ decay) with negligible gamma emissions. The bremsstrahlung radiation yield is a function of the initial kinetic energy of the beta particles and increases as the atomic number of the absorber material increases. Therefore, high-energy betas interacting with dense, high-Z materials will more likely produce significant bremsstrahlung radiation (see Section 3.1.3). The depletion and decay code ORIGEN (see Section 3.6.1) can calculate the bremsstrahlung photon sources from beta emitters in selected materials but not for a case-specific waste material. Therefore, based on the available options, the bremsstrahlung photon sources might be either significantly overpredicted (e.g., assuming UO_2) or underpredicted (e.g., assuming water). This source also can be approximated using a simple method, such as that provided by Turner [53], or determined by rigorous beta particle simulations with a Monte Carlo code such as MCNP. For example, the simple method predicts that the radiation yields of a beta particle with the initial energy of 2.27 MeV would be approximately 1.7, 3.4, and 5.2% if the waste materials were Al, Fe, and Zr, respectively. The energy spectrum of the bremsstrahlung radiation cannot easily be determined, but the photon energy can be conservatively approximated as equal to the beta energy end point. Based on this example, the highest-Z material among the anticipated waste streams is recommended for the purpose of generating the bremsstrahlung radiation produced by beta emitters with high end point energies.

3.4 Neutron Source from Subcritical Multiplication

The neutrons emitted by spontaneous fissions and (α, n) reactions in spent fuel will further induce fission reactions with fissile nuclides in the spent fuel (i.e., ^{235}U , ^{239}Pu , and ^{241}Pu). This neutron source is often called a *subcritical multiplication neutron source*. Because this neutron source is not included in the neutron source term determined with depletion and decay codes, it must be considered as a separate source in dose rate calculations. This additional neutron source can be treated explicitly in dose rate calculations with shielding codes that track the neutrons produced by fission reactions. An approximate approach to account for this neutron source is to update the neutron source strength calculated by the depletion code with the $S^* = S/(1-k_{eff})$ formula for systems that are subcritical, where:

- S^* is the neutron source strength that includes subcritical multiplication,
- S is the neutron source strength calculated with depletion codes, and
- k_{eff} is the effective neutron multiplication factor, which is determined by a criticality calculation for the specific cask design and fuel loadings.

The fissile content in spent fuel is significantly depleted compared to fresh fuel. Therefore, the subcritical multiplication neutron source is higher if a fresh fuel composition is conservatively specified in the shielding model compared with irradiated fuel compositions. Similar effects are observed for the secondary gamma dose rate, which is correlated with the neutron source (see Section 3.5). The fractional contribution of the neutron source from subcritical multiplication to the total neutron dose rate and the effect on dose rate of modeling fresh fuel compositions in place of irradiated fuel compositions were evaluated ORNL/SPR-2021/2373 [16] for a generic storage cask model. The findings are summarized in Section 4.2.2.1.

3.5 Secondary Gamma Source

Secondary gamma sources comprise photons from capture reactions of neutrons with nuclei in source, overpack, and environmental materials. The radiative capture reaction produces one or more energetic photons with energies of up to several MeV. An important source of secondary gamma radiation is capture gamma photons from (n,γ) reactions caused by thermal neutrons inside the neutron shield [91]. Therefore, secondary gamma sources from (n,γ) reactions produced near the outer surface of a neutron shield undergo significantly less attenuation than primary gamma radiation originating in the fuel and may be a significant contributor to external dose rates. Environmental materials such as soil and/or concrete also can contribute secondary gamma sources from radiative neutron capture. Therefore, the secondary gamma source must be considered in shielding analyses.

Secondary gamma sources are generated during neutron transport simulations from coupled neutron gamma transport calculations. The energy and photon intensity data are available from the Evaluated Nuclear Structure and Decay Data File (ENSDF) library, which contains recommended nuclear structure and decay data for all the known nuclides. The ENSDF database is maintained by the National Nuclear Data Center [92], Brookhaven National Laboratory. The dose rate produced by secondary gamma radiation is directly proportional to the neutron source intensity, but its magnitude depends on material compositions. The fractional contribution of the total dose rate from secondary gamma radiation can vary significantly, depending on SNF characteristics, overpack design, and distance from the cask. For example, the shielding calculations summarized in Section 4.2.2.3.1 show that the dose rate contribution from secondary gamma radiation increases with increasing distance from a dry storage cask and can dominate the total far-field dose rate from high-burnup fuel at longer cooling times.

3.6 Source Term Computer Codes and Validation

Radiation source term calculations require point-depletion methods for solving a system of differential equations describing nuclide generation, depletion, and decay. Problem-specific calculations require a method for calculating spectrum-averaged neutron absorption cross sections. NUREG/CR-6802 has extensively presented the depletion capabilities and limitations of SAS2H, a 1D depletion module available in SCALE 4 used to perform the various analyses published in that report. However, SAS2H was superseded by improved depletion capabilities in subsequent SCALE releases. The recommendations provided in this report are based on depletion calculations with SCALE 6.2 or later releases. Therefore, ORIGEN, TRITON, Polaris, and ORIGAMI, the depletion and decay capabilities available in the current version (6.2.4) of the SCALE code system, are further discussed in this section. Other popular depletion codes used throughout the world include CASMO, HELIOS, WIMS, APOLLO, KORIGEN, and TransLAT [68,93], but these codes are not discussed in this report.

The SCALE computer code system [19,20] is a comprehensive modeling and simulation suite for nuclear safety analysis and design developed and maintained by ORNL. SCALE provides computer codes and analysis sequences for criticality, reactor physics, source term, shielding, and cross-section sensitivity and uncertainty analyses. The cross-section data provided with SCALE 6.2.4 include comprehensive continuous-energy neutron and coupled neutron–gamma data based on Evaluated Nuclear Data File (ENDF)/B-VII.0 and ENDF/B-VII.1 as well as multigroup data. Comprehensive ORIGEN data libraries, based on ENDF/B-VII.1 and recent JEFF evaluations, include nuclear decay data, neutron reaction cross sections, neutron-induced fission product yields, and delayed gamma ray and neutron emission data for over 2,200 nuclides.

3.6.1 ORIGEN

The ORIGEN code [20,94] is used within SCALE to solve the system of differential equations that describes nuclide generation, depletion, and decay. The ORIGEN code within SCALE is the industry standard and one of most popular codes [68] for point-depletion calculations. It can be used as a standalone code and as a functional module within SCALE’s depletion modules (i.e., TRITON, Polaris, and ORIGAMI).

ORIGEN can compute alpha, beta, neutron, and gamma emission spectra during decay. SNF neutron source terms calculated with ORIGEN include neutrons from spontaneous fission and from (α ,n) reactions with light elements in the fuel oxide material. SNF photon source terms calculated with ORIGEN include photons (i.e., x-rays and gamma rays) from radionuclide decay, spontaneous fission, and (α ,n) reactions, as well as bremsstrahlung. For bremsstrahlung photon source calculation, the option for the medium is either UO₂ (the default option), water matrix, or no material. A case-specific material option is not available in ORIGEN.

3.6.2 TRITON

Starting with the SCALE 5.0 release, TRITON ([95,96], a rigorous two-dimensional (2D) depletion module, superseded SAS2H, which is the SCALE 1D depletion module mentioned in NUREG/CR-6802. The TRITON module in the current version of SCALE [20] provides multiple capabilities for 1D, 2D, and 3D depletion analyses, cross-section processing sequences, transport sequences, and sensitivity/uncertainty analysis sequences. TRITON provides options to request depletion by power (i.e., assuming constant specific power) or depletion by flux (i.e., assuming constant flux) for selected materials. Depletion by flux is appropriate for non-fuel materials that do not significantly contribute to the total power. The SCALE 252- or 56-group library based on ENDF/B-VII.1 data may be used in TRITON depletion calculations.

Problem-dependent ORIGEN cross-section libraries can be generated with the TRITON 2D lattice physics capability (=T-DEPL), which uses burnup-dependent cross-section preparation, the 2D NEWT flexible mesh discrete ordinates code, and ORIGEN to perform depletion of user-specified materials. TRITON calculations generate a series of output files—including one containing stacked ORIGEN binary output data (.ft71) for each material depleted or irradiated in the problem at the end of each burnup state point, as well as ORIGEN binary library files (.ft33).

3.6.3 POLARIS

Polaris is a module dedicated to 2D LWR lattice physics analyses. This module uses the embedded self-shielding method for multigroup cross-section processing, and a transport solver based on the method of characteristics. Polaris provides an easy-to-use input format that allows

users to set up lattice models with minimal lines of input and effort. Polaris calculations generate a series of output files, including one containing stacked ORIGEN binary output data (.ft71) for each material depleted or irradiated in the problem at the end of each burnup state point, as well as ORIGEN binary library files (.ft33) (SCALE 6.3 only). The SCALE 252- or 56-group library based on ENDF/B-VII.1 data may be used in Polaris depletion calculations.

3.6.4 ORIGAMI

ORIGAMI is a SCALE [20,97] module dedicated to source term calculations for irradiated LWR fuel assemblies, which typically exhibit radial and/or axial burnup variations. This module performs fast point-depletion calculations with the ORIGEN code using pre-generated problem-dependent cross sections (.ft33 files). ORIGEN cross-section libraries can be generated for a variety of fuel types and irradiation conditions. Varying parameters in ORIGEN cross-section data are fuel enrichment, burnup, and moderator density (optional). ORIGAMI performs interpolations on the ORIGEN cross-section data using a previously validated method, which is documented in ORNL/TM-13584 [98]. This is a very practical method for generating nuclide compositions and radiation source terms for criticality and shielding calculations specifying various fuel assembly average burnup values and axial burnup profiles.

A series of 1,470 pre-generated libraries for use in ORIGAMI calculations are provided with SCALE 6.2.4 for 61 fuel assemblies from commercial and research reactors. These libraries have been generated with TRITON using input parameters documented in the SCALE manual [20]. Additional ORIGEN cross section libraries can be generated with TRITON by users using other application-specific input parameters.

ORIGAMI produces several types of output files, including: 1) a file containing stacked ORIGEN binary output data (.ft71) for each depletion zone; 2) files with nuclide concentrations at the last time-step for each axial depletion region, in the format of SCALE standard composition input data or MCNP material input data; 3) a file containing the axial decay heat at the final time-step; and 4) gamma and neutron radiation source spectra.

3.6.5 Depletion Code Validations

Depletion code validations are primarily based on comparisons to radiochemical assay (RCA) data. Publicly available RCA data and assembly decay and irradiation condition data required for fuel depletion simulations are consolidated in the Spent Fuel Composition database [99], which has been developed and is maintained by members of the Organisation for Economic Co-operation and Development (OECD) Nuclear Energy Agency (NEA) in close collaboration with ORNL. Measurement data for a total of 750 fuel samples from 44 different reactors are included in SFCOMPO 2.0, which was released in 2017. The data in SFCOMPO have been independently reviewed for consistency with the original reports. An effort of the SFCOMPO Technical Review Group (TRG) is underway to publish the first isotopic evaluations of individual assay data using a standard data evaluation format, including uncertainty analyses. A summary of current publicly available RCA data for PWR and BWR nuclide inventory validations is provided in ORNL/SPR-2022/2518 [17].

A review of recent ORNL publications [100,101] providing nuclide inventory validations is available in ORNL/SPR-2022/2692 [18]. These validation studies used (1) SCALE 6.2.4 and nuclear cross sections based on ENDF/B-VII.1 [102] and (2) SCALE 6.1 and nuclear cross sections based on ENDF/B-VII.0 [103]. Nuclides identified as important contributors to radiation source terms and dose rates for cooling times relevant to dry storage include fission products

^{144}Ce , ^{106}Ru , ^{134}Cs , ^{154}Eu , and ^{137}Cs and actinides ^{242}Cm (cooling times < 3 years) and ^{244}Cm (up to approximately 100 years of cooling). Actinides ^{238}Pu , ^{241}Am , ^{246}Cm , ^{240}Pu , ^{239}Pu , and ^{242}Pu become important at longer cooling times (e.g., 100 years or longer). These nuclides are discussed in greater detail in Sections 3.1.1 and 3.1.2. Bias and bias uncertainty values are available for all the nuclides of interest except for ^{242}Cm in PWR fuel and ^{246}Cm in BWR fuel. The number of evaluated PWR fuel samples varies as a function of nuclide from 14 (^{246}Cm) to 92 (^{240}Pu and ^{239}Pu) [100]. The SCALE 6.2.4/ENDF/B-VII.1 validation study [100] for BWR fuel provides bias and bias uncertainty values for ^{137}Cs and most actinides of interest. However, a SCALE 6.1/ENDF/B-VII.0 validation study [101] provides bias and bias uncertainty values for fission products ^{144}Ce , ^{106}Ru , ^{134}Cs , ^{154}Eu , and ^{90}Sr , but not for actinides ^{244}Cm and ^{242}Cm , based on RCA data for six fuel samples from a BWR 10×10 fuel assembly.

On average, SCALE overpredicted the concentrations of ^{106}Ru and ^{154}Eu and underpredicted the concentrations of ^{144}Ce , ^{134}Cs , ^{90}Sr , ^{137}Cs , ^{244}Cm , and ^{242}Pu for both PWR and BWR fuel with SCALE 6.2.4/ENDF-B/VII.1 and SCALE 6.1/ENDF-B/VII.0. For the PWR fuel, the bias values associated with nuclide concentrations from SCALE 6.2.4/TRITON/ENDF-B/VII.1 and SCALE 6.1/TRITON/ENDF-B/VII.0 depletion calculations are less than approximately 10%. The associated bias uncertainty values are less than approximately 11% for all nuclides of interest except for ^{106}Ru , ^{241}Am , and ^{246}Cm . For these nuclides, the bias uncertainty values vary from 20% to approximately 26%. For the BWR fuel, bias values associated with nuclide concentrations from SCALE 6.2.4/Polaris/ENDF-B/VII.1 depletion calculations are less than approximately 10%. The bias uncertainty values vary from 6% for ^{137}Cs to 68% for ^{244}Cm in the BWR fuel. The SCALE 6.1/TRITON/ENDF-B-VII.0 validation results show an isotopic bias of less than approximately 14% and bias uncertainty values less than 18%.

The nuclide concentration bias and bias uncertainty that are based on validation against RCA measurement data are affected by uncertainties in the measurement data, uncertainties in the modeling data (e.g., fuel operating history and assembly characteristics), uncertainties associated with nuclear cross-section data, and intrinsic uncertainties and approximations associated with the computational methods used for simulations. Measurement uncertainties might be significant for nuclides found in very small quantities in spent fuel. The depletion modules in the SCALE code system have been extensively validated based on available RCA data for UO_2 fuel samples, primarily for burnup credit criticality safety applications. Very limited code-to-code studies exist that show comparisons between the SCALE 6 releases and other depletion codes. Comparison of code predictions to high-quality experimental data [104] for one PWR UO_2 fuel sample shows that nuclide concentration predictions by SCALE 6.2.2/ENDF-B/VII.1 are in good agreement with the measured values for most of the measured nuclides, and these predictions are similar to nuclide concentrations calculated with other depletion codes. For example, the differences between the SCALE/TRITON isotopic inventory predictions and measurement values varied from 0.3% for ^{235}U to -12.5% for ^{241}Pu . Differences among different depletion code predictions were attributed to differences in the transport computational method (i.e., Monte Carlo vs. deterministic) and various nuclear data used in the simulations.

The uncertainties associated with nuclear cross-section data and depletion computational methods should be considered in the assessment of the overall safety margin. The consequences of these uncertainties may be mitigated by various analysis approaches, such as employing conservative assumptions, increasing design margins in the analysis, and establishing bounding design-basis source terms with justified conservatism.

4 SHIELDING CALCULATIONS

This section describes updated information and recommendations concerning computational methods for shielding calculations, modeling approaches with illustrations of dose rate spatial distributions for generic transportation package and dry storage cask models, and code validations. Specific issues in the generation of shielding and dose rate solutions that typically arise in preparation of a safety application are also addressed.

4.1 Methods

Computational methods for shielding calculations, representative shielding codes, various computational approaches to the solution of radiation protection problems, and factors to consider when deciding which methods and models are appropriate for a given application are provided in NUREG/CR-6802. These methods include the point kernel method, deterministic methods, and the Monte Carlo method. This section provides updated information and recommendations, focusing on Monte Carlo transport codes used to perform shielding calculations for safety applications. The Monte Carlo transport method provides a rigorous solution to shielding calculations because it can (1) simulate radiation/particle interactions with matter within the accuracy limitations of existing nuclear data and (2) implement actual material specifications and 3D geometry details. This method is widely used to perform shielding calculations for a variety of applications because of these capabilities. Almost all Monte Carlo computer codes used to solve deep-penetration problems use variance reduction techniques to accelerate the stochastic transport calculations. Some of these variance reduction techniques have significantly evolved since NUREG/CR-6802 was published.

4.1.1 Deterministic Transport Codes

Deterministic transport codes are generally used to obtain global neutron and photon flux solutions based on a transport model that is discretized in space, energy, and angle. Deterministic codes have also been used to calculate approximate energy- and spatial-dependent adjoint and forward fluxes for use in preparation of variance reduction parameters (e.g., source biasing and weight windows) for Monte Carlo shielding calculations, as discussed in the next section. Examples of newer discrete ordinates codes for shielding applications include Denovo [105], a 3D massively parallel discrete ordinates solver; ATTILA^{®4} [106], a serial 3D unstructured-tetrahedral-mesh neutral/charged-particle discrete ordinates code; and PARTISN [107], a parallel 3D rectangular-mesh neutral-particle discrete ordinates code.

4.1.2 Monte Carlo Transport Codes

Use of Monte Carlo radiation transport computer codes to perform shielding calculations in support of license applications for SNF and other radioactive material transportation packages and SNF dry storage casks is the current industry norm. The MCNP [61] code and the MAVRIC module in the SCALE code system [20] are described in this section.

4.1.2.1 MCNP

MCNP is a versatile code widely used to perform Monte Carlo transport calculations for a variety of applications, including spent fuel applications. MCNP has numerous capabilities, including

⁴ Attila[®] is a trademark of Silver Fir Software.

continuous-energy cross sections; general, criticality, and surface sources; multiple tally types; and multiple variance reduction techniques. It provides several quantities that aid the user in assessing the quality of the confidence interval of the tally calculation results. MCNP provides a series of variance reduction techniques that can be used to increase the efficiency of Monte Carlo simulations for deep-penetration problems. These include particle splitting and Russian roulette that can be implemented by subdividing shield materials into multiple cell sublayers with increasing particle importance values for the outer layers to bias particle transport to the outside of the cask, the weight window generator, and others. However, variance reduction parameters for MCNP can also be automatically generated with ADVANTG [108] and ATTILA [106]. These variance reduction methods also implemented in SCALE/MAVRIC—which use moderate-fidelity forward and/or adjoint fluxes from deterministic calculations to generate source biasing and weight window parameters—are discussed in greater detail in the next section.

MCNP can also generate surface source files that can be used in subsequent MCNP calculations. These surface source files are particularly useful for far-field dose rate calculations required to demonstrate compliance with 10 CFR Part 72 requirements. A surface source at the external surface of a dry storage cask describes the energy and angular distributions of the neutrons and photons exiting the cask. Confirmatory calculations [109] indicate that this two-step calculation method produces dose rate values similar to those obtained by explicit calculations employing volumetric sources.

4.1.2.2 MAVRIC

MAVRIC features neutron and photon continuous-energy and multigroup energy Monte Carlo transport capabilities; point detector, geometry region, and mesh tallies; and simplified source descriptions that include direct use of f71 ORIGEN binary files produced by ORIGAMI source term calculations. The default behavior for MAVRIC is to create neutrons from fission events and create secondary gammas from neutron collisions. The results of the shielding validations for the MAVRIC module in SCALE 6.2.4 are summarized in Section 4.3.

MAVRIC has the capability to automatically generate variance reduction parameters based on input geometry and source specifications. MAVRIC performs both forward and adjoint discrete ordinates calculations with Denovo, a discrete ordinates code, to determine energy- and space-dependent particle importance functions. Denovo input data, including the SCALE 27n-19g library, problem geometry discretization on a Cartesian grid, and a response function definition, are specified in the MAVRIC input. The forward-weighted consistent adjoint driven importance sampling (FW-CADIS) variance reduction method is implemented in MAVRIC, which enables estimation of dose rate with good statistical accuracy everywhere outside a heavily shielded system. The CADIS method can also be used to optimize Monte Carlo solutions for specific locations. These variance reduction methods and their implementation have been extensively documented [110,111,112], but a concise description is further provided in this report. These variance reduction methods bias source energy distributions as a function of source particle location based on forward- and/or adjoint-flux information. The solution of the integral equation of the adjoint formulation is optimal for importance function biasing in deep-penetration problems [113]. The purpose of source biasing is to increase the sampling frequency of energy ranges and spatial regions that make significant contributions to dose rates external to shielded sources while decreasing the sampling frequencies of unimportant particles/regions. Source particle weight is also adjusted to maintain a fair game (i.e., to produce unbiased dose rate results when using biasing techniques). Energy- and space-dependent weight windows are constructed consistently with the adjusted source particle weights (i.e., particle weight is delimited by the weight window upper and lower bounds). If necessary, particle weight is

maintained within the weight window by applying splitting for particle weights above the weight window upper bound and Russian roulette for particle weights below the weight window lower bound. Although weight window parameters can differ by many orders of magnitude in a source region, depending on particle energy, they generally converge to narrow ranges at the dose rate locations of interest. Therefore, the benefits of these biasing techniques are twofold compared to analog calculations. First, the use of these biasing techniques significantly reduces the compute time because only particle energies and spatial locations that make contributions to external dose rate will be simulated. Second, the particle weights at the dose rate locations of interest generally form narrow distributions (i.e., small variances) if a large number of source particles are sampled. The forward- and/or adjoint-flux information is obtained from prior discrete ordinate calculations using a discretized geometry model of the detailed geometry model based on Cartesian mesh and adjoint source location input specifications. The computer requirements for discrete ordinates calculations can be very high, depending on input specifications, and high-fidelity calculations are neither practical nor required for the purpose of generating variance reduction parameters for Monte Carlo simulations. Moderate-fidelity solutions of the forward- and/or adjoint-flux are adequate for this purpose [114]. However, the user should always assess the quality of the deterministic solutions because variance reduction parameters based on poor forward- and/or adjoint-flux solutions can have detrimental effects on the Monte Carlo transport simulations.

A mesh tally is recommended to be specified for the external regions of the transportation package/dry storage cask model because it enables 3D visualizations of dose rate spatial distributions and identification of locations with high dose rate values. Region and/or point detector tallies can be used for verification purposes along with mesh tallies. Fulcrum, a visualization tool available in SCALE can be used to render the geometry model and associated dose rate maps.

The MAVRIC module in the SCALE code system has been used primarily to perform confirmatory shielding calculations to support NRC reviews of license applications for dry storage casks and transportation packages, as well as canister-specific dose rate calculations with UNF-ST&DARDS [69]. UNF-ST&DARDS, which is an integrated data and analysis tool for assembly-specific depletion and decay calculations and cask-specific SNF criticality, thermal, dose rate, and containment analyses, is an important tool within the DOE's Integrated Waste Management program.

4.2 Modeling

The development of geometry models for shielding applications is a very important part of the overall analysis. NUREG/CR-6802 [9] provides a series of modeling approaches for the fuel assembly and the fuel basket as well as approximation methods for the treatment of radiation streaming paths within the packaging. The various assembly/source material smearing techniques may be used to simplify the pin-by-pin assembly geometry model. However, the various approximation methods for the treatment of radiation streaming paths recommended in NUREG/CR-6802 are no longer recommended herein because improved Monte Carlo computer code capabilities and increased computing power are currently available to explicitly model a streaming path. Additional recommendations are presented in Section 4.2.1 for transportation packages and in Section 4.2.2 for dry storage casks. Generic spent fuel transportation package and dry storage cask models are presented, and the results of MAVRIC shielding calculations are illustrated and discussed. The results of several studies that analyzed specific issues associated with modeling the broad range of SNF and activated NFH characteristics are also presented in this section. These studies were intended to illustrate the dose rates from (1)

representative fuel assembly types used in the calculation model; (2) neutron sources from subcritical multiplication; (3) reconstituted fuel assemblies with stainless-steel replacement rods; and (4) activation sources associated with various PWR NFH. The calculations used either a generic transportation package model or a generic dry storage cask model. In addition, the far-field dose rate produced by a generic dry storage cask is analyzed, its sensitivity to various model parameters is discussed, and specific recommendations are provided.

4.2.1 Spent Fuel Transportation Package Model

Modeling approaches for the spent fuel transportation package under HAC are presented in Section 4.2.1.1. Shielding calculation results for a generic spent fuel transportation package under NCT and HAC are presented in Section 4.2.1.2. Dose rate sensitivities to fuel assembly type are analyzed in Section 4.2.1.3.

4.2.1.1 Spent Fuel Transportation Package Modeling

Spent fuel transportation package models describe the packaging based on licensing drawings and incorporate features that are consistent with transportation conditions. Therefore, different shielding models are required to support shielding analyses of spent fuel transportation packages under NCT and HAC. The geometry model for the transportation package under NCT is generally consistent with the assumption that packaging, package contents, and impact limiters maintain their integrity under normal conditions. However, the geometry model for the transportation package under HAC should incorporate a series of assumptions that are consistent with the effects of the drop, crush, puncture, and fire tests specified in 10 CFR 71.73 on the transportation package. These assumptions and their rationales must be clearly documented in the safety analyses. Under HAC, the integrity of the neutron shield and impact limiter materials is expected to be significantly affected, and the lead shield may slump under the 30-foot drop impact, thereby diminishing the initial shielding effectiveness of the package shielding. Typically, slump of the lead shield is modeled, the neutron shield material and the impact limiter are replaced with air, and the cask surface is used as the reference for the location of the HAC dose rate limit. The maximum axial/radial slump of the lead shield should be consistent with the results of structural and thermal analyses for the package under HAC.

Transportation overpacks may be designed to accommodate canisters of different lengths. A support is typically required either above or underneath shorter canisters to prevent their movement during transportation. It is recommended to consider a reduction of the support with associated canister displacement inside the overpack cavity under HAC. Thus, the effects of canister displacements with greatest potential of increasing external dose rate relative to nominal configurations can be analyzed. This is particularly important for evaluating the effects of axial lead slump because the gaps that may be produced in the gamma shield are essentially radiation streaming paths.

Damaged/failed fuel is typically loaded in failed fuel cans, and a limited number (e.g., up to four) of such cans may be permitted in a single storage cask or package. For shielding purposes, applicants may assume that failed fuel cans have the same average assembly burnup, enrichment, and cooling time as intact fuel. The shielding analyses are required to address issues related to long-term storage (i.e., dry storage beyond 20 years, as defined in NUREG-2224 [115]) of high-burnup fuel. It is well known that hydride reorientation could have detrimental effects on the mechanical properties of the zirconium-based cladding alloys and that the potential of hydride reorientation increases as fuel burnup increases [116]. NUREG-2216 [7] indicates that the shielding analysis of packages that include high-burnup fuel (i.e., SNF with burnup exceeding 45

GWd/MTU) should address credible and bounding reconfigurations of the fuel and associated source terms within the package. Potential effects of various hypothetical fuel reconfiguration scenarios on external package dose rates have been analyzed in NUREG/CR-7203 [117] using simplifying assumptions. The analyzed fuel reconfiguration scenarios include cladding failure, rod/assembly deformation without cladding failure, changes to assembly axial alignment without cladding failure, and gross fuel failure resulting in a collective collapse of all fuel rods. The previous studies have shown that fuel redistribution toward the package internal cavity bottom and/or top regions has the potential to significantly increase external dose rates relative to intact fuel, especially at the transportation package/dry storage cask surface. NUREG-2224 identifies a series of scenarios addressing the impact of possible fuel reconfiguration on external dose and dose rates that were analyzed in NUREG/CR-7203 and are acceptable for the staff. However, NUREG-2224 indicates that the results in NUREG/CR-7203 should not be considered generally applicable with respect to external dose and dose rate evaluations. Therefore, applicants would have to assess the impact of fuel reconfiguration on external dose and dose rates for their particular designs using insights from NUREG/CR-7203. The effects of fuel reconfiguration may be mitigated by increasing SNF cooling time requirements for high-burnup fuel assemblies.

4.2.1.2 Representative Spent Fuel Transportation Package Shielding Calculation Results

Dose rate calculation results for a generic SNF transportation package model are presented herein. This generic transportation package has design characteristics that are similar to existing SNF transport systems. It features a cask body, bottom plate, and top lid made of carbon steel, a radial gamma shielding consisting of lead with a thickness of 8 cm, a radial neutron shield consisting of borated polymer with a thickness of 16 cm, slabs of lead and borated polymer inserted into the bottom plate, and two upper and two lower trunnion plugs made of stainless steel. Trunnion plugs are penetrations through the gamma and neutron shielding materials needed to support lifting and tie-down of the package. The impact limiter materials were neglected in this model for the package under NCT, but the locations of the surface and 2 m dose rates were established relative to the outer boundary of the impact limiter. Assumed effects of the HAC were implemented into the model for the generic transportation package under HAC. The borated polymer was replaced by air and the lead gamma shield features a radial slump of 1.5 cm and an axial slump of 1 cm. The fuel configuration is intact in the model for HAC. The generic transportation package models for NCT and HAC are illustrated in Figure 4-1.

The package contains 37 PWR SNF assemblies loaded into a canister, the fuel region is represented pin by pin, and the hardware outside the fuel region is represented as homogenous material uniformly distributed within the boundaries of the gas plenum, upper end fitting, and lower end fitting regions. The design basis NFH is a BPRA with the ^{60}Co activation source presented in Section 3.2, the absorber rods of which are inserted into the guide tubes of each fuel assembly. Dose rate 3D maps are illustrated for PWR fuel assemblies with an initial fuel enrichment of 4.2%, an average burnup of 60 GWd/MTU, a representative PWR axial burnup profile, and a cooling time of 15 years. The 3D shielding model and dose rate maps produced by each type of radiation source are illustrated for the generic transportation package under NCT in Figure 4-2. These are illustrated in Figure 4-3 for the generic transportation package under HAC. The dose rate maps shown were produced by the neutron source, the secondary gamma radiation from neutron capture reactions, the primary gamma source, the ^{60}Co activation sources in the fuel assembly top and bottom hardware, and the BPRA ^{60}Co activation source. The front-right quarter of the model was removed to enable visualization of the model and dose rate spatial variation.

In this example, the external dose rate for NCT is dominated by the neutron dose rate, followed by the secondary gamma dose rate. The highest external neutron dose rate is observed above and below the package and outside the trunnion plugs because these regions are less shielded against neutrons than the radial region. Primary gamma, secondary gamma, and BPRA activation sources have larger effects on the external radial dose rate within the axial extent of the active fuel region than on the external regions at the top and the bottom of the package. The ^{60}Co activation source in hardware produces higher dose rates in the external radial regions near these sources than in the other external regions.

For HAC, the external dose rate is dominated by the neutron dose rate, followed by the dose rate produced by the ^{60}Co activation sources in fuel assembly hardware. The HAC neutron dose rate values are much higher than the NCT neutron dose rate values because the package neutron shield material was replaced with air. The lead slump is seen to increase the primary gamma dose rate in the external radial region outside the slump location.

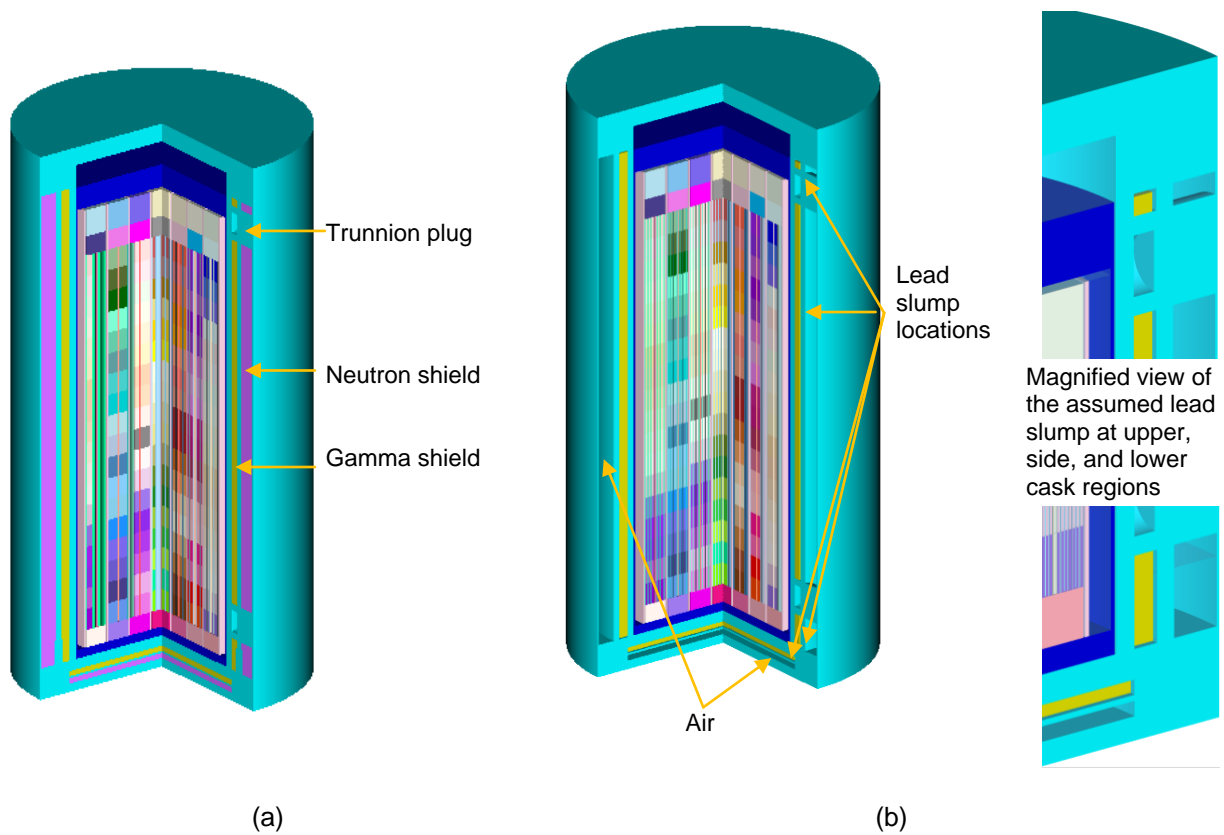


Figure 4-1 Illustration of Generic Transportation Package Models for (a) NCT and (b) HAC

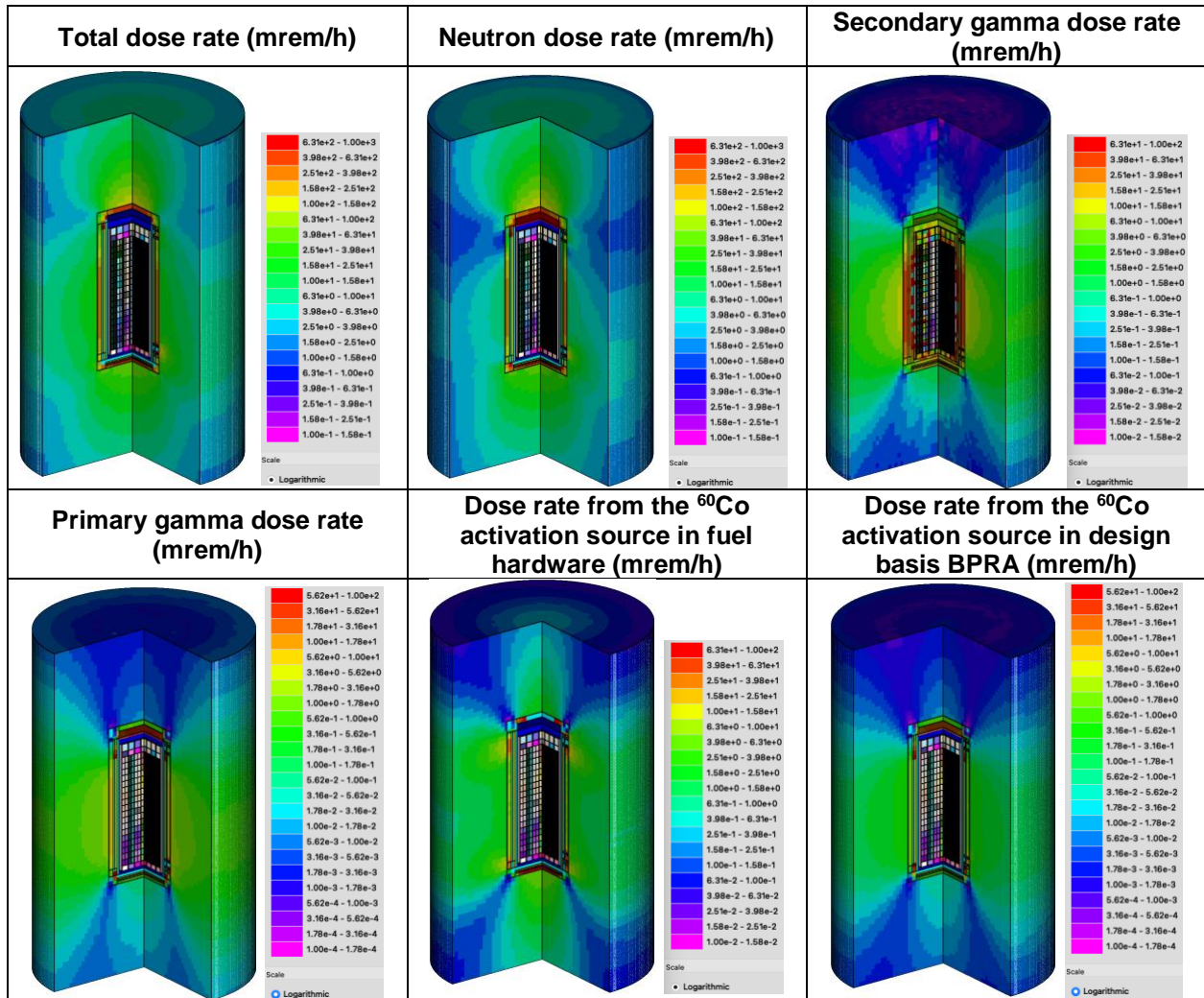


Figure 4-2 Spatial Dose Rate Distribution Produced in the Air Region External to a Generic Transportation Package under NCT by Each Radiation Source (Selected dose rate ranges are shown: 1E-01 – 1E+03 mrem/h for the total and neutron sources; 1E-02 – 1E+02 mrem/h for the secondary gamma source and the cobalt activation source in fuel hardware; and 1E-04 – 1E+02 mrem/h for primary gamma source and the cobalt activation source in BPA. Air region extends 2 m radially and 3 m axially from the package external surface. Front-right quarter of the 3D model was removed to enable detailed visualization.)

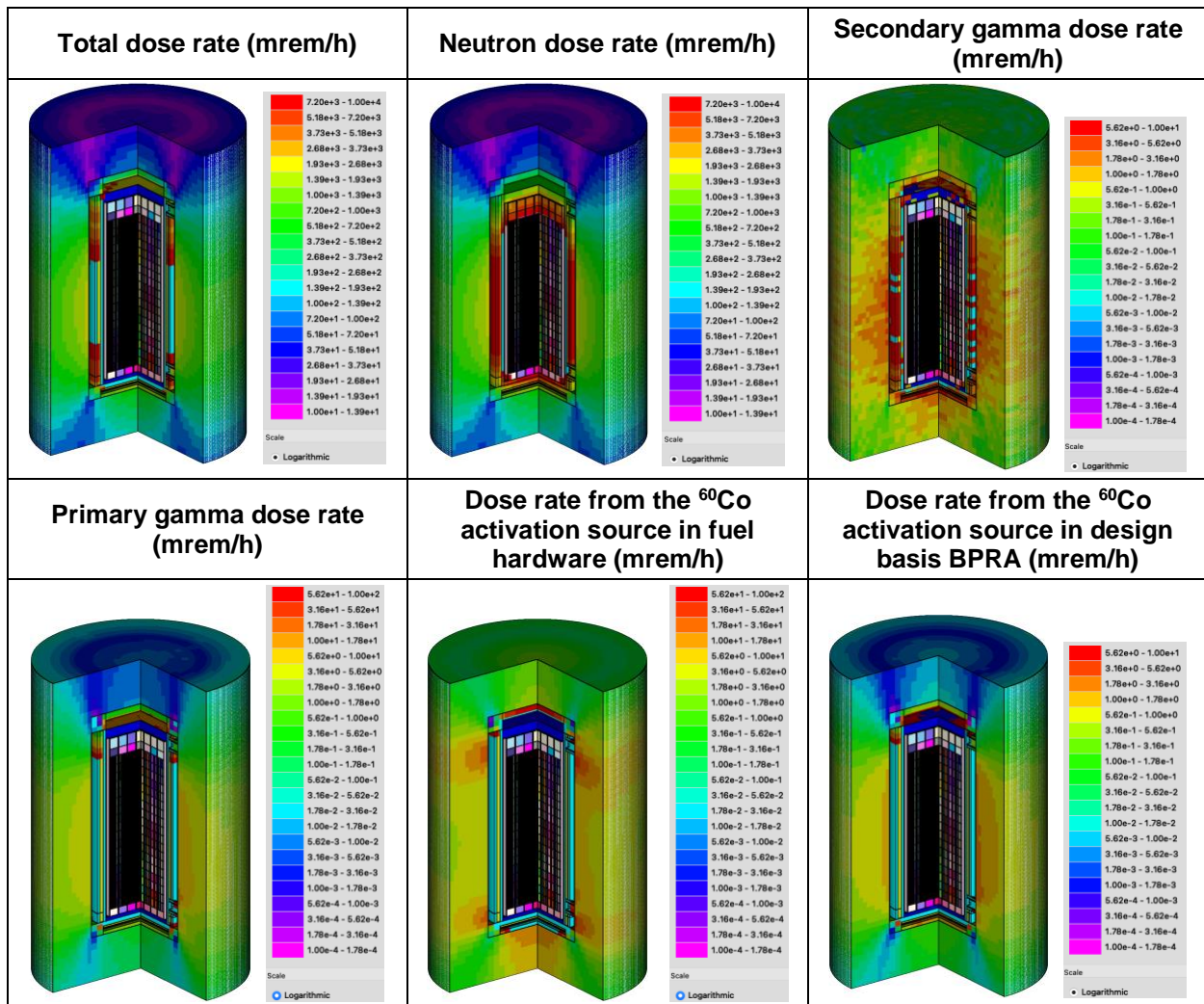


Figure 4-3 Spatial Dose Rate Distribution Produced in the Air Region External to a Generic Transportation Package under HAC by Each Radiation Source (Selected dose rate ranges are shown: 1E+01 – 1E+04 mrem/h for the total and neutron sources; 1E-04 – 1E+02 mrem/h for the primary gamma source and the cobalt activation source in fuel hardware; and 1E-04 – 1E+01 mrem/h for the secondary gamma source and the cobalt activation source in BPRA. Air region extends 1 m from the package external surface. Front-right quarter of the 3D model was removed to enable detailed visualization.)

4.2.1.3 Dose Rate Sensitivities to Fuel Assembly Type

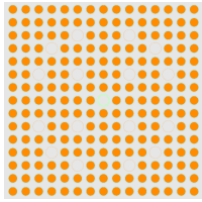
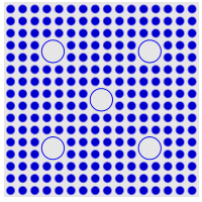
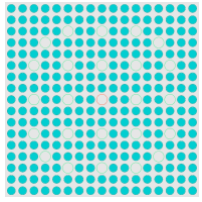
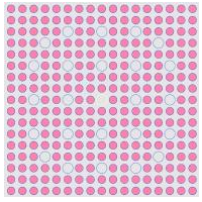
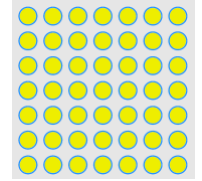
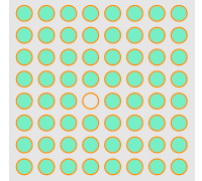
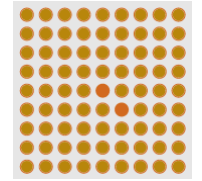
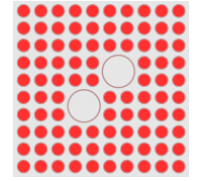
4.2.1.3.1 Fuel Assembly Design

A fuel assembly with a higher initial uranium mass is typically used to generate radiation source terms because assembly source strength is directly proportional to the initial uranium mass at a fixed burnup. However, a heavier fuel assembly also provides greater self-shielding effects than a lighter fuel assembly. Self-shielding effects may partly cancel out the effects of a higher

radiation strength associated with a higher initial uranium mass. The overall effect on external dose rate was evaluated in ORNL/SPR-2021/2373 [16] for four representative PWR and four representative BWR fuel assembly types, using the model of the generic transportation package under NCT described in Section 4.2.1.2. The main design characteristics for representative fuel assembly types are presented in ORNL/SPR-2021/2093 [15].

The evaluated PWR fuel assembly types were B&W 15×15, WE 17×17 LOPAR (low parasitic) fuel, WE 17×17 OFA (optimized fuel assembly), and Combustion Engineering 16×16. The evaluated BWR fuel assembly types are General Electric (GE) 7×7, GE 8×8, ANF 9×9, and GE 10×10. Irradiation conditions (e.g., moderator density and soluble boron concentration for the PWR fuel, void fraction and exposure to control blade for BWR fuel, etc.) used in source term calculations were identical among the PWR/BWR fuel assemblies. The highest initial uranium mass for these assembly types, based on the GC-859 survey data [63], was used in the geometry models and radiation source term calculations. Each fuel assembly had an average fuel assembly burnup value of 50 GWd/MTU, a 4.2 wt % initial ²³⁵U enrichment, and a 10-year cooling time. Axial burnup profiles representative of PWR and BWR SNF were applied. Maximum total, neutron, secondary gamma, and primary gamma dose rate values were determined at the radial surface and at 2 m from the radial surface of the generic package model under NCT. Cross-sectional views of the fuel assembly models and normalized maximum dose rate values at 2 m from the NCT transportation package model are provided in Table 4-1. The B&W 15×15 fuel assembly model was bounding for the PWR fuel, but the WE 17×17 LOPAR fuel assembly model produced approximately the same maximum radial gamma dose rate values within the range of statistical uncertainty as the B&W 15×15 fuel assembly type. The evaluated BWR fuel assembly models produced practically the same maximum radial dose rates within the statistical uncertainties. This study confirms that fuel assembly types that have significantly higher initial uranium mass (e.g., B&W 15×15, WE 17×17 LOPAR) than other fuel assembly types (e.g., WE 17×17 OFA) produce conservative external dose rates. Cobalt activation sources were not included in this analysis because a conservative activation source may be specified independently.

Table 4-1 Two Meter NCT Dose Rate Ratios for PWR and BWR Fuel Assembly Designs

Assembly	B&W 15×15	CE 16×16	WE 17×17 LOPAR	WE 17×17 OFA
kg U/ assembly	491.72	433.20	469.20	429.58
Neutron ^a	1.00	0.92 ± 0.06	0.96 ± 0.06	0.91 ± 0.07
Secondary gamma ^a	1.00	0.91 ± 0.08	0.94 ± 0.08	0.85 ± 0.08
Primary gamma ^a	1.00	0.90 ± 0.02	1.06 ± 0.03	0.97 ± 0.03
Total ^a	1.00	0.90 ± 0.04	0.96 ± 0.04	0.88 ± 0.04
Assembly model cross-sectional view				
Assembly	GE 7×7	GE 8×8	ANF 9×9	GE 10×10
kg U/ assembly	197.60	187.89	175.66	183.37
Neutron ^a	1.00	0.99 ± 0.05	0.96 ± 0.06	1.01 ± 0.04
Secondary gamma ^a	1.00	0.98 ± 0.08	0.99 ± 0.08	1.00 ± 0.06
Primary gamma ^a	1.00	0.99 ± 0.03	0.89 ± 0.03	0.94 ± 0.02
Total ^a	1.00	0.99 ± 0.05	0.95 ± 0.05	0.98 ± 0.04
Assembly model cross-sectional view				

^aMaximum dose rate ratio ± 2 sigma uncertainty values. Reference PWR fuel type: B&W 15×15. Reference BWR fuel type: GE 7×7.

4.2.1.3.2 BWR Fuel Assemblies with Partial-Length Rods

Modern BWR fuel assemblies contain both full-length and partial-length fuel rods. Calculations of radiation source terms and shielding model development for fuel assemblies with partial-length rods require more detailed knowledge of the BWR fuel designs and complicated modeling. The effects on the external dose rates of a generic BWR transportation package model were analyzed in ORNL/SPR-2021/2373 [16] for two different BWR fuel assembly models. The generic transportation package model consisted of the packaging model presented in Section 4.2.1.2, but the package contents consisted of 68 BWR fuel assemblies. The two fuel assembly models consisted of (1) a fuel assembly with full-length fuel rods and (2) a fuel assembly with two axial zones including the dominant lattice and the vanished lattice. The active fuel zone was represented as individual fuel pins in these models. All fuel assemblies in the transportation cask model had identical initial enrichment, discharge characteristics (i.e., assembly average burnup, cooling time, axial burnup profile), and identical irradiation conditions (e.g., bladed lattice and the same moderator density). The location of the axial burnup profile peak was within the dominant lattice region. More details about the model are available in ORNL/SPR-2021/2373 [16].

The dose rate values produced by primary gamma, neutron, and associated secondary gamma sources were calculated at the package surface and compared between the two assembly models. Both models produced the same axial dose rate profiles along the axial extent of the dominant lattice, and the full-length fuel rod assembly model produced a bounding axial dose rate profile for the vanished lattice of the partial-length rod fuel assembly. The axial dose rate profiles of the primary gamma, neutron, and secondary gamma radiation produced by the two assembly models at the cask surface are illustrated in Figure 4-4. The relative statistical uncertainty of the dose rate estimate was less than 2% for neutrons and less than 1% for primary gamma radiation; however, the uncertainty values are not shown in the graphs for clarity. Therefore, a BWR full-length fuel rod assembly model is recommended for use in shielding analyses. This model is more conservative with respect to dose rate than a partial-length rod fuel assembly model.

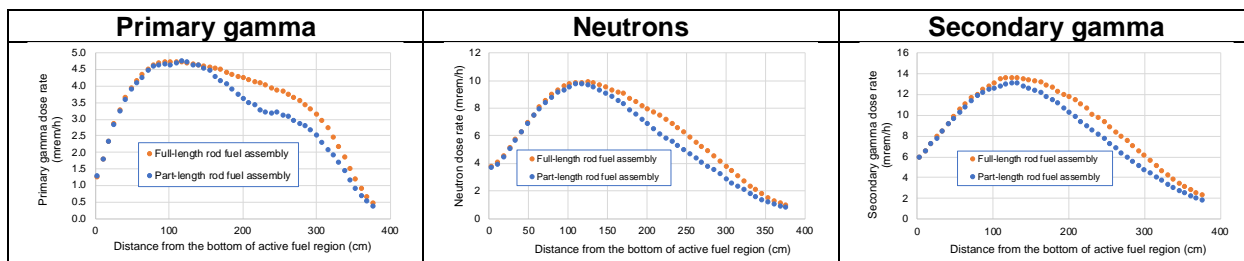


Figure 4-4 Axial Dose Rate Profiles Produced by Full-length Rod and Part-length Rod Fuel Assemblies at the Radial Surface of a Generic Transportation Package Model

4.2.2 Spent Fuel Storage Model

Studies have been performed in this report on the contributions of the various SNF radiation sources discussed in Section 3 of this report. The near-field dose rate for a generic dry storage cask during normal operations is addressed in Section 4.2.2.1, and its sensitivity to various parameters (e.g., fuel composition, geometry representation, activation sources in steel replacement rods) are analyzed in Section 4.2.2.2. Far-field dose rates for a generic dry storage cask and its sensitivity to various input parameters (e.g., air volume and density, soil composition specification) are presented in Section 4.2.2.3. More details about these studies are provided in ORNL/SPR-2021/2373 [16].

4.2.2.1 Generic Storage Cask Model and Near-Field Dose Rates

The dose rates produced by each major radiation source in the air region extending 1 m from the cask surface are illustrated in Figure 4-5 for a generic dry storage cask model. This is a generic vertical concrete cask (VCC) model featuring a concrete radial shell with a thickness of approximately 70 cm and inlet and outlet vents for cooling the fuel. The 3D dose rate maps are shown for the cask model containing 37 PWR SNF assemblies, where each assembly has an initial fuel enrichment of 4%, an average burnup of 60 GWd/MTU, and a cooling time of 5 years. Typical of VCC casks and the selected cooling time, the external dose rate is dominated by the gamma radiation originating in the active fuel region and by the ^{60}Co activation sources in assembly hardware materials. The neutron dose rate is lower than the gamma dose rate for these SNF characteristics because concrete contains light elements, which have effective attenuation properties against neutrons but are less effective against gamma radiation. The

streaming paths at the top and bottom of the cask did not cause a significant increase in the external neutron dose rates because the neutron source based on the axial burnup profile is low in these regions. However, the gamma dose rate is higher near the lower cask region because less shielding material exists in that region. The gamma dose rate spatial distributions in the external region of the generic dry storage cask model that are produced by ^{60}Co activation sources in irradiated BPRA and ORA (see Section 3.2) are illustrated in Figure 4-6.

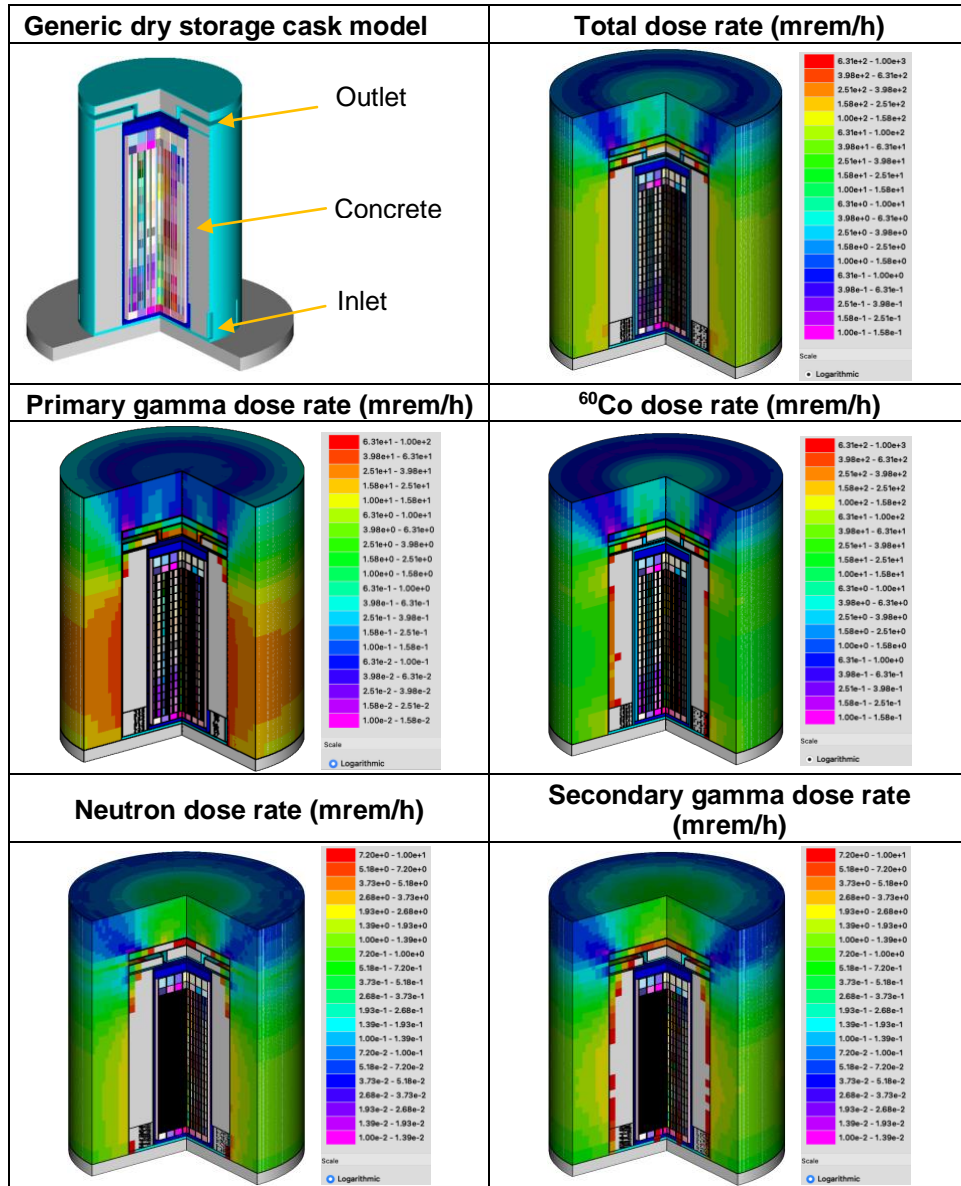


Figure 4-5 Spatial Dose Rate Distribution Produced in the Air Region External to a Generic Dry Storage Cask Model by Each Radiation Source (Selected dose rate ranges are shown: $1\text{E}-01$ – $1\text{E}+03$ mrem/h for the total sources and the cobalt activation sources in fuel hardware; $1\text{E}-02$ – $1\text{E}+02$ mrem/h for the primary gamma source; and $1\text{E}-02$ – $1\text{E}+01$ mrem/h for the neutron and secondary gamma sources. Air region extends 1 m from the cask external surface. Front right-quarter of the 3D model was removed to enable detail visualization.)

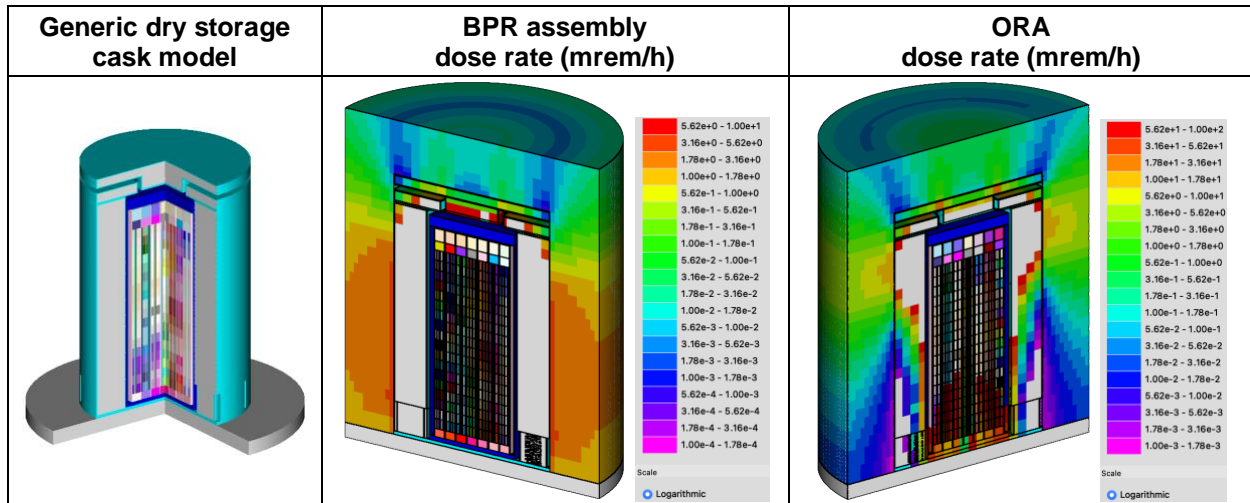


Figure 4-6 Spatial Dose Rate Distribution Produced by BRPA and ORA in the Air Region External to a Generic Dry Storage Cask Model (Selected dose rate ranges are shown: 1E-04 – 10 mrem/h for BPR assembly; 1E-03 – 100 mrem/h for ORA).

4.2.2.2 Near-Field Dose Rate Sensitivities to Various Model Parameters

4.2.2.2.1 Fuel Composition Used in Fuel Assembly Model

Typical shielding calculations for SNF storage casks and transportation packages use fresh fuel compositions in place of irradiated fuel compositions to reduce model complexity. Effects of fuel composition specifications on external storage cask dose rates were evaluated and documented in ORNL/SPR-2021/2373 [16]. The fresh fuel assumption is conservative regarding dose rate because fresh fuel contains a higher fissile amount than SNF. The generic VCC model was used in MAVRIC calculations with either a fresh fuel composition or an irradiated fuel composition. For both cases, the average burnup of the PWR fuel assembly was 60 GWd/MTU, the initial enrichment was 4%, the cooling time was 5 years, the SNF had an axial burnup profile, and maximum dose rate values were calculated at 1 m from the cask. The irradiated fuel composition produced a slightly higher dose rate value from primary gamma radiation (i.e., by approximately 2%, including the statistical uncertainty) as well as lower dose rate values from neutrons (i.e., by approximately 15%) and secondary gamma radiation (i.e., by approximately 17%) than the fresh fuel composition. The two different fuel compositions produced approximately the same maximum total dose rate values within statistical uncertainty because gamma radiation dominated the external dose rates for the 5-year cooling time. However, this overall effect is not expected to be generally valid for transportation packages because transportation packaging includes effective shielding materials against neutrons as well as gamma radiation (e.g., steel, lead, and resins), and the neutron source might make significant contributions to the external dose rates of transportation packages under NCT and HAC.

For the fresh fuel composition with an initial enrichment of 4%, the percentage contribution made by the neutron source from subcritical multiplication to the total neutron dose rate was approximately 37%, and the percentage contribution to the total secondary gamma dose rate of the secondary gamma radiation associated with the neutrons from subcritical multiplication was approximately 60%. The neutron and secondary gamma dose rate increases associated with a 5% initial enrichment were approximately 45% and 70%, respectively. These dose rate

increases characterize dose rate locations at the cask surface approximately corresponding to axial location of the fuel midplane. Fresh fuel compositions assuming an enrichment of 5% may be used for conservative neutron and secondary gamma dose rate values. Although the fresh fuel composition slightly reduces the primary gamma dose rate as compared to the irradiated fuel composition, the neutron and secondary gamma dose rates are significantly higher for the fresh fuel composition than for the irradiated fuel composition. The overall effect of the fresh fuel composition assumption on the total external dose rate depends on the SNF system design. If the total external dose rate is dominated by the total of neutron and secondary gamma dose rates, fresh fuel compositions will produce higher total external dose rate than irradiated fuel compositions. The overall effect is expected to be relatively negligible if the total dose is dominated by the primary gamma radiation, as shown in ORNL/SPR-2021/2373 [16] for a generic storage cask model. Therefore, fresh fuel compositions are recommended because this approach will either increase or have insignificant effects on the total external dose rate, depending on the system design, and because fresh fuel specifications significantly reduce the complexity of fuel assembly models.

4.2.2.2.2 Pin-by-pin Model Compared with Homogeneous Material Model for Active Fuel Zone

The active fuel zone of a fuel assembly is typically modeled as homogeneous material within its geometry boundary because this model is easy to implement, and it also generates conservative cask/package external dose rates compared to a detailed pin-by-pin fuel model. The conservatism associated with the homogeneous fuel model was evaluated in ORNL/SPR-2021/2373 [16]. The gamma dose rate produced by the pin-by-pin model was approximately 5% lower than that produced by the homogeneous material model. The total dose rate contributions from neutrons and secondary gamma rays from neutron capture were practically identical within the statistical uncertainty for the two models. Therefore, this study showed that the homogeneous material model is slightly conservative in comparison with the pin-by-pin model. Although the homogeneous model is conservative, a detailed pin-by-pin model for the active fuel region is acceptable because modern 3D Monte Carlo codes are capable of modeling fuel pin by pin with accurate results.

4.2.2.2.3 Dose Rate Effects of Stainless-Steel Replacement Rods in Reconstituted Fuel Assemblies

As discussed in Section 3.1.9, reconstituted SNF fuel assemblies might contain irradiated steel rods that were used to replace leaking fuel rods. Loadings that contain reconstituted fuel assemblies have the potential to increase the dose rate in the external regions of spent fuel storage casks and transportation packages, depending on the location of the reconstituted fuel assembly in the fuel basket and fuel assembly cooling time. The potential effects of different loadings were evaluated in a previous study [16] by comparing the maximum external gamma dose rates produced by reconstituted fuel assemblies with the external gamma dose rates produced by regular fuel assemblies (i.e., fuel assemblies that do not contain irradiated steel rods). The comparison was limited to the gamma radiation sources in the active fuel region of PWR fuel. The assumed cobalt impurity concentration in the replacement rods was 800 ppm, and the replacement rods were placed in peripheral assembly locations for maximum impact on external cask dose rate. The activation sources in irradiated stainless-steel rods included ^{60}Co sources based on activation rates from exposure to the neutron flux from a fuel assembly that would achieve average assembly burnup values of 60 and 40 GWd/MTU. The 60 GWd/MTU burnup value, which corresponds to the average burnup value of the regular assembly, was a conservative assumption. The effects were analyzed for different assembly cooling times from 2 to 75 years using the generic dry storage cask model discussed in Section 4.2.1.

Two different scenarios were analyzed: (1) all 37 PWR fuel assemblies containing replacement rods; and (2) reconstituted fuel assemblies in the 9 innermost basket locations and regular fuel assemblies in the remainder of basket locations, as seen in Figure 4-7. For each of these scenarios, a reconstituted fuel assembly contained either 8 to 10 replacement rods or 3 to 4 replacement rods. In the first scenario, the ^{60}Co activation source in irradiated replacement steel rods was a major contributor to the external gamma dose rate up to approximately 30 years of cooling, and its contributions extended to 45 years of cooling. The fuel assemblies containing irradiated replacement steel rods produced a maximum increase of 30% to 130% in the external gamma dose rate relative to regular fuel assemblies at 10 years of cooling, depending on the number of steel rods and assembly-average burnup. However, the second scenario produced the same gamma dose rate as the cask loaded with regular fuel assemblies for the analyzed range of cooling time 2 to 75 years because inner basket locations are shielded by outer fuel assemblies. Therefore, the study showed that reconstituted fuel assemblies with irradiated fuel rods can be placed safely in the inner locations of the fuel basket inside the cask because these reconstituted assemblies are shielded by the regular fuel assemblies in the outer basket locations.

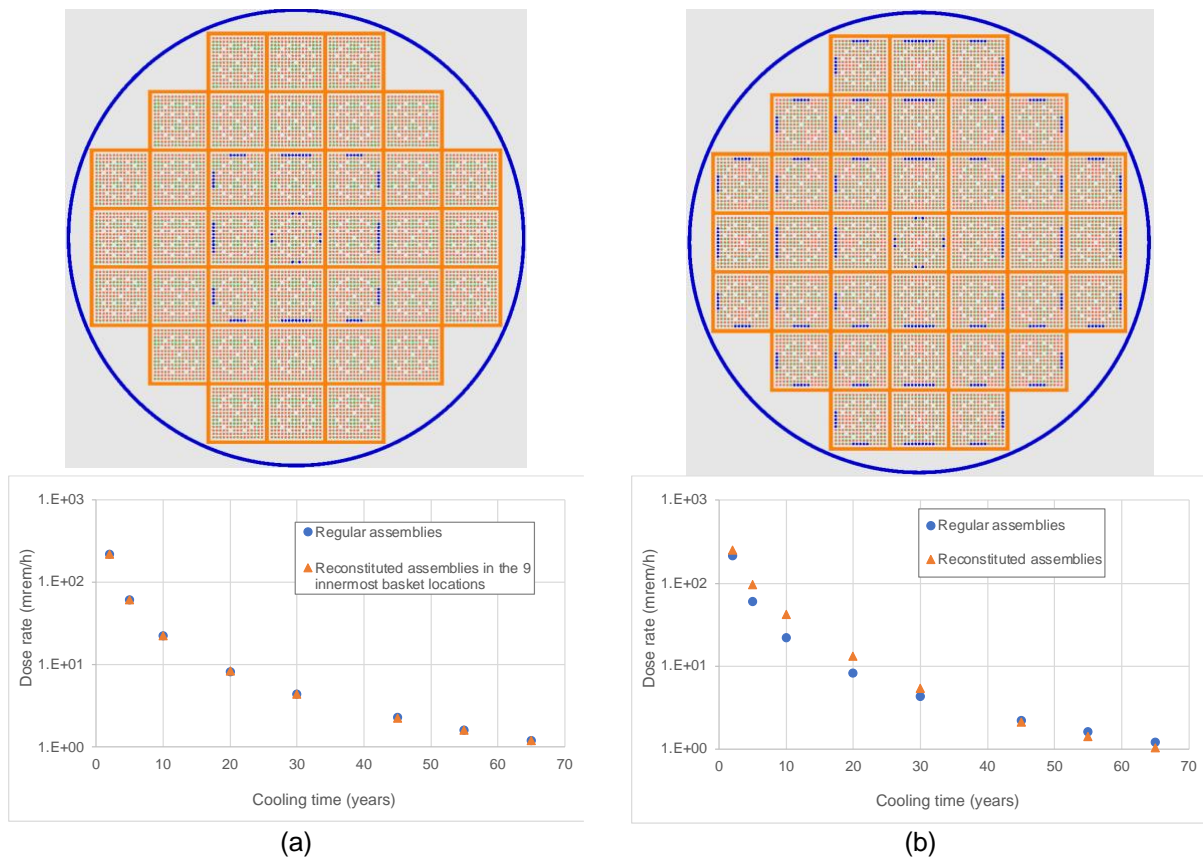


Figure 4-7 Spatial Distributions of Irradiated Steel Replacement Rods in Reconstituted Fuel Assemblies and their Effects on External Gamma Dose Rate for a Generic Dry Storage Cask Model: (a) Reconstituted Assemblies in 9 Innermost Basket Locations; (b) All Assemblies Reconstituted (Stainless-steel replacement rods are shown in blue.)

4.2.2.3 Far-Field Dose Rates

Far-field dose rate refers to dose rate at large distances from a shielded radiation source, such as an individual dry spent fuel storage cask or arrays of storage casks. Far-field dose rate calculations are required to establish the location of the controlled area boundary based on criteria specified in 10 CFR 72.104(a) and 72.106(b) [6]. Typically, dose rate is calculated in the air regions above the ground, where people are expected to reside. The dose rate at a location external to a dry storage cask is produced by neutrons and photons escaping from the cask and reaching that location unobstructed or through multiple scattering interactions with nuclei/atoms in the environment (e.g., air, soil, concrete). Radiation that reemerges into the air as a result of scattering processes within the ground is referred to as *groundshine*; the dose rate contribution from air scattering events is known as *skyshine* dose rate. It has been demonstrated that the contribution of direct radiation to the total dose rate decreases as a function of distance from the cask [118]. For a dry storage cask loaded with SNF of average assembly burnup of 40 GWd/MTU and a cooling time of 10 years, skyshine has been shown to have a larger effect on the neutron dose rate than on the photon dose rate, and the skyshine neutron dose rate was a significant component of the total dose rate at distances greater than approximately 100 m from the cask [118].

Variation of dose rate with average fuel assembly burnup and cooling time as well as the fractional dose rate contributed by each type of radiation that originates in SNF assemblies and surrounding materials are discussed in Section 4.2.2.3.1. Far-field dose rate sensitivity to various modeling parameters (e.g., air mass density and volume and soil composition) is analyzed in Section 4.2.2.3.2.

4.2.2.3.1 Fractional Dose Rate Contribution by Radiation Component

A parametric study in ORNL/SPR-2021/2373 [16] provides far-field dose rate calculations using the dry storage cask model illustrated in Figure 4-5, and average fuel assembly burnup values of 45, 60, and 70 GWd/MTU and cooling times of 1, 5, and 40 years. Total maximum dose rate and fractional contributions from primary gamma radiation, ^{60}Co activation sources in assembly hardware, neutrons, and secondary gamma radiation were calculated as a function of distance up to 1,600 m from the cask center. Tally regions were specified in the air above the ground, within horizontal concentric cylindrical annuli that surrounded the cask. The width and height of a tally regions were 1 m and 2 m, respectively. The dose rate produced by secondary gamma rays from neutron capture reactions was calculated with coupled neutron-photon Monte Carlo simulations. More information about the model parameters is provided in ORNL/SPR-2021/2373 [16].

The graph in Figure 4-8 shows the variation of the total dose rate as a function of distance from the center of the cask with average fuel assembly burnup of 70 GWd/MTU for cooling times of 1, 5, and 40 years. The graphs in Figure 4-9 show the fractional dose rate contributions of primary gamma, ^{60}Co activation, neutron, and secondary gamma sources.

The external cask dose rate decreased by approximately three orders of magnitude within 100 m from the center of the cask and by approximately nine orders of magnitude at 1,600 m from the center of the cask. At 1 year of cooling, the external cask dose rate was predominantly produced by the primary gamma radiation originating in the fuel. At 5 years of cooling, the external cask dose rate was predominantly produced by the primary gamma and the ^{60}Co activation source, where the ^{60}Co activation source had a similar contribution as the primary gamma source. At 40 years of cooling, the external cask dose rate was dominated by the primary gamma source up to

approximately 700 m from the cask center. The contribution of secondary gamma radiation to the far-field dose rate significantly increased with increasing assembly burnup, fuel cooling time, and the distance from the cask. Secondary gamma radiation dominated the total dose rate at distances beyond approximately 700 m from the center of the cask for each of the average assembly burnup values analyzed and a 40-year cooling time. The secondary gamma source is proportional to the neutron source, and it is expected to increase with increasing fuel burnup. The relative contribution of secondary gamma radiation to the total external dose rate increases with increasing fuel cooling time because of the decay of fission products and activation sources that are principal gamma emitters. In addition, the secondary gamma source has high energies and is more penetrating than primary gamma radiation originating in the fuel. This indicates the importance of performing coupled neutron–photon transport calculations and analyzing the impact of material specifications on the secondary gamma contributions.

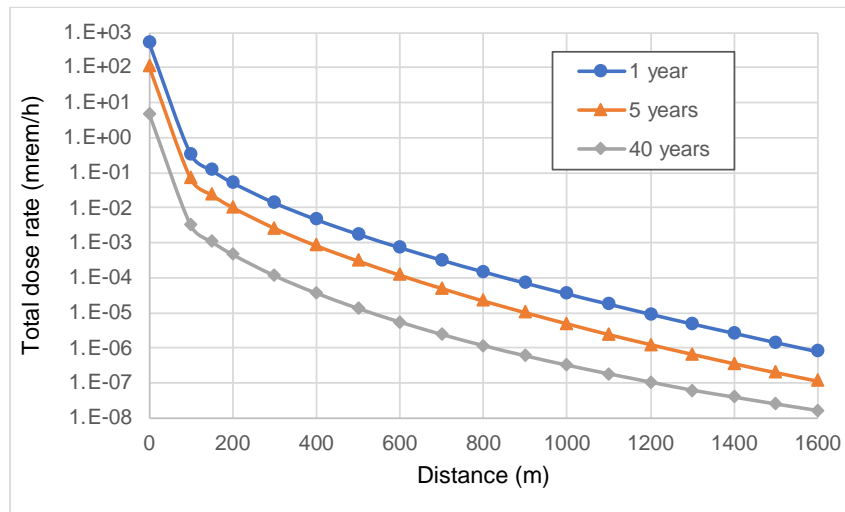


Figure 4-8 Dose Rate Variation as a Function of Distance and Fuel Assembly Cooling Time (Average fuel assembly burnup is 70 GWd/MTU.)

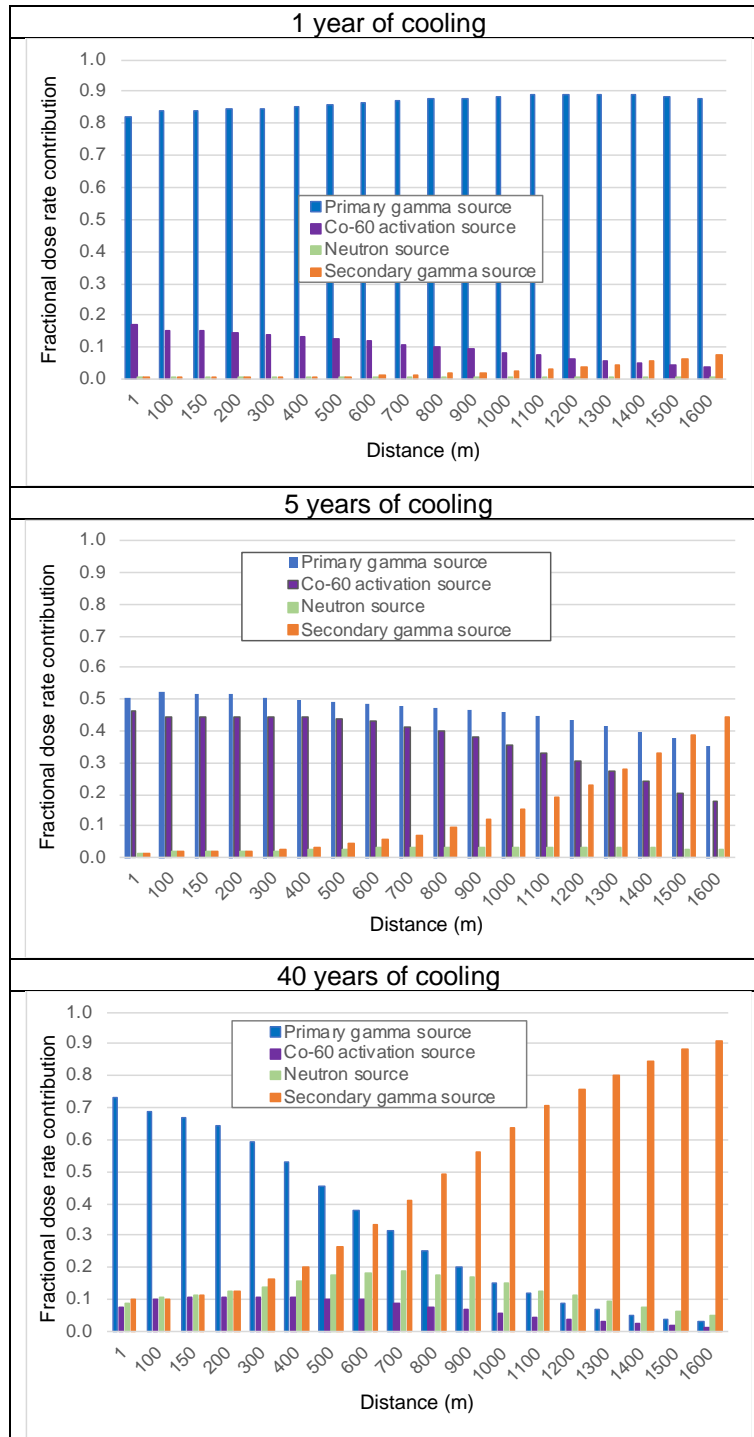


Figure 4-9 Fractional Dose Rate Contribution by Each Radiation Source as a Function of Distance from a Generic Storage Cask and Cooling Time (Average fuel assembly burnup is 70 GWd/MTU.)

A relatively limited study documented in ORNL/SPR-2021/2373 [16] showed that two different cask loadings that produced the same near-field maximum dose rate values also produce the

same maximum far-field dose rate up to 400 m from the cask center, but the maximum dose rate values were different beyond that distance. The dose rates produced by a fuel assembly with higher burnup (i.e., 55 GWd/MTU) and longer cooling time (20 years) were higher than the dose rates produced by a fuel assembly with lower burnup (i.e., 35 GWd/MTU) and shorter cooling time (i.e., 15 years) for dose rate locations beyond 400 m from the cask center. More studies considering higher burnup assemblies are needed to confirm the conclusions of this limited study.

4.2.2.3.2 Sensitivity to Various Modeling Parameters

The far-field dose rate is typically calculated as a function of distance from a shielded source within the air regions above the ground. For generic calculations, the earth–air interface can be represented as a flat surface. However, known local topographic features are recommended to be included in the geometry model for site-specific calculations. Ample volumes of air and soil extending beyond the location of interest for dose rate calculations should be included in the model to properly simulate important radiation scattering events that contribute the dose rates at remote locations. To determine the radial and axial extents of the air volume required to accurately determine dose rate at a location of interest, the volume of air beyond that location may be gradually increased until minimal changes are noticed on the total dose rate at that location.

Although air has very low mass density, small air density variations can have a very significant impact on dose rates at long distances from a cask because of the large volume of air considered in the geometry model. Specifically, dose rate increases with decreasing air density (i.e., less attenuation). For example, the total dose rate increased by 60% at 1,000 m from a cask model because of a 9% air density decrease [119]. Air density decreases with increasing altitude [120] and varies with atmospheric conditions. For example, the air density of the standard atmosphere decreases from 1.225 kg/m³ at sea level to 1.1673 kg/m³ at an altitude of 500 m. The specific air physical characteristics for shielding analyses should be justified, especially for site-specific applications.

Depending on the type, soil elemental compositions can affect the groundshine dose component because of the various scattering, neutron moderation, and absorption characteristics of the elements in soil. Neutron scattering, in general, approaches an isotropic distribution for most nuclides; photons, on average, are scattered in the forward direction. The concentration of hydrogen in soil is very important because neutron interaction with hydrogen nuclei effectively reduces the neutron energy to very low values and increases the probability of radiative capture reactions, thereby decreasing neutron groundshine but generating new secondary gamma sources. Previous studies [119,121] showed that dry soil, an idealized representation of soil, is conservative with respect to neutron dose rate above the ground, because more neutrons are scattered back into the atmosphere from dry soil and these backscattered neutrons are more energetic as compared to the backscattered neutrons from moist soil. The gamma dose rate did not show sensitivity to the water content in soil.

4.3 Computer Code Validation

Shielding materials typically used in transportation packages include carbon steel, lead, and neutron absorber materials such as polymers and/or borated materials, and the primary shielding material used in dry storage casks is concrete. Therefore, it is of interest to validate shielding code results against benchmark experiments designed to test neutron and gamma radiation transport through typical shielding materials. A dry storage cask typically features a set

of inlet and outlet vents or openings through the shielding layers that maintain an air flow around the fuel canister. To prevent a direct streaming path from the radiation source, these vents are typically shaped as a labyrinth. Therefore, it is important to benchmark the computer codes against measurements of radiation streaming through shielding labyrinths. At large distances from a dry storage installation, the skyshine and groundshine components become a dominant part of the far-field dose rate from the installation. Thus, it is important to benchmark radiation transport codes against measurements of skyshine and groundshine radiation. Validations based on comparisons to measurement data are affected by uncertainties in the measurement data, uncertainties in the modeling data, uncertainties associated with nuclear cross section data, and intrinsic uncertainties and approximations associated with the computational methods used for simulations. Therefore, it is recommended that shielding code validations use benchmark data that have been thoroughly evaluated and include uncertainty analyses.

A summary of publicly available shielding benchmarks is provided in ORNL/SPR-2022/2518 [17]. Databases reviewed in this work include the Shielding Integral Benchmark Archive and Database (SINBAD) [122] and the International Criticality Safety Benchmark Evaluation Project (ICSBEP) Handbook [123]. These databases are developed and maintained by members of the OECD NEA. A summary of applicable shielding benchmark experiments is provided in ORNL/SPR-2022/2518. These experiments have tested radiation attenuation in shielding materials (e.g., iron, steel, lead, water, elements found in concrete and soil) and radiation scattering phenomena (e.g., radiation streaming through ducts with labyrinth-like configurations, skyshine and groundshine), which are relevant to shielding calculations for SNF transportation packages/dry storage casks. The typical radiation sources in these selected experiments are ^{252}Cf sources, thermal-neutron reactors, and ^{60}Co sources. Experimental data include detector count rates, detector energy response functions, leakage neutron fluxes, neutron and gamma doses, foil neutron activation rates, and skyshine dose rates. The quality of information for measured reaction rates is likely much higher than that of measured neutron spectra, which depends on the quality of the processing of pulse heights through an unfolding algorithm [124]. The SINBAD TRG has recently initiated new benchmark evaluations and modernization of the database. Therefore, thorough evaluations of measurement data and uncertainties as well as their systematic documentation are expected to be available in the future for use in shielding code validations.

Validation of the MAVRIC module in SCALE 6.2.4 is documented in ORNL/TM-2020/1500/v4 [125]. Validation was based on eight representative benchmark experiments available from SINBAD, the ICSBEP Handbook, and other publicly available shielding validation studies. Either continuous-energy cross-section libraries generated from ENDF/B-VII.1 nuclear data or ENDF/B-VII.0 multigroup libraries (200 neutron groups and 47 gamma groups) were used in the validation study. The set of selected experiments included four types: (1) shielding experiments testing radiation attenuation in individual shielding materials (e.g., iron, steel, polyethylene, lead, and tungsten) as well as combinations of various thicknesses of steel and polyethylene; (2) an experiment involving neutron streaming through ducts; (3) a skyshine experiment using ^{60}Co sources; and (4) a criticality alarm experiment providing foil activation measurements. In addition, a code-to-code comparison was performed between MAVRIC and existing MCNP validation results. These calculations agreed within estimated measurement uncertainties. The differences observed between MAVRIC and MCNP calculation results, generally within 20%, were primarily attributed to the different response functions and nuclear data used with the two computer codes [125].

Thousands of points of comparison between experiment and calculation are documented in the validation report. Generally, MAVRIC calculations and the experimental values agreed within

measurement uncertainty. Rare outliers were explained by either a lack of information or large uncertainties in the experiment conditions, material, or dimensions. The measurement uncertainties varied greatly among these experiments. For example, the uncertainty associated with the selected foil activation measurements from the criticality alarm experiment was approximately 7%. For this experiment, the maximum difference between the calculated and measured activities was 18%. However, the uncertainty associated with the leakage neutron spectrum measurements provided by the type 1 experiments varied as a function of neutron energy, from 1% to 100%. For these experiments, calculations generally agreed with the experimental results within 50%, except for rare outliers with larger discrepancies. For the skyspine experiment, the agreement between calculations and experimental data for the close-range measurement locations (less than 300 m from source) and far-range measurement locations (beyond 500 m from source) was within 2σ measurement uncertainty (14%), and a disagreement of approximately 25% between the calculated and measured dose rates was observed for mid-range measurement locations (300 m to 500 m from source). The relative uncertainties for the experiment involving neutron streaming through ducts varied between 5% and 30%. For this experiment, calculations were within 30% of the measurement values for all measurement locations, except for a measurement location that was farthest away from the source. For this location, the experimental neutron count was low, and the maximum difference between calculated and measured values was 70%.

Measurement uncertainties and the quality of experimental data greatly vary among shielding experiments, depending on the measured physical quantity and available documentation provided by the authors of the experiments. Large disagreements between measurement data and shielding simulation results of the order of tens of percentage are typical, but these disagreements are not necessarily an indication of the magnitude of the errors and uncertainties associated with nuclear cross section data and computational methods. The consequences of uncertainties associated with the shielding code may be mitigated by various analysis approaches, such as employing conservative assumptions, increasing design margins in the analysis, and establishing bounding design-basis source terms with justified conservatisms.

5 CONCLUSIONS

This report provides updated recommendations for the important areas of the shielding review of applications for NRC Certificates of Compliance for spent fuel storage cask and Type B radioactive material transportation package designs. Other recommendations are documented in NUREG/CR-6802 and NUREG/CR-6716, which were published in 2003 and 2001, respectively. Previous recommendations in NUREG/CR-6716 and NUREG/CR-6802 that are not computer code-related are still applicable, but the computer codes and modeling techniques presented in those reports are no longer representative of modern codes currently used for source term and shielding calculations. The recommendations in this report are intended to support reviews of license applications that accommodate current industry needs. The new recommendations are based on a series of individual research studies, including radiation source term and shielding calculations with the SCALE code system developed at ORNL. However, the recommendations provided in this report are not code dependent. A summary of the conclusions of the main individual studies is provided here.

Fuel assembly decay heat specifications are sometimes proposed to replace fuel assembly burnup, enrichment, and cooling time specifications for shielding analyses of dry storage casks because decay heat is typically the limiting parameter for canister loadings. A study, which is summarized in Section 3.1.7, analyzed the relationship between dose rate and decay heat for SNF transportation and storage systems. In this study, dose rates were calculated for 198 cases which evaluated various SNF systems, SNF discharge characteristics, and loading maps while a constant decay heat was maintained. The results of this study showed that a given decay heat does not correspond to a unique dose rate for a variety of fuel characteristics and package designs. The large variation in dose rates for a constant decay heat indicates that casks loaded based on decay heat—that is, allowing any burnup, cooling time, and enrichment combinations that yield the qualified decay heat limit(s)—cannot ensure that an ISFSI or a spent fuel transportation package will meet the regulatory limits set forth by the respective regulations, that is, 10 CFR Part 72 or 71.

The contents of SNF dry storage and transportation systems consist of SNF assemblies with a variety of assembly designs, broad ranges of average fuel assembly burnup, enrichment, cooling time, and irradiation conditions, as well as different types of irradiated NFH. Fuel assembly minimum initial enrichment, maximum burnup, and minimum cooling time are more appropriate for use as loading controls and limits. However, a set of input depletion parameters that is bounding with respect to radiation source terms and dose rates can be used as bounding conditions to further increase the safety margin. A study, which is summarized in Sections 3.1.5 and 3.1.6, analyzed the effects of various depletion parameters on neutron, primary gamma, and ^{60}Co activation sources. Most depletion conditions that were demonstrated to produce conservative neutron source terms also produce conservative source terms for primary gamma rays originating in active fuel and the ^{60}Co activation sources in fuel hardware regions. However, different trends of variation of the individual source types with certain input parameters were identified in previous studies. For example, the neutron dose rate increases as initial fuel enrichment decreases at fixed burnup, but the primary gamma dose rate increases with decreasing initial fuel enrichment only up to approximately 10 years of cooling and then increases as initial fuel enrichment increases after 10 years of cooling at fixed burnup. Fuel assembly models that include inserts such as BPRs will produce conservative neutron and primary gamma radiation source terms, but non conservative ^{60}Co activation sources for fuel assembly hardware. Fuel parameters and depletion conditions for design basis source term

calculations should be selected based on their overall dose rate effects and most dominating source regarding external dose rates, for all burnups and cool times allowed.

Irradiated PWR NFH rods are usually inserted into the guide tubes of PWR SNF assemblies that are loaded in canisters for storage. Therefore, activation sources in irradiated NFH might have significant contributions to dry storage cask/transportation package external radiation dose rates. There are many types of spent NFH that contribute additional radiation sources in various regions of the host fuel assembly. A limited study determined the activation sources dose rate contributions made by BPRAs and TPDs/ORAs, which are frequently used as design basis activated NFH in shielding analyses because of the ^{60}Co activation source in the materials (see Section 3.2, 4.2.1.2, and 4.2.2.1). This contribution depends on the minimum cooling time permitted for these inserts. BPRAs increase the radial dose rate along the active fuel length, whereas TPDs/ORAs increase the radial dose rate above the active fuel region.

The contents of Type B waste transportation packages may include a broad range of nuclides, geometries, and non-fuel materials that may not be very well defined before loading. The materials, geometry shapes, and spatial source distributions of individual waste pieces may exhibit variations that cannot be easily characterized and/or considered in safety analysis models. Therefore, idealized bounding shielding models are typically developed for shielding analyses. A study presented in Section 3.3 analyzed the effects of localized activation source peaks and the contributions of activation products in irradiated steel and Inconel alloys from reactor pressure vessel and other internals on external dose rates for a steel cask. The results of the study showed that ^{60}Co contribution to the total external package dose rate is approximately 60% to 95%, depending on material, initial cobalt impurity concentration, and shield thickness, at 30 days after reactor shutdown. Its maximum contribution of approximately 100% was reached within the time interval of 2 to 5 years after shutdown and was maintained for up to 45 to 60 years after shutdown, depending on material, initial cobalt impurity concentration, and shield thickness. Localized activation source peaks would significantly increase external dose rate if their locations were near the cask shielding.

The uncertainties associated with nuclear cross-section data and computational methods are important in the assessment of the overall safety margin. A summary of the SCALE capabilities for depletion and shielding calculations is provided in Sections 3.6 and 4.1.2.2, respectively. Depletion code validations are primarily based on comparisons to RCA data. Bias and bias uncertainty values for nuclides important to radiation source terms and dose rate from existing SCALE validations are provided in this report. The results of SCALE shielding validations based on comparisons to experimental shielding benchmarks are also provided.

A summary of recommendations for shielding analyses for Type B SNF and other radioactive material transportation packages and SNF dry storage casks is provided in Section 1.4.

6 REFERENCES

1. Ux Consulting. 2022. *StoreFUEL and Decommissioning Report*. StoreFUEL VOL 24, No. 287, 05 Jul 2022. Roswell, GA.
2. Maheras S., et al. 2022. *Nuclear Power Plant Infrastructure Evaluations for removal of Spent Nuclear Fuel*, M3SF-20N0203020412 (PNNL-30429). Pacific Northwest National Laboratory, Richland, WA.
3. Interim Storage Partners, LLC. 2020. *WCS Consolidated Interim Storage Facility Safety Analysis Report*, Docket Number 72-1050, Revision 3.
4. Holtec International. 2022. *Licensing Report on the HI-STORE CIS Facility*, Docket # 72-1051. Holtec Report #HI-2167374, Rev. 0T.
5. Title 10 of the *Code of Federal Regulations*, Part 71. "Packaging and Transportation of Radioactive Material." Available at <https://www.govinfo.gov/app/collection/cfr/2022/title10/chapterI/part71>.
6. Title 10 of the *Code of Federal Regulations*, Part 72. "Licensing Requirements for the Independent Storage of Spent Nuclear Fuel, High-Level Radioactive Waste, and Reactor-Related Greater Than Class C Waste." Available at <https://www.govinfo.gov/app/collection/cfr/2022/title10/chapterI/part72>.
7. U.S. Nuclear Regulatory Commission. 2020. *Standard Review Plan for Transportation Packages for Spent Fuel and Radioactive Material*. NUREG-2216. Washington, DC.
8. U.S. Nuclear Regulatory Commission. 2020. *Standard Review Plan for Spent Fuel Dry Storage Systems and Facilities*. NUREG-2215. Washington, DC.
9. Broadhead, B. L. 2003. *Recommendations for Shielding Evaluations for Transport and Storage Packages*. NUREG/CR-6802 (ORNL/TM-2002/31). US Nuclear Regulatory Commission, Washington, DC.
10. Bowman S. M., I. C. Gauld, and J. C. Wagner. 2001. *Recommendations on Fuel Parameters for Standard Technical Specifications for Spent Fuel Storage Casks*. NUREG/CR-6716 (ORNL/TM-2000/385). US Nuclear Regulatory Commission, Washington, DC.
11. Gauld, I. C. and J. C. Ryman. 2001. *Nuclide Importance to Criticality Safety, Decay Heating, and Source Terms Related to Transport and Interim Storage of High-Burnup LWR Fuel*. NUREG/CR-6700 (ORNL/TM-2000/284). US Nuclear Regulatory Commission, Washington, DC.
12. Shappert L. B., Ed. 1998. *The Radioactive Materials Packaging Handbook, Design, Operations, and Maintenance*. ORNL/M-5003. Oak Ridge National Laboratory, Oak Ridge, TN.

13. Cumberland R., G. Radulescu, and K. Banerjee. 2020. *A Study on the Relationship between Dose Rate and Decay Heat for Spent Nuclear Fuel Casks*. ORNL/SPR-2020/1441. Oak Ridge National Laboratory, Oak Ridge, TN.
14. Radulescu G. and K. Banerjee. 2020. *Best Practices for Shielding Analyses of Activated Metals and Spent Resins from Reactor Operation*. ORNL/SPR-2020/1586. Oak Ridge National Laboratory, Oak Ridge, TN.
15. Radulescu G., B. R. Grogan, and K. Banerjee. 2021. *Fuel Assembly Reference Information for SNF Radiation Source Term Calculations*. ORNL/SPR-2021/2093. Oak Ridge National Laboratory, Oak Ridge, TN.
16. Radulescu G. and P. Stefanovic. 2023. *A Study on the Characteristics of the Radiation Source Terms of Spent Fuel and Various Non-Fuel Hardware for Shielding Applications*. ORNL/SPR-2021/2373 Rev. 1. Oak Ridge National Laboratory, Oak Ridge, TN.
17. Radulescu G. and P. Stefanovic. 2022. *Review of Experimental Data for Validating Computer Codes Used in Shielding Calculations for Spent Fuel Storage and Transportation Systems*. ORNL/SPR-2022/2518. Oak Ridge National Laboratory, Oak Ridge, TN.
18. Radulescu G. and A. Alpan. 2022. *Review of SCALE Validations Applicable to Spent Nuclear Fuel Shielding Calculations*. ORNL/SPR-2022/2692. Oak Ridge National Laboratory, Oak Ridge, TN.
19. SCALE 6.2.4, available from Radiation Safety Information Computational Center and The Organisation for Economic Cooperation and Development, Nuclear Energy Agency, as CCC-834 package.
20. Wieselquist W. A., R. A. Lefebvre, and M. A. Jessee, Eds. 2020. *SCALE Code System*, ORNL/TM-2005/39, Version 6.2.4. Oak Ridge National Laboratory, Oak Ridge, TN.
21. Title 10 of the *Code of Federal Regulations*, Part 61. "Licensing Requirements for Land Disposal of Radioactive Waste," Available at <https://www.govinfo.gov/app/collection/cfr/2022/title10/chapterI/part61>.
22. <https://www.nrc.gov/waste/spent-fuel-storage/designs.html> (accessed Oct 2022).
23. <https://rampac.energy.gov> (accessed Oct 2022).
24. American National Standards Institute. 2014. *American National Standard for Radioactive Materials - Leakage Tests on Packages for Shipment*. ANSI N14.5-2014. Washington, DC.
25. Carter J. T., S. Maheras, and R. Jones. 2016. "Containers for Commercial Spent Nuclear Fuel." *Presentation to Nuclear Waste Technical Review Board*. Washington, DC, August 24, 2016.
26. U.S. Nuclear Regulatory Commission. 2020. *Certificate of Compliance for Spent Fuel Storage Casks*. Certificate Number 1031. Washington, DC.

27. U.S. Nuclear Regulatory Commission. 2022. *Certificate of Compliance for Spent Fuel Storage Casks*. Certificate Number 1032. Washington, DC.
28. U.S. Nuclear Regulatory Commission. 2021. *Certificate of Compliance for Spent Fuel Storage Casks*. Certificate Number 1004. Washington, DC.
29. U.S. Nuclear Regulatory Commission. 2021. *Certificate of Compliance for Spent Fuel Storage Casks*. Certificate Number 1040. Washington, DC.
30. U.S. Nuclear Regulatory Commission. 2018. *Certificate of Compliance for Radioactive Material Packages*, Certificate Number 9373. Washington, DC.
31. U.S. Nuclear Regulatory Commission. 2019. *Certificate of Compliance for Radioactive Material Packages*. Certificate Number 9356. Washington, DC.
32. U.S. Nuclear Regulatory Commission. 2019. *Certificate of Compliance for Radioactive Material Packages*. Certificate Number 9302. Washington, DC.
33. U.S. Nuclear Regulatory Commission. 2019. *Certificate of Compliance for Radioactive Material Packages*. Certificate Number 9235. Washington, DC.
34. U.S. Nuclear Regulatory Commission. 2021. *Certificate of Compliance for Spent Fuel Storage Casks*. Certificate Number 1008. Washington, DC.
35. U.S. Nuclear Regulatory Commission. 2019. *Certificate of Compliance for Radioactive Material Packages*. Certificate Number 9261. Washington, DC.
36. U.S. Nuclear Regulatory Commission. 2015. *License for Independent Storage of Spent Nuclear Fuel and High-Level Radioactive Waste*. License No. SNM-2506. Washington, DC.
37. U.S. Nuclear Regulatory Commission. 2017. *Certificate of Compliance for Radioactive Material Packages*. Certificate Number 9313. Washington, DC.
38. U.S. Nuclear Regulatory Commission. 2022. *Certificate of Compliance for Spent Fuel Storage Casks*. Certificate Number 1027. Washington, DC.
39. U.S. Nuclear Regulatory Commission. 2021. *Certificate of Compliance for Radioactive Material Packages*. Certificate Number 9293. Washington, DC.
40. U.S. Nuclear Regulatory Commission. 2017. *Certificate of Compliance for Radioactive Material Packages*. Certificate Number 9168. Washington, DC.
41. U.S. Nuclear Regulatory Commission. 2011. *Certificate of Compliance for Radioactive Material Packages*. Certificate Number 9204. Washington, DC.
42. U.S. Nuclear Regulatory Commission. 2015. *Certificate of Compliance for Radioactive Material Packages*. Certificate Number 9212. Washington, DC.
43. U.S. Nuclear Regulatory Commission. 2022. *Certificate of Compliance for Radioactive Material Packages*. Certificate Number 9218. Washington, DC.

44. U.S. Nuclear Regulatory Commission. 2022. *Certificate of Compliance for Radioactive Material Packages*. Certificate Number 9279. Washington, DC.
45. U.S. Nuclear Regulatory Commission. 2014. *Certificate of Compliance for Radioactive Material Packages*. Certificate Number 9365. Washington, DC.
46. U.S. Nuclear Regulatory Commission. 2022. *Certificate of Compliance for Radioactive Material Packages*. Certificate Number 9390. Washington, DC.
47. American National Standards Institute. 2022. *Radioactive Materials – Leakage Tests On Packages For Shipment*. ANSI N14.5-2022. Washington, DC.
48. Murata T. and K. Shibata. 2002. "Evaluation of the (α ,n) Reaction Nuclear Data for Light Nuclei," *Journal of Nuclear Science and Technology*, Supplement 2, 76-79.
49. Fernandes A. C., et al. 2016. "Comparison of thick-target (α ,n) yield calculation codes," *Proceedings, 13th International Conference on Radiation Shielding (ICRS-13) & 19th Topical Meeting of the Radiation Protection & Shielding Division of the American Nuclear Society - 2016 (RPSD-2016)*. Paris, France, October 3-6, 2016.
50. Pigni M. T., S. Croft, and I. C. Gauld. 2016. "Uncertainty Quantification in (α ,n) Neutron Source Calculations for an Oxide Matrix." *Progress in Nuclear Energy*, 91, 147-152.
51. Häkkinen S. 2019. *Impurities in LWR fuel and structural materials*. VTT-R-00184-20. VTT Technical Research Center of Finland, Ltd., Espoo, Finland.
52. Nichols A. L., D. L. Aldama, and M. Verpelli. 2008. *Handbook of Nuclear Data for Safeguards: Database Extensions, August 2008*. INDC(NDS)-0534. International Atomic Energy Agency, Vienna, Austria.
53. Turner J. E. 2007. *Atoms, Radiation, and Radiation Protection*. John Wiley & Sons, LTd.
54. Karpus P. J. 2017. *Beta Emission and Bremsstrahlung*. LA-UR-17-30388. Los Alamos National Laboratory, Los Alamos, NM.
55. Hermann O. W. and C. W. Alexander. 1986. *A Review of Spent-Fuel Photon and Neutron Source Spectra*. ORNL/CSD/TM-205. Oak Ridge National Laboratory, Oak Ridge, TN.
56. Mughabhab S. F. 2003. *Thermal Neutron Capture Cross Sections Resonance Integrals and G-Factors*. INDC(NDS)-440. International Atomic Energy Agency, Vienna, Austria.
57. U.S. Department of Energy, Office of Civilian Radioactive Waste Management. 1992. *Characteristics of Potential Repository Wastes*. DOE/RW-0184-R1, Volume 1. Washington, DC.
58. Electric Power Research Institute. 2010. *Cobalt Reduction Sourcebook*, EPRI-1021103. Palo Alto, CA.
59. Electric Power Research Institute. 1999. *Advanced Light Water Reactor Utility Requirements Document*. TR-016780-V2R8. Palo Alto, CA.

60. Luksic A. 1989. *Spent Fuel Assembly Hardware: Characterization and 10CFR 61 Classification for Waste Disposal, Volume 1-Activation Measurements and Comparison with Calculations for Spent Fuel Assembly Hardware*. PNL-6906-vol. 1. Pacific Northwest National Laboratory, Richland, WA.
61. Wermer C. J. Ed. 2017. *MCNP Users Manual – Code Version 6.2*. LA-17-29981. Los Alamos National Laboratory, Los Alamos, NM.
62. Godfrey A. T. 2014. *VERA Core Physics Benchmark Progression Problem Specifications, Revision 4*. CASL-U-2012-0131-004, Rev 4. Oak Ridge National Laboratory, Oak Ridge, TN.
63. U.S. Department of Energy, Energy Information Administration. 2013. *Nuclear Fuel Data Survey Form GC-859*. Washington, DC.
64. Hall R., et al. 2021. *Isotopic and Fuel Lattice Parameter Trends in Extended Enrichment and Higher Burnup LWR Fuel, Vol. I: PWR Fuel*. ORNL/TM-2020/1833. Oak Ridge National Laboratory, Oak Ridge, TN.
65. Radulescu G. and K. Banerjee. 2021. *Demonstration of the On-the-Fly Shielding Analysis Method*. ORNL/SPR-2021/1913. Oak Ridge National Laboratory, Oak Ridge, TN.
66. Nuclear Energy Institute. 2019. *The Economic Benefit and Challenges with Utilizing Increased Enrichment and Fuel Burnup for Light-Water Reactors*. White Paper. Palo Alto, CA.
67. DeHart M. D. 1996. *Sensitivity and Parametric Evaluations of Significant Aspects of Burnup Credit for PWR Spent Fuel Packages*. ORNL/TM-12973. Oak Ridge National Laboratory, Oak Ridge, TN.
68. International Atomic Energy Agency. 2006. *Optimization Strategies for Cask Design and Container Loading in Long Term Spent Fuel Storage*. IAEA-TECDOC-1523. Viena, Austria.
69. Lefebvre R. A., et al. 2017. “Development of Streamlined Nuclear Safety Analysis Tool for Spent Nuclear Fuel Applications.” *Nucl. Technol.*, 199, 227-244.
70. Geelhood K. J. 2019. *Fuel Performance Considerations and Data Needs for Burnup above 62 GWd/MTU*. PNNL-29368. Pacific Northwest National Laboratory, Richland, WA.
71. Adamson R., et al. 2003. *High Burnup Fuel Issues*. ZIRAT-8 Special Topics Report. Advanced Nuclear Technology International. Sweden.
72. Cacciapouti R. J. and S. Van Volkinburg. 1997. *Axial Burnup Profile Database for Pressurized Water Reactors*. YAEC-1937. Yankee Atomic Electric Company, Rowe, MA.
73. Wimmer L. B. and C. W. Mays. 2004. *BWR Axial Burnup Profile Evaluation*. 32-5045751-00, Framatome ANP, Lynchburg, VA.

74. Hannah M. A. 1980. *Axial Fuel Blanket Design and Demonstration, First Semi-Annual Progress Report: January-September 1980*. DOE/ET/34020-1. Babcock & Wilcox, Lynchburg, VA.
75. Alonso G., S. Bilbao, and E. del Valle. 2015. "Impact of the moderation ratio over the performance of different BWR fuel assemblies." *Annals of Nuclear Energy*, 85, 670-678.
76. U.S. Nuclear Regulatory Commission. 1992. *Alternative Requirements for Fuel Assemblies in Design Features Section of Technical Specifications*. Generic Letter 90-02, Supplement 1. Washington, DC.
77. https://www.westinghousenuclear.com/Portals/0/flysheets/NFCM-0012_SFA.pdf (accessed Dec 2022).
78. U.S. Department of Energy, Office of Civilian Radioactive Waste Management. 1992. *Characteristics of Potential Repository Wastes*. DOE/RW-0184-R1, Volume 1. Washington, DC.
79. Migliore R. J., et al. 1994. *Non-Fuel Assembly Components: 10 CFR 61.55 Classification for Waste Disposal*. PNL-10103. Pacific Northwest Laboratory, Richland, WA.
80. Lepel, E. A., et al., Radiological Characterization of Spent Control Rod Assemblies, NUREG/CR-6390 (PNL-10806), U.S. Nuclear Regulatory Commission, Washington, D.C. (1995).
81. Ferreux L., et al. 2014. "Photon emission intensities in the decay of ^{108m}Ag and ^{110m}Ag ." *Applied Radiation and Isotopes*, 87, 101-106.
82. U.S. Department of Energy, Yucca Mountain Site Characterization Project Office. 1998. *Summary Report of Commercial Reactor Criticality Data for Crystal River Unit 3*. B00000000-01717-5705-00060 Rev. 01. Las Vegas, NV.
83. Secker J. R., et al. 2005. "Optimum Discharge Burnup and Cycle Length for PWRs." *Nucl. Technol.*, 151(2), 109–119.
84. Evans J. C., et al. 1984. *Long-Lived Activation Products in Reactor Materials*. NUREG/CR-3474. U.S. Nuclear Regulatory Commission, Washington, DC.
85. Phlippen P-W, et al. 2018. "Numeric Determination and Validation of Neutron-Induced Radioactive Nuclide Inventories for Decommissioning and Dismantling of Light Water Reactor," *Nucl. Technol.*, 201, 66–79.
86. Smith R. I., G. J. Konzek, and W. E. Kennedy, Jr. 1978. *Technology, Safety and Costs of Decommissioning a Reference Pressurized Water Reactor Power Station*. NUREG/CR-0130 Vol1. U.S. Nuclear Regulatory Commission, Washington, DC.
87. Oak H. D., et al. 1979. *Technology, Safety and Costs of Decommissioning a Reference Boiling Water Reactor Power Station*, NUREG/CR-0672 Vol2. U.S. Nuclear Regulatory Commission, Washington, DC.

88. MacKenzie D. R., M. Lin, and R. E. Barletta. 1983. *Permissible Radionuclide Loadings for Organic Ion Exchange Resins from Nuclear Power Plants*. NUREG/CR-2830. U.S. Nuclear Regulatory Commission, Washington, DC.
89. Robertson D. E., et al. 2000. *Low-Level Radioactive Waste Classification, Characterization, and Assessment: Waste Stream and Neutron-Activated Metals*. NUREG/CR-6567. U.S. Nuclear Regulatory Commission, Washington, DC.
90. U.S. Department of Energy. 2016. *Final Environmental Impact Statement for the Disposal of Greater-Than-Class C (GTCC) Low-Level Radioactive Waste and GTCC-Like Waste*. DOE/EIS-0375, Volume 2: Chapter 9 through Appendix I. Washington, DC.
91. Shultis J. K. and R. E. Faw. 2000. *Radiation Shielding*. American Nuclear Society edition.
92. <https://www.nndc.bnl.gov/ensarchivals/> (accessed Dec 2022).
93. Organisation for Economic Co-operation and Development, Nuclear Energy Agency. 2022. *State-of-the-art report on Nuclear Fuel Behaviour Under Reactivity-initiated Accident Conditions*. NEA No. 7575. Vienna, Austria.
94. Gauld I. C., et al. 2011. "Isotopic Depletion and Decay Methods and Analysis Capabilities in SCALE," *Nuclear Technology*, 174, 169–195.
95. DeHart M. D. and S. M. Bowman. 2005. "Improved Radiochemical Assay Analyses Using TRITON Depletion Sequences in SCALE," *Proceedings, International Atomic Energy Agency (IAEA) Technical Committee Meeting on Advances in Applications of Burnup Credit to Enhance Spent Fuel Transportation, Storage, Reprocessing and Disposition*, London, UK, August 29 – September 2, 2005.
96. Ade, B. J.. 2012. *SCALE/TRITON Primer: A Primer for Light Water Reactor Lattice Physics Calculations*. NUREG/CR-7041 (ORNL/TM-2011/21). U.S. Nuclear Regulatory Commission, Washington, DC.
97. Skutnik S. E., M. L. Williams, and R. A. Lefebvre. 2015. "ORIGAMI: A New Interface for Fuel Assembly Characterization with ORIGEN." *Proceedings, IHLRWM 2015*. Charleston, SC, April 12-16, 2015.
98. Leal L. C., O. W. Herman, S. M. Bowman, and C. V. Parks. 1998. *ARP: Automatic Rapid Process for the Generation of Problem-Dependent SAS2H/ORIGEN-S Cross-Section Libraries*. ORNL/TM-13584. Oak Ridge National Laboratory, Oak Ridge, TN.
99. Michel-Sendis F., et al. 2017. "SFCOMPO-2.0: An OECD NEA Database of Spent Nuclear Fuel isotopic Assays, Reactor Design Specifications and Operating Data," *Annals of Nuclear Energy*, 110, 779–788.
100. Ilas G., J. R. Burns, B. D. Hiscox, and U. Mertyurek. 2022. *SCALE 6.2.4 Validation: Reactor Physics*. ORNL/TM-2020/1500/v3. Oak Ridge National Laboratory, Oak Ridge, TN.
101. Smith H. J., I. C. Gauld, U. Mertyurek. 2012. *Analysis of Experimental Data for High Burnup BWR Spent Fuel Isotopic Validation—SVEA-96 and GE14 Assembly Designs*.

- NUREG/CR-7162 (ORNL/TM-2013/18). U.S. Nuclear Regulatory Commission, Washington, DC.
102. Chadwick M. B., et al. 2011. "ENDF/B-VII.1 Nuclear Data for Science and Technology: Cross Sections, Covariances, Fission Product Yields and Decay Data," *Nuclear Data Sheets*, 112(12), 2887-2996.
 103. Chadwick M. B., et al. 2006. "ENDF/B-VII.0: Next Generation Evaluated Nuclear Data Library for Nuclear Science and Technology." *Nuclear Data Sheets*, 107(12), 2931-3060.
 104. Eysermans J., et al. 2022. "REGAL International Program: Analysis of experimental data for depletion code validation." *Annals of Nuclear Energy*, 172, 109057.
 105. Evans T. M., et al. 2010. "Denovo: a new three-dimensional parallel discrete ordinates code in SCALE." *Nuclear Technology*, 171(2), 171-200.
 106. Wareing T. A., J. M. McGhee, and J. E. Morel. 1996. "ATTILA: a three-dimensional, unstructured tetrahedral mesh discrete ordinates transport code," *Transactions of the American Nuclear Society*, vol. 75, article 146.
 107. Alcouffe R. E., et al. 2018. *PARTISN: A Time-Dependent, Parallel Neutral Particle Transport Code System*. LA-12969-M. Los Alamos national Laboratory, Los Alamos, NM.
 108. Mosher S. W., et al. 2015. *ADVANTG-An Automated Variance Reduction Parameter Generator*. ORNL/TM-2013/416, Rev. 1. Oak Ridge National Laboratory, Oak Ridge, TN.
 109. Radulescu G., T. M. Miller, K. Banerjee, and D. E. Peplow. 2021. *Dose Rate Analysis of the WCS Consolidated Interim Storage Facility*. ORNL/TM-2019/1070. Oak Ridge National Laboratory, Oak Ridge, TN.
 110. Wagner J. C., et al. 2011. "Review of Hybrid (Deterministic/Monte Carlo) Radiation Transport Methods, Codes, and Applications at Oak Ridge National Laboratory." *Progress in Nuclear Science and Technology*, 2, 808-914.
 111. Peplow D. E. 2011. "Monte Carlo Shielding Capabilities with MAVRIC," *Nuclear Technology*, 174(2), 289-313.
 112. Wagner J. C., D. E. Peplow, and S. W. Mosher. 2014. "FW-CADIS Method for Global and Regional Variance Reduction of Monte Carlo Radiation Transport Calculations." *Nuclear Science and Engineering*, 176(1), 37-57.
 113. Coveyou R. R., V. R. Cain, and K. J. Yost. 1967. "Adjoint and Importance in Monte Carlo Applications." *Nuclear Science and Technology*, 27, 219-234.
 114. Haghghat A. and J. C. Wagner. 2003. "Monte Carlo Variance Reduction with Deterministic Importance Functions," *Progress in Nuclear Energy*, 42(1), 25-53.
 115. U.S. Nuclear Regulatory Commission. 2020. *Dry Storage and Transportation of High Burnup Spent Nuclear Fuel*. NUREG-2224. Washington, DC.

116. U.S. Nuclear Regulatory Commission. 2003. *Spent Fuel Project Office Interim Staff Guidance – 11, Revision 3*. Washington, DC.
117. Scaglione J. M., et al. 2015. *A Quantitative Impact Assessment of Hypothetical Spent Fuel Reconfiguration in Spent Fuel Storage Casks and Transportation Packages*. NUREG/CR-7203 (ORNL/TM-2013/92). U.S. Nuclear Regulatory Commission, Washington, DC.
118. Shultis J. K. 2000. *Radiation Analysis of a Spent Fuel Storage Cask*. Report No. 290. Kansas State University, Manhattan, KS.
119. Radulescu G., et al. 2001. "Skyshine Calculations for a Large Spent Nuclear Fuel Storage Facility with SCALE 6.2.3," *Nucl. Technol*, 207(11), 1768-1783.
120. National Oceanic and Atmospheric Administration. 1976. *US Standard Atmosphere 1976*. U.S. Government Printing Office, Washington, DC.
121. Radulescu G. and K. J. Connolly. 2016. "A Parametric Analysis of Factors Affecting Calculations of Estimated Dose Rates from Spent Nuclear Fuel Shipments," *Proceedings of the WM2016 Conference*. Phoenix, Arizona, March 6-10, 2016.
122. SINBAD 2017.12, Shielding Integral Benchmark Archive and Database, Version February 2016, available from Radiation Safety Information Computational Center as DLC-237.
123. International Criticality Safety Benchmark Evaluation Project (ICSBEP) Handbook (database), <https://www.oecd-nea.org/download/science/icsbep-handbook/CD2019/> (accessed June 2022).
124. Kodeli I. A. and E. Sartori. 2021. "SINBAD – Radiation shielding benchmark experiments." *Annals of Nuclear Energy*, 159, 108254.
125. Celik C., D. Peplow, M. Dupont, and G. Radulescu. 2022. *SCALE 6.2.4 Validation: Radiation Shielding*. ORNL/TM-2020/1500/v4. Oak Ridge National Laboratory, Oak Ridge, TN.

BIBLIOGRAPHIC DATA SHEET

(See instructions on the reverse)

NUREG/CR-7302, Revision 1
ORNL/TM-2023/2679

2. TITLE AND SUBTITLE

Updated Recommendations Related to Spent Fuel Transport and Dry
Storage Shielding Analyses

3. DATE REPORT PUBLISHED

MONTH

YEAR

January

2024

4. FIN OR GRANT NUMBER

5. AUTHOR(S)

Georgeta Radulescu

6. TYPE OF REPORT

Technical

7. PERIOD COVERED (Inclusive Dates)

8. PERFORMING ORGANIZATION - NAME AND ADDRESS (If NRC, provide Division, Office or Region, U. S. Nuclear Regulatory Commission, and mailing address; if contractor, provide name and mailing address.)

Oak Ridge National Laboratory
Oak Ridge, TN 37831-6283

9. SPONSORING ORGANIZATION - NAME AND ADDRESS (If NRC, type "Same as above", if contractor, provide NRC Division, Office or Region, U. S. Nuclear Regulatory Commission, and mailing address.)

Division of Safety Analysis
Office of Nuclear Regulatory Research
U.S. Nuclear Regulatory Commission
Washington, D.C. 20555-0001

10. SUPPLEMENTARY NOTES

11. ABSTRACT (200 words or less)

This report provides updated recommendations for important areas of the shielding review of applications for U.S. Nuclear Regulatory Commission (NRC) Certificates of Compliance for spent fuel dry storage cask and Type B radioactive transportation material package designs. The recommendations are based on a series of research studies sponsored by the NRC and performed by Oak Ridge National Laboratory. The main findings of this research are described and illustrated with graphs that allow for examination of representative source terms and dose rates, as well as expected effects of various input parameters on source terms and dose rates for transportation packages and storage casks. The principal recommendations cover: spent nuclear fuel limiting characteristics for loadings; relationships between decay heat and external dose rate; bounding depletion parameters for fuel assembly radiation source term calculations; the neutron source from subcritical multiplication; secondary gamma dose rates; reconstituted fuel assemblies with irradiated stainless-steel fuel rods; air density and soil composition specifications for storage cask far-field dose rate calculations; and models for activated metals in Type B waste packages. The recommendations are intended to provide staff with updated guidance on the performance of shielding analyses that account for modern methods, different application systems, and benchmark experiments.

12. KEY WORDS/DESCRIPTORS (List words or phrases that will assist researchers in locating the report.)

Shielding analyses
Spent nuclear fuel
Transportation packages
Dry storage casks
Guidance
Recommendations
SCALE
ORNL

13. AVAILABILITY STATEMENT

unlimited

14. SECURITY CLASSIFICATION

(This Page)

unclassified

(This Report)

unclassified

15. NUMBER OF PAGES

16. PRICE



Federal Recycling Program



UNITED STATES
NUCLEAR REGULATORY COMMISSION
WASHINGTON, DC 20555-0001

OFFICIAL BUSINESS



@NRCgov



NUREG/CR-7302 Revision 1 Updated Recommendations Related to Spent Fuel Transport and Dry Storage February 2024
Shielding Analyses